Uncertainty in climate change impacts on Southern Alps river flow: the role of hydrological model complexity

Ryan Jones

A thesis submitted in partial fulfilment of the degree of Masters of Science, at the University of Otago, Dunedin, New Zealand

October 2017

Abstract

Climate change scenario modelling for New Zealand indicates a series of hydrological changes can be expected. Hydrological modelling is a critical tool to assess the likely impacts of future climate change on river runoff. A hydrological model no matter the complexity can be viewed as a simplified representation of the real-world environment. The most comprehensive hydrological models, i.e. fully-distributed (e.g. TopNet and MIKESHE), are generally complex and require large amounts of input data, computer power and time. The use of a semi-distributed model like HBV-light to perform essentially the same function can yield a relatively efficient method of scenario hydrological modelling. As such, the aim of this research is to assess the use of the HBV-Light hydrological model to simulate observed river flow data from within the Shotover Catchment, situated in Queenstown, New Zealand, and compare projected changes to future river runoff under climate change conditions to that of a more complex hydrological model (TopNet).

The HBV-Light model performed well in the Shotover Catchment when replicating an observed data set of 13 years (1972−1984), returning a monthly NSE of 0.72 for the calibration period and 0.61 for the validation period (1985−1997). The use of HBV-Light to simulate river flow under future climate change conditions, and the potential influence such changes could have on New Zealand's freshwater resources were also assessed. HBV-Light, using an IPCC SRES A1B climate scenario, and an ensemble of 12 GCM's suited to New Zealand's climate conditions, projected runoff increases to the Shotover River in the magnitude of 13.43 % for 2040 over a 20-year average (2030 − 2049), and 17.44 % in 2090 (2080 − 2099). In comparison to the more complex model (TopNet) used assess the impact of climate change on river flow for the same future time periods using the same 12 GCM ensemble and IPCC SRES A1B climate scenario, HBV-Light simulates a yearly projection for 2040 that is 3.5 % higher than TopNet, 1.65 % lower in 2090. Monthly comparisons of future runoff show the HBV-Light model drastically over-simulates TopNets assessment of the Shotover Catchment (by 35 % in 2090 for August) and other research in the Clutha Catchment, in some cases by up to 50 %. HBV-Light under-simulated soil moisture by 300 mm/yr^{-1} and over-simulated AET consistently, but simulated snowmelt relatively well in comparison to TopNet. Therefore, the current research concludes that the role of hydrological model complexity outweighs the role of other modelling uncertainties such as input data. HBV-Light was run with physical input

data which is more accurate but limited in the spread of the catchment, whereas TopNet was run using interpolated data (VCSN) which covers the catchments upper reaches but is only an interpolation. TopNets performance was more in line with other research from the Clutha Catchment and its sub-catchments, such as the Matukituki and the Lindis. However, in the absence of large comprehensive data sets (VCSN) required to run complex models such as TopNet, HBV-Light could be an acceptable alternative for assessing future impacts to river runoff under climate change conditions in New Zealand.

Acknowledgements

I want to thank first and foremost the University of Otago for giving me the opportunity to undertake this MSc. The support and services available really helped me get to where I am today. To my supervisors Dr Daniel Kingston and Dr Sarah Mager, the time, guidance and patience you have shown me have been second to none, and am truly grateful for every minute of it. To my family, Dad, Mum, Brett, Nan and Grandad, your support, love and encouragement throughout the six years I've spent at university has meant the world to me. Finally, to flatmates and friends, thanks for the putting up with me and the memories that were created, there are somethings I will surely never forget.

Table of Contents

List of Figures

Chapter Two

Chapter Three

Chapter Four

Chapter Five

List of Tables

Chapter Two

Chapter Three

Chapter Four

Chapter Five

Chapter One
Introduction

Increasing atmospheric greenhouse gas concentrations (GHG) are the primary cause of global warming/climate change (Houghton *et al*., 1996; Hurd *et al.* 1999; Wigley 1999; IPCC 2000; 2007). One of the greatest impacts global warming will have is likely to be on the hydrological cycle at all scales, from global to singular catchments (Bates *et al*. 2008). Impacts on the hydrological cycle have the potential to change the distribution of water resources both spatially and temporally, with the consensus of most researchers indicating evidence of changes to the intensity and frequency of future hydrological events such as precipitation and draughts (Huntington 2006). The intensification of the hydrological cycle will see increased precipitation and evaporation in some parts of the world, with increases in precipitation thought to be unequally distributed globally, leaving other parts with significant reduction in precipitation (Collins *et al.* 2013).

Due to the dependency of the hydrological cycle on climate, any changes to future climate regimes will affect a variety of human settlements worldwide that depend on the existing spatial and temporal patterns of water resources for irrigation and consumptive use (Frederick and Gleick 1999; Cisneros *et al.* 2014). Many aspects of human civilisation such as the environment, economy and society are dependent on water resources, and changes to it could influence humanity (Arnell 1999; Cisneros et al. 2014). Therefore, understanding and estimating the magnitude of climate change and the corresponding influence on the hydrological cycle is important, as such changes have the potential to affect the fresh water supply of humans and animals, peoples current dependency on floods and draughts, hydropower generation, and navigation (Christensen and Lettenmaier 2007; Bae *et al.* 2011).

1.1 Use of hydrological models for impact assessment

A hydrological model is a simplification of a hydrological catchments true physical complexity (Beven 2010). The use of hydrological modelling as a tool for both climate change and runoff assessment are well established (Andersson *et al.* 2006; Beyene *et al.* 2010; Elsner *et al.* 2010). Hydrological models are used for a variety of hydrological applications. These can include more complex processes of the water cycle such as runoff, infiltration of the surface,

surface flow, subsurface flow, canopy interception, snow melt, precipitation and evapotranspiration (Willmott and Rowe 1985). The use of simpler models, essentially requiring less input data and calibration (time spent running the model), could potentially produce the same degree of runoff certainty as more complex, physically based hydrological models (Wagener and McIntyre 2007). Within New Zealand, hydrological modelling has focused predominantly on climate change (e.g. Poyck *et al.* 2011), groundwater (e.g. Hattermann *et al.* 2004; Fenicia *et al.* 2006) and flood modelling (e.g. Clark *et al.* 2008; Devkota and Bhattarai 2015), and the associated effects these hydrological pathways have on catchment runoff.

To date, many studies have been carried out in catchments across both the North and South Islands of New Zealand, aiming to understand how future impacts of climate change will affect the overall condition of catchments. The most commonly used hydrological modelling tool in New Zealand is TopNet. TopNet is a fully distributed hydrological model with the ability to simulate water balance over a number of sub-catchments in a basin, and routes stream flow from each sub-basin (Clark *et al.* 2008). The use of TopNet has been shown satisfactory for New Zealand conditions (e.g. Clark *et al.* 2008; Woods *et al.* 2008; Poyck *et al*. 2011; Srininvasan *et al*. 2011; Gawith *et al.* 2012). However, running and calibrating the model can prove difficult, requiring considerable data and time inputs (McMillan *et al.* 2016). Therefore, it is advantageous to determine whether an accurate representation of catchment river runoff under the potential influences of climate change can be simulated using a less complex, more user friendly hydrological model.

There are two aims for this research. The first aim is to determine whether a relatively simple hydrological model can realistically simulate an observed flow in an alpine catchment in New Zealand. Secondly, if a simple model can realistically simulate an alpine flow, the research will compare future climate change impacts on river flow between the simple hydrological model and that of a complex model. Thus, the objectives of this research are:

- To set up and calibrate a simple conceptual model for the Shotover Catchment,
- Run the calibrated hydrological model for climate change impacts in two future periods, to compare runoff outputs with that of a more complex hydrological model, using the same set of climate scenarios.

Chapter Two that follows this introduction (Chapter One) presents an overview of hydrological modelling which focuses primarily on the current research surrounding the uncertainty

associated with hydrological modelling and areas requiring further exploration. Chapter Three provides details of the field area chosen to run HBV-Light, the characteristics of the area including geography, geology and climatology, followed by the hydrological modelling process undertaken for this research, and a description of both hydrological models used (HBV-Light and TopNet). Chapter Four assesses the HBV-Light model's replication of an observed flow from within the Shotover Catchment for the calibration and validation periods, with comments and conclusions on HBV-Lights suitability drawn from visual and statistical analysis. A brief summary of how TopNet was incorporated in this research and how the odel performed over an observed period is also included in Chapter Four. Chapter Five presents the projected changes to river runoff under the same climate change conditions of both HBV-Light and TopNet, and compares projected snowmelt, soil moisture and AET outputs of both models. Chapter Six compares and discusses the differences in the respective model outputs, the limitations surrounding the research, and where improvements could be made in future understanding. Chapter Seven concludes the thesis by summarising the key findings and contribution of the research to current literature.

Chapter Two

Hydrological Modelling: An Overview

Hydrologic processes such as precipitation, snowmelt, interception, evapotranspiration, infiltration, surface runoff, and sub-surface flow have complex interrelationships within any river basin or watershed (Islam 2011). Due to the complex relationships between variables in a catchment, developing a hydrological model to represent those interactions is difficult. A hydrological model is a mathematical model used to simulate stream flow by estimating the inter-relationships of soil, water, climate, and land use variables associated with a hydrological catchment through mathematical abstraction (Gosain *et al.* 2009). In order to calibrate and run a hydrological model for the present day and future runoff, the compounding uncertainty that is inherently bestowed on runoff projections must be acknowledged in order to quantitate and understand the credibility of such projections.

The purpose of this chapter is to compile and evaluate the current literature focusing on the uncertainty associated with hydrological modelling, and identify areas of research where uncertainty is unknown. The hydrological modelling process on a general level is explored in Section 2.1. Following the general modelling process, the uncertainty that global climate models (GCMs) present due to their large-scale nature is acknowledged, and the common approaches to refining them are explained (Section 2.2). Section 2.3 follows on from methods of downscaling data, by examining the uncertainty that hydrological modelling bestows on the final runoff projection, and the role that model complexity has. Section 2.4 details how the accumulation and precision of climate and hydrological input data to run the model can impact the overall model performance during the calibration period, followed by uncertainties of calibrating a hydrological model (Section 2.5). The chapter ends with some examples of New Zealand specific impact studies that have been conducted within the Southern Alps (Section 2.6) and the justification for this research is presented (Section 2.7).

2.1 Hydrological modelling process

There are four main processes to climate change hydrological modelling: emissions, climate projections, downscaling and hydrological projections (Fig. 2.1). Emissions projections primarily drive General Circulation Models (GCMs), stage 1, where the projected emissions are then used to drive the climate projections, stage 2. GCMs incorporate the atmosphere, oceanic and terrestrial surfaces, the cryosphere, and biogeochemical processes, all of which are governed by complex and continually evolving inter-relationships that are simulated 3-dimentionally. All GCMs are complex, however they run at different spatial resolutions e.g. anywhere between 100 to 600 km^2. Each individual GCM involves parameterisation owing to gaps in a real-world knowledge and processes, insufficient computing power to simulate complex aspects of the real world, i.e. the presence of sub-grid scale processes where information hasn't been ascertained (Gosling *et al.* 2011).

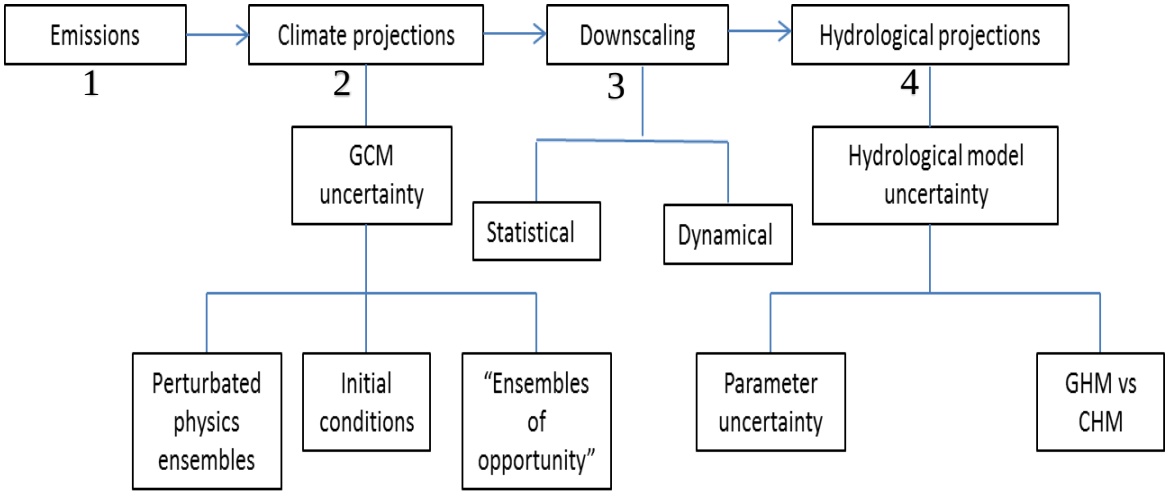

Figure 2.1: *The four main processes of climate change hydrological modelling, and the common sources of uncertainty associated with each process.* Source: Gosling *et al.* (2011).

2.2 GCM Uncertainty

Confidence in future climate projections derived from large scale GCMs depend on the application of well understood physical climate processes, the chosen GCMs ability to simulate observed climates and replication of simulated projections by other models (Daniels *et al.* 2012). Due to local climate processes such as topography, vegetation and hydrology being fine-scaled, the magnitude of variability between model projections increases as GCMs are primarily course-scaled. The development and integration of statistical relationships between some large and local scale climate processes can be included in GCMs, but not all (PCIC 2014).

In regions with less rainfall, the use of different GCMs can simulate opposing projections of rainfall change, highlighting the uncertainty with the use of sophisticated GCM tools that have statistical relationships between local and large-scale climates integrated still have. Therefore, the disparity between coarse and fine scaled resolutions present a need for the mitigation of GCM uncertainty to refine the precision of future climate projections (stage 3 of Fig. 2.1). To mitigate GCM uncertainty there are three common approaches; ensembles of opportunity, perturbed physics ensemble and downscaling of GCMs.

2.2.1 Ensembles of Opportunity

The first deals with uncertainty associated with GCM structure. Researchers use a range of projections from a group of plausible GCMs, producing a multitude of scenarios to compare, often referred to as "ensembles of opportunity" (Meehl *et al.* 2007). An ensemble of opportunity is a collection of GCMs that identify a possible trend in the climate, instead of taking a single GCM as confirmation of what future climate conditions could yield. Ensembles of opportunity can often lead to wide variation in global and regional variations of future temperature and precipitation estimates, as some researchers putting their GCM estimates forward could use different model variations to derive outputs (Haughton *et al.* 2014).

2.2.2 Perturbed Physics Ensemble

The second approach to mitigating uncertainty is to generate a "perturbed physics ensemble" (PPE), which cause a disturbance within physical parameterisations of a climate model. Essentially, this approach looks at GCM uncertainty again however this time deals with different versions of a single GCM. An advantage of PPE is that if there is a disturbance within the model, it can be accounted for as noise within the output, where an analysis of the models output can be readjusted for the sensitive parameter, and plausible versions can be assessed. PPE's largest weakness is its highly dependent on computer power, but if available, large groups of climate scenarios can be generated for comparison. A PPE of 2578 simulations was run by Stainforth *et al.* (2005) for high, medium and low emissions values for 6 parameters: the representation of clouds and precipitation: the threshold of relative humidity for cloud formation, the cloud to-rain conversion threshold, the cloud-to-rain conversion rate, the ice fall speed, the cloud fraction at saturation and the convection entrainment rate coefficient.

2.2.3 Downscaling GCM outputs

The third approach to mitigating uncertainty of GCMs is downscaling. Downscaling of GCM's is essential in most forms of climate change impact assessment, as mismatch between GCM resolution in all but the largest river systems is too great to assess the possible microclimates associated with individual catchments. Although GCMs are heavily relied upon for future estimations of climate change impact studies they cannot account for natural heterogeneity of fine-scale climate variability as their resolutions are generally coarse (100 to 500 km). Therefore, downscaling is used to derive finer-resolution spatial and temporal aspects of climate projections. Spatial downscaling methods essentially take a coarse GCM resolution e.g. a 500-km grid cell output, to a finer resolution; e.g. 20 km or a specific location. Temporal downscaling aims to derive fine-scale climate data from coarse GCM outputs such as turning monthly or seasonal rainfall into daily rainfall time-series data.

Downscaling can be done in two ways, dynamical downscaling and statistical downscaling. Dynamical downscaling uses a regional climate model (RCM) which is essentially a higher resolution GCM, with similar principles. An RCM uses large-scale climate processes that are imbedded in a GCM and applies more complex topography and the corresponding surface heterogeneities, the land-sea contrast, and a greater description of the associated physical processes at the local scale to project realistic climate information at finer resolutions (20 to 50 km) than a GCM (100 to 600 km). Statistical downscaling uses established relationships between current and historical local climate variables and large-scale atmospheric processes, which then have to be validated. The large-scale future atmospheric variables that a GCM projects is then processed using the relationships determined and validated between the local scale climate variables and large scale atmospheric processes to produce site specific climate projections that are finer (>10 km) than an RCM which is generally limited to a spatial resolution between 20 and 50 km.

Downscaling techniques have both advantages and disadvantages (Giorgi and Mearns 1991). The dynamic approach is similar to a large scale GCM and when used with a local RCM system can provide better dynamic and physical consistency of parameters that are more representative of real world processes than statistical downscaling can (Kim *et al.* 2000). The primary advantage of an RCM is the ability to model atmospheric processes and land cover changes explicitly. Although computationally expensive, the dynamic downscaling method does not rely on central assumption like statistical methods, where it is assumed present day relationships between climate variables such as temperature and precipitation through natural

events like the ENSO cycle will be replicated in the future, allowing for natural variation of parameter values (Gosling *et al.* 2011). On the point of RCMs, it is important to note as a disadvantage that RCMs inherit the same bias as their parent GCM, and are themselves a source of uncertainty owing to imperfect simulations of small-scale climate from large-scale (Seaby *et al.* 2013). Even though RCMs greatly improve spatial resolution, a RCM output still needs statistical downscaling and bias correction for higher resolution data.

The main advantage to statistical downscaling techniques is that they are computationally inexpensive compared to dynamical downscaling that can be validated through physical field observations that can be expensive, and are easily applied to various GCM outputs. GCM downscaling provides information of local parameters that give a more representative perspective of the changing climate between differing regional morphologies, as each one is spatially and temporally significant to a specific area (Gosling *et al.* 2011). Statistical downscaling also allows the links between large-scale and small-scale climates to be analysed as downscaling provides the framework for small-scale physical models to verify large-scale empirical models, thus allowing more confidence in the modelled outputs (Osborn *et al.* 1999). Theoretical disadvantages of statistical downscaling are that the outputs under boundary forcing for present day climates may hold true and could be verified by physical observation, but the basic assumption of possible future scenarios with those same boundaries may not (Zorita and von Storch 1999). Another disadvantage with statistical downscaling is that input data used for parameter refining between individual catchments may not be readily available as more diverse and remote regions are accompanied by topographic complexities. A third downscaling caveat is that systematic changes, regional forcing boundaries and feedback processes are not accounted for by statistically-based techniques (Mearns *et al.* 1999).

With both advantages and disadvantages known about dynamical and statistical downscaling, researchers can often use both approaches in conjunction with each other. Dynamical-statistical downscaling essentially downscales a coarse resolution GCM through the use of a finer scaled RCM (dynamical approach), and then further downscales the RCM using statistical equations based on local scale relationships for finer resolution climate outputs (statistical approach). Dynamically downscaling an RCM provides more precise climate predicters that can be further improved through statistical downscaling to provide finer resolution outputs, ultimately improving the precision of future climate change impacts (Guyennon *et al.* 2013).

2.3 Applying Downscaled Climate Data

The last component of hydrological modelling process is where the downscaled climate data is applied to a hydrological model (stage 4 of Fig. 2.1). Imperfections of hydrological models arise through abstraction and simplification of catchments natural patterns and processes, which themselves are often poorly understood (Bastola *et al.* 2011). Different hydrological models create uncertainty, e.g. catchment scale hydrological models (CHM) and global scale hydrological models (GHM) which contribute uncertainty to the hydrological projection, but not to the extent of uncertainty that a GCM "ensemble of opportunity" may introduce and is often overlooked (Prudhomme and Davies 2009, A). The so-called "cascade of uncertainty" as coined by Schneider (1983), highlights the compounding uncertainty that accumulates through the climate change impact assessment process (Fig. 2.1), as each stage of analysis adds its own unique form of uncertainty to the output credibility. In addition to the assumptions already bestowed on the modelling process through the so-called cascade of uncertainty, the final stage (4) presents further uncertainty. Hydrological modelling presents its own set of local scale assumptions surrounding relationships between catchment characteristics and atmospheric interactions (Section 2.3.1), as well as the role that hydrological model complexity contributes to further increases in future runoff projection uncertainty (Section 2.3.2).

2.3.1 Uncertainties associated with hydrological modelling

All hydrological models are subject to the same two issues, non-linearity and scale. Despite attempts to counteract the association of increased catchment non-linearity with increasing catchment size, which most models aim to do anyway, models are designed to focus mainly on the physical interactions between local scale surface and subsurface runoff, and not the implications of non-linear equations themselves. The problems associated with using non-linear equations to describe water movement through a catchment, are that the calculations do not average simply (Beven 2001), and is essentially another criticism of lumped and semi-distributed models. The disadvantage being that any extremes in equational runoff distribution may be reflected in the observed response of runoff, and not attributed to a response of actual catchment variation.

The problem of scale is inherently linked to that of non-linearity, where even the simple assessment of rainfall distribution is more difficult as the catchment area increases. As hydrological models have different grid scales (10 m to 10 km) which are generally smaller than land surface parameterisations (5 km to 100 km) such as Numerical Weather Prediction (NWP) and GCM models, there can be a disparity between the resolutions of parameter values

on a sub-grid scale. The implication of having data points for parameters larger than the resolution of a hydrological model means at the sub-grid scale the actual parameter values could vary, decreasing precision of catchment data. There is a failure among researchers to develop a scale consistent reconstruction of hydrological processes to describe the influences on observed runoff that are derived from sub-grid scale heterogeneity and nonlinearity (Beven *et al.* 1995; Bloschl 2010). The principles of scale that arise in most hydrological models are known in a qualitative manner, not quantitative, and therefore the principles are general, and applying them to model equations is made all the more difficult because models are usually applied to a particular catchment, where each catchment as mentioned has its own level of complexity.

2.3.2 The role of hydrological model complexity

Hydrological models are classified based on model input variables, parameters and the extent of physical principles applied in the model (Devi *et al.* 2015). Hydrological models can be classified as either deterministic or stochastic (Beven 2001; Abbott and Refsgaard 1996). The main differences between the two classifications is one allows a single outcome based on one set of parameter values (deterministic), and the other permits randomness of the outcomes (stochastic), associated with the uncertainties of the input variables (Gosling *et al.* 2011). There are two main approaches to simulating spatial variation in hydrological processes within deterministic models (the most common), lumped and distributed (Breuer *et al.* 2009; Beven 2001). Lumped models only account for part of the hydrological pathways, mainly the catchment as a whole and the aquifer as a separate unit from the land surface, and not accounting for sub-catchment variations. A lumped model regards hydrological pathways as a single unit and represents variables as an average across the catchment e.g. average storage of water in the saturated zone is assumed spatially constant across the entire area (Gosling *et al.* 2010). Due to such assumptions being about spatial diversity, a lumped models inability to recognise spatial diversity of hydrological processes (Moradkhani and Sorooshian 2008), including variations in land use/cover and soil properties, may be a considerable limitation (Gosling *et al.* 2010). Therefore, the distributed hydrological model can be considered more representative of the diverse spatial nature of catchments, as the model recognises variation in data sets by dividing the entire catchment's parameters into small units (Devi *et al.* 2015) e.g. land use, soil, vegetation, canopy interception and other inputs like sub-units and grid cells (Abbott and Refsgaard 1996).

Table 2.1*:* Characteristics of empirical, conceptual and physically based hydrological models, sourced from Devi *et al.* (2015).

Empirical model	**Conceptual model**	**Physically based model**
Data based on metric or black box model	Parametric or grey box model	Mechanistic or white box model
Involve mathematical equations, derive value from available time series	Based on modelling of reservoirs and include semi empirical equations with physical basis	Based on spatial distribution, evaluation of parameters describing physical characteristics
Little consideration of features and processes of system	Parameters derived from field data and calibration	Require data about initial state of model and morphology of catchment
High predictive power, low explanatory depth	Simple and can be easily implemented in computer code	Complex model, requires human expertise and computation capability
Cannot be generated to other catchments	Require large hydrological and meteorological data	Suffer from scale related problems
ANN, unit hydrograph	HBV model, SWAT	SHE or MIKESHE model, TOPMODEL
Valid within the boundary of given domain	Calibration involves curve fitting make difficult physical interpretation	Valid for wide range of situations.

Another important classification to make is whether the hydrological model is empirical, conceptual or physically based (Table 2.1). Empirically based models are statistically driven, whereby the model does not take into account the nature and complexity of the hydrological system, only accounting for existing data such as observations of rainfall (Devi *et al.* 2015). The basic principle being that the use of empirical input and output time series data to drive

mathematical equations, presents the limitation of assuming water balance is heterogeneous, where in reality most catchments if not all are heterogeneous. Therefore, as empirical models are only driven by the statistical relationship between input and output data time series, calibration isn't able to refine the model's ability to simulate runoff, as there are no catchment parameters to calibrate.

Conceptual models combine both semi empirical equations and physical time series data, with the ability to calibrate model parameters with field data, and model curve fitting of simulated and observed runoff (Devi *et al.* 2015). Conceptual models generally describe all the interconnected hydrological processes that govern water balance, including recharge components; rainfall, infiltration, percolation and removal components; evaporation, runoff and drainage. Most conceptual models come with varying degrees of complexity, where often the more complex the model the more likely the model requires large amounts of meteorological and hydrological data to run and calibrate. Daily or monthly discharge hydrographs between observed and simulated runoff is often compared visually and can present interpretation challenges such as differences in seasonal variation, where one season could replicate runoff well, and another poorly, a problem associated with all types of models. To aid visual comparisons between observed and simulated data, model performance can be analysed statistically using NSE vales and r-values similar to most other models. Some conceptual hydrological models such as HBV have proven to be very cost effective compared to field work, computationally inexpensive to run and can operate on most continents (Bergstrom 2006, Clark *et al.* 2008).

The most comprehensive of hydrological models are physically based. Such models have been described as mechanistic, as they include idealised scenarios of physical catchment processes, to portray mathematically idealized representation of runoff (Devi *et al.* 2015). The main difference between physical and conceptual hydrological models are the input data required, where unlike conceptual models, physically based models can be calibrated with comparatively smaller hydrological and meteorological data, as the majority of input parameters are real-world physical values from within a catchment. However, as there are more variables needing values at higher spatial and temporal resolutions to be able to calculate spatio-temporal variation in these processes, the time taken to fill the data requirements can be immense depending on the model (Abbott *et al.* 1986). The tendency of physical models to require large amounts of input data (many different physical parameters from within a catchment) allow

them to overcome deficiencies that conceptual and empirical models may face because the parameters are open to physical interpretation, meaning that parameter values have to be calibrated and not raw input data. The main benefit of a hydrological model having the use of physical parameters stem from the input data being a representation of measurable changes in both space and time, therefore changes in actual hydrological and meteorological records can be replicated within the model. A second benefit of the variability of input parameters allows physical models to be applied outside of the catchment boundary originally calibrated for, and can be used for a wide range of situations (Abbott *et al.* 1986).

Distributed models can be applied to spatial scales from a grid cell resolution of a few tens of metres e.g. small basins and urban settings (Cuo *et al.* 2008), to medium sized catchments using catchment scale hydrological models (CHMs), up to a global scale using global hydrological models (GHMs) (Doll *et al.* 2003). Representation of precise hydrologic variables such as soil water, groundwater, snow/ice or river channel losses usually vary between models of scale. CHMs are able to represent parameter impacts with higher accuracy due to more confident representation of catchment resources through spatial grids, than that of GHM's (Gosling *et al.* 2010). Distributed models display elements of complexity. Fully distributed models are most complex (e.g. TopNet, Clark *et al.* 2008; MIKESHE), typically dividing the catchment into spatially even grids (Abbott *et al.* 1986; Collischonn *et al.* 2007). However, such detailed models have been questioned as to the reliability of the input parameters as they are based on theory (Breuer *et al.* 2009). The problem with theory being that assumptions made about hydrological parameters in nature are linear, where in reality they are non-linear (Beven 2001). Less complex semi-distributed models (e.g. HBV, Bergstrom 1976; SWAT) simulate all the hydrological processes within spatially non-explicit Hydrological Response Units (HRU) (Arnold *et al.* 1998). The HRU is the smallest spatial unit of the model, and the standard HRU definition approach lumps all similar land uses, soils, and slopes within a sub-basin based upon user-defined thresholds. Each HRU is then lumped together within sub-catchments and routed downstream (Gosling *et al.* 2010).

2.4 Uncertainty of input data

Inputs of precipitation data are critical for any hydrological model no matter the sophistication of the model or calibration of other parameters (Beven 2004). Assessing the degree of spatial and temporal uncertainty in precipitation data is most commonly achieved through analysing

the sensitivity of output data to other input parameters (Segond *et al.* 2007). Therefore, inaccuracies in rainfall interpretation could cause a failure to observe variation within other input parameters during calibration that are dependent on precipitation (McMillan *et al.* 2011). Furthermore, precipitation within a catchment can vary drastically due to climate conditions and location to large topographical features, making precipitation lapse rates difficult to measure. The most commonly used method to obtain precipitation data is using point rain gauges. The cheaper of methods for collecting raw precipitation data, which is still relied on by flood forecasting hydrological applications and gauged catchments, but only allows for precise quantitative data at a specific rain gauge. Areas of a catchment not covered by rain gauges are estimated between stations, and therefore certain areas of catchments both large and small, depending on the density of rain gauges, remain a source of uncertainty (Moulin *et al.* 2009).

Temperature data used for running a hydrological model can also be a large source of uncertainty if incomplete records are kept, or if the climate station used for a particular study is located at the end point of the catchment, especially if the catchment is Alpine in nature. Hydrological models with a snow accumulation threshold factor rely on temperature data to calculate how much precipitation is occurring as snow when temperatures reach freezing points, and how much of the snowpack is lost when temperatures are above the set melt point. If the temperature data is sourced from lower in the catchment the actual temperature higher up in the head waters may be lower, meaning more precipitation would be occurring as snow than what is projected by the model, where there will be a miss-match between the observed and simulated from the outset.

Actual Evapotranspiration (AET) is the total terrestrial and oceanic evaporation, plus the total plant transpiration to the atmosphere, where evaporation drawn from the soil, vegetation canopy, and all waterbodies are incorporated (Penman 1948). Transpiration is the movement of water through a plant, where water is lost as vapour through the stomata (Cummins 2007). Potential evapotranspiration (PET) is the maximum loss of water vapour that would be possible under the ideal conditions, e.g. a continuous area of vegetation, and no shortage of water (Gangopadhyay *et al.* 1966). The two differences between AET and PET are: AET has two processes, evaporation of water from the soil, and transpiration from the leaves of plants. PET is characterised by McKenney and Rosenberg (1991) as a mass transport process driven by the vapour pressure gradient of the surrounding atmosphere, and is limited by both energy (solar

radiation) and water availability (precipitation) (McMahon *et al.* 2013). Robust estimations of evapotranspiration (ET) are paramount as ET is often a substantial source of uncertainty where most global and catchment scale hydrological models use PET for estimation, as ET can be constrained by available soil moisture content (Arnold *et al.* 1998; Arnell 1999). Therefore, assessing hydrological change is dependent on understanding PET dynamics, and currently, there are over 50 different methods of doing so (Lu *et al.* 2005).

The most common method of estimating PET is Penman-Monteith, recommended by The United Nations Food and Agriculture Organisation (FAO) (Allen *et al.* 1998), the American society of Civil Engineers (ASCE), and by the European Union (EU), as the metrological variables that control PET: Solar radiation, temperature, humidity and wind, are adequately accounted for. The Penman-Monteith method accounts for temperature as an average of the daily minimum or maximum air temperature in degrees Celsius (˚C). If minimum or maximum air temperature is not available, the mean air temperature can be used; however, can have a lower reference evapotranspiration estimate. Solar net radiation is taken as an average in mega joules per square metre per day (MJ m^{-2} day^{-1}). As net radiation is not commonly recorded directly, net radiation is calculated using an average of the incoming shortwave radiation that is measured using a pyranometer, or by taking an average of sunshine hours per day that is measured with a Campbell-Stokes sunshine recorder. Clearly problems can arise when estimating radiation through natural occurrences of atmospheric change such as cloud coverage. The Penman-Monteith method requires daily actual vapour pressure (kPa), and in the absence off, can still be derived from relative humidity percentages, or dry and wet bulb temperatures (˚C). Wind speed for the Penman-Monteith method are recorded as a daily average (m s^{-1}) at 2 m from the surface, as speeds between the soil and measuring device can vary. The large amount of data used to run the equation is both a strength and a weakness, as it accounts for all variables associated with evapotranspiration, but input of the data is incredibly time consuming. Another weakness of the Penman-Monteith equation is the large emphasis on evaporation in a water balance equation, but measuring evapotranspiration is weak and is not as precise as directly measured components such as precipitation and stream flow. In addition to weather variation, the equation is sensitive to both stomatal resistance and conductance (Beven 1979), as a multitude of vegetation in a catchment is difficult to conceptualise accurately.

Estimating PET for hydrological modelling is important because of the uncertainty already surrounding the parameter. The recommended use of the Penman-Monteith methods by the FAO is constrained by large data requirements, dependence on numerous parameters, i.e. maximum and minimum temperature, vapour pressure, net radiation and wind speed (Tilahun 2006; Fooladmand *et al.* 2008) and when data is limited, other PET estimation methods must be explored (Moeletsi *et al.* 2013). Since the Penman-Monteith equation is a net radiation based method, other radiation methods with less intensive data requirements such as Makkink, Ritchie-type and Priestley-Taylor could be implored (Pereira and Pruitt 2004; Berengena and Gavilán 2005), but in the absence of radiation (cloud cover), temperature-based models could substitute efficiently, e.g. Hargreaves and Samani, Thornthwaite or the Blaney-Criddle equations (Pereira and Pruitt 2004; Berengena and Gavilán 2005).

2.5 Calibration uncertainties

Conceptual hydrological models, such as HBV have proved to be a cost-effective alternative to physical field studies and can operate on most continents (Bergstrom 2006). A key part of a functioning hydrological model is the calibration process, which aims to limit model uncertainty, however, calibration processes impose their own form of uncertainty. Calibrating a hydrological model is the trial and error process of determining appropriate parameter values based on a comparison of simulated and observed flow (Cao *et al.* 2006) by manipulating key or single parameters to assess the simulated runoff response (Gupta *et al*. 1998; Anderton *et al.* 2002). It has been suggested that calibration processes for spatially distributed hydrological model has the potential for equifinality (Beven 2001; Cao *et al.* 2006), although true for all models, equifinality becomes more of an issue for complex models as greater combinations of parameter sets can produce acceptable results. The implication of equifinality is of importance to physically based models as their distributed structure requires a large number of parameters, all of which need to be calibrated and therefore can be computationally expensive and time consuming. To offset such problems, automatic calibration techniques have evolved like the use of a Monte Carlo approach, however the parameter sets settled upon can be unrealistic of real-world catchment values unless constraints (if known) for parameter values are set. If real-world catchment parameter values are unknown, the uncertainty of model values and their acceptability becomes less uncertain.

Calibrating a hydrological model sets it up for a stationary catchment, where in fact no hydrological catchment is linear or straight forward. Calibration takes time, as each individual parameter must be tested by changing others to see how the goodness of fit (such as the Nash Sutcliffe Efficiency value) reacts. A well-defined parameter value with a high goodness of fit (closer to 1 than 0) between the modelled discharge and the observed can change in response to changes made to a single parameter. Likewise, if a good simulation is achieved using a wide range of parameter values, a single parameter may not be as well defined or realistic of catchment values, casting uncertainty surrounding the observed verse simulated goodness of fit that can increase even with unrealistic input parameter values (Seibert 1997). In ungauged catchments (no recorded data), the input data is estimated or assumed, and therefore there has to be confidence in the input data to accept the output data (Bergstrom 2006).

2.6 New Zealand specific impact assessment

The use of TopNet in New Zealand spans a wide range of hydrological modelling applications, including operational flow forecasting (McMillan *et al.* 2013; Ibbitt *et al.* 2005), the impacts of future climate change on catchment runoff (Gawith *et al.* 2012; Poyck *et al.* 2011; Srinivasan *et al.* 2011; Woods *et al.* 2008), and current national water accounting (Henderson *et al.* 2011). On impacts of climate change to future runoff, a consistent trend across New Zealand using a 12 GCM ensemble suggests that under the IPCC SRES A1B 'middle of the road' scenario (IPCC 2000), precipitation and temperature will increase for both 2040 (2030-2049) and 2090 (2080-2099) time periods (MfE 2008; Poyck *et al.* 2011; Srinivasan *et al.* 2011; Gawith *et al.* 2012). As a result, the contribution of snowmelt to runoff is expected to decrease in spring with increased temperature. However, despite less meltwater contributing to spring runoff, the future runoff is expected to increase in winter and spring as a result of higher precipitation totals and less snow storage (Poyck *et al.* 2011; Gawith *et al.* 2012).

The first paper to explore the use of TopNet as a freshwater modelling tool for the Clutha Catchment was Poyck *et al*. (2011). Three periods were investigated using TopNet: the calibration period (1980-1999), and two future periods (2030-2049, and 2080-2099). The model was calibrated using streamflow data from three areas of the catchment (Balclutha, Matukituki and the Lindis) recorded over 20 years and recorded a weekly NSE of 0.90 (Balclutha), 0.81 (Lindis) and 0.86 (Matukituki). Future periods were run using a "middle of the road" (A1B) emissions data set from the IPCC Fourth Assessment Report. The results

showed there to be an increase in annual streamflow of around 6% in 2040, and 17% in 2090 (Poyck *et al.* 2011), where the main focus of the research looked at climate change impacts to the snow pack and the resulting effects to runoff.

A study very similar to Poyck *et al*. (2011) was conducted by Gawith *et al.* (2012). TopNet was run for the Lindis and Matukituki catchments also, with monthly NSE values of 0.69 and 0.68 respectively over a 20-year observed period (1980 to 1999). When run for future climate change impact assessment, the authors used the same ensemble of GCMs as Poyck *et al.* (2011) and utilised the SRES A1B emissions scenario also. The results showed that there was a projected mean annual runoff increase of 7 % in 2040 and 12.8 % in 2090 for the Matukituki Catchment, and larger increases for the Lindis Catchment of 10 % in 2040 and 20.4 % in 2090. An example of TopNets other performance runs in New Zealand is demonstrated in Ibbitt *et al.* (2005) where researchers ran the model for 14 river basins with previous observed flood data, in different climate regimes. Ten out of the 14 rivers studied showed medium to good accuracies (r^2 = 70-90%).

As evident, the use of the relatively complex model TopNet in New Zealand has worked reasonably well, returning good NSE and daily hydrograph replication between observed and simulated data (Gawith *et al.* 2012; Poyck *et al*. 2011; Srinivasan *et al.* 2011; Woods *et al.* 2008). TopNet has successfully been used to model a range of different functions focused around how New Zealand's freshwater is used and how it could be impacted by future changes to the climate, but performance against other models is rarely assessed. The complexity and time-consuming nature of TopNet could warrant the use of a simpler model like HBV-Light that has been used successfully in a small number of New Zealand studies (Koedyk and Kingston 2016), to essentially assess the same thing.

2.7 Research Justification and Summary

In New Zealand, the possibility of using a relatively simple hydrological model to perform essentially the same climate change impact assessment task as more complex hydrological models, essentially due to time and data constraints, is currently underexplored (Devi *et al.* 2015). To assess and comment on the respective runoff outputs between a simple conceptual model to simulate future runoff under climate change conditions, and a complex one, it is advised to quantify, if possible, the magnitude of uncertainty inherently associated with all

aspects of hydrological modelling. The scope of research generally undertaken in New Zealand when assessing the potential impacts that climate change could have on freshwater resources, and the uncertainty associated with such investigations, primarily focuses on GCM and climate related uncertainty (Srinivasan *et al.* 2011; Poyck *et al.* 2011; Gawith *et al.* 2012), neglecting model related uncertainty. On a larger scale, Prudhomme and Davis *et al.* (2009, A) suggest hydrological model induced uncertainty is also overlooked in impact assessment research undertaken across the world.

It has been suggested by Gosling and Arnell (2011), and Haddeland *et al.* (2011), that when using the same climate forcing scenario, the runoff simulation for a future time period may differ when assessed with alternate hydrological models, even if the respective models produce an acceptable result of an observed baseline period. The reason for lack of research surrounding hydrological uncertainty, and the use of alternative models over the same catchment, as suggested by Thompson *et al.* (2013), is that different models are invariably developed for different purposes, by different institutions, and rarely used for assessing the same climate change scenarios. The few researchers that have explored uncertainties associated with impact assessment studies (Dibike and Coulibaly 2005; Haddeland *et al.* 2011; Hagemann *et al.* 2012) have all suggested model-derived uncertainty may not be negligible, and therefore is an area of research that needs to be explored when undertaking model comparisons in New Zealand.

It is argued that even complex hydrological models like TopNet do not provide better results, and the use of other distributed models such as the variable infiltration capacity model (VIC), HBV-Light, MIKESHE and SWAT, could prove valuable for time and data constraints of future research (Devi *et al.* 2015). The fully distributed hydrological model TopNet (Clark *et al.* 2008) was developed by the National Institute for Weather and Atmosphere (NIWA) and is New Zealand's first national-scale water resources simulation model. Using TopNet, NIWA has successfully produced the most detailed national-scale water resources map to date, however, running and calibrating the model can prove difficult (Clark *et al.* 2008), and as TopNet was developed and is owned by NIWA, access to it is difficult, and not always granted. Use of the semi-distributed hydrological model HBV-Light (Seibert and Vis 2012) to assess the impact of climate change on freshwater catchments in New Zealand is limited and very much in its infancy, where the same could be said about most other models compared to the extensively used TopNet. However, the parent model of HBV-Light (HBV) has been proven

suitable for use in over 30 different countries, spanning most continents (Vehvilainen and Lohvansuu 1991; Vehvilainen and Huttunen 1997; Saelthun *et al.* 1998; 1999; Graham 2000).

Furthermore, certain hydrological models perform better in different environments compared to others. Catchments with well-defined boundaries both vertically and laterally with accurate records of precipitation and climate records with a small amount of threshold driven processes would expect higher model performance (McMillan *et al.* 2016). Therefore, due to New Zealand's diverse scales of geology, topography and the resulting climate complexity (Snelder and Biggs 2002), catchments such as the Shotover provide exemplary opportunities to assess model strengths and weaknesses, as such controls on catchment runoff should be strongly replicated through model performance (McMillan *et al.* 2016). If the HBV-Light model can reproduce observed runoff to similar or the same standard previously shown by TopNet, this research will provide confidence for the use of HBV-Light in simulating the future implications posed by climate change to New Zealand's hydrological catchments. If proven useful, the applicability of this research will benefit scientists, conservational institutes, regional councils and students alike. The accessibility and simplicity of the hydrological modelling software HBV-Light in assessing future climate change impacts on New Zealand's freshwater resources, will provide further understanding and knowledge surrounding potential effects to catchment characteristics.

Chapter Three
Field Area and Methods

The Shotover Catchment was chosen for this research as it provided three unique characteristics. Firstly, it is located in New Zealand's largest Catchment, the Clutha, which drains snowmelt from the Southern Alps for large parts of the year, and as it is parallel to the main divide of the Alps, is subject to a very complex climate (Section 3.1 & 3.4). Secondly, the research's second aim focuses on the comparison of HBV-Light and TopNets simulated runoff output, where TopNet has be shown to perform well in the Clutha, Lindis and Matukituki Catchments (Section 2.6), and therefore provides substantial insight into positives and negatives of TopNet in similar catchments like the Shotover. Thirdly, the Shotover Catchment has many hydrometric and climate stations situated throughout, providing a reasonable time period of overlapping catchment variables to run HBV-Light with.

The following chapter has 9 sections (3.1 to 3.9) followed by a summary of the Chapter (3.10). Sections 3.1 to 3.4 details the geology, topography, soil composition, land cover, climate and hydrology of the Shotover Catchment. Section 3.5 explains the differences between the input data used to run both hydrological models and attempts to quantify the uncertainty that is introduced by the input data used i.e. point source data verse interpolation. Section 3.6 details the climate change emissions scenario used in this research and how the data was used. An overview of the hydrological models HBV-Light and TopNet are presented in Sections 3.7 and 3.8 respectively and why TopNet was chosen as the model of comparison is explained. Section 3.9 details the calibration procedure undertaken by this research, and what techniques were chosen to justify the use of HBV-Light to model future impacts of climate change on freshwater within the Shotover Catchment.

3.1 Geology and Topography

The Shotover catchment has a total area of 1078 km^2 (Hicks *et al*. 2011), situated east of the main divide, separating the drier Central Otago region and the West Coast of New Zealand (Fig. 3.1). The Shotover River is deeply entrenched in a steeply walled valley except for the

uppermost and lowermost reaches which open out into wide shingle beaches, and is primarily controlled by the Harris Mountain range in the east of the catchment and the Richardson Mountain belt to the west, both aligned in a north to south orientation. Capping the upper Shotover catchment in the north is Mt Tyndall (2496 m) and Headlong Peak (2510), the second and third highest peaks within the catchment boundary. Much of the valley's structure is geologically controlled by the steep-walled (20-50˚), predominantly schist, Richardson and Harris Mountains, that align the river channel in a north-south alignment, with a Strahler stream order of 6. The Shotover has a mean annual flood flow (based on observed records at the Bowen Peaks site from 1967 to 2002, Fig. 3.1) of 420 $m^{3/s}$, with a range of 150 to 918 $m^{3/s}$ **(**Shotover Country – Plan Change 2010).

The Shotover catchment's elevation ranges from 300 m at the outwash confluence with the Kawarau River, to 2525 m (Centaur Peak) in the north-west, a part of the Richardson Ranges. Nineteen percent of the catchment area lies above 1500 m, 66 % lies between 900 m and 1500 m, and the remaining 13 % between 300 m and 900 m (National Water and Soil Conservation Organisation 1977). The drainage pattern of the Shotover River is considered to be a 'Trellis' formation, as such structures tend to form between parallel, elongated landforms, often with regular tributary junctions forming at right angles, indicating geometric control of underlying structures (Bloom 1972; Clark *et al.* 2004). The two constraining mountain ranges have been significantly incised by tributaries draining west-east (Richardson Range) and east-west (Harris Range), including lower Stony Creek, Flood Burn, Sixteen Mile Creek, Glencairn Creek, and Moonlight Creek.

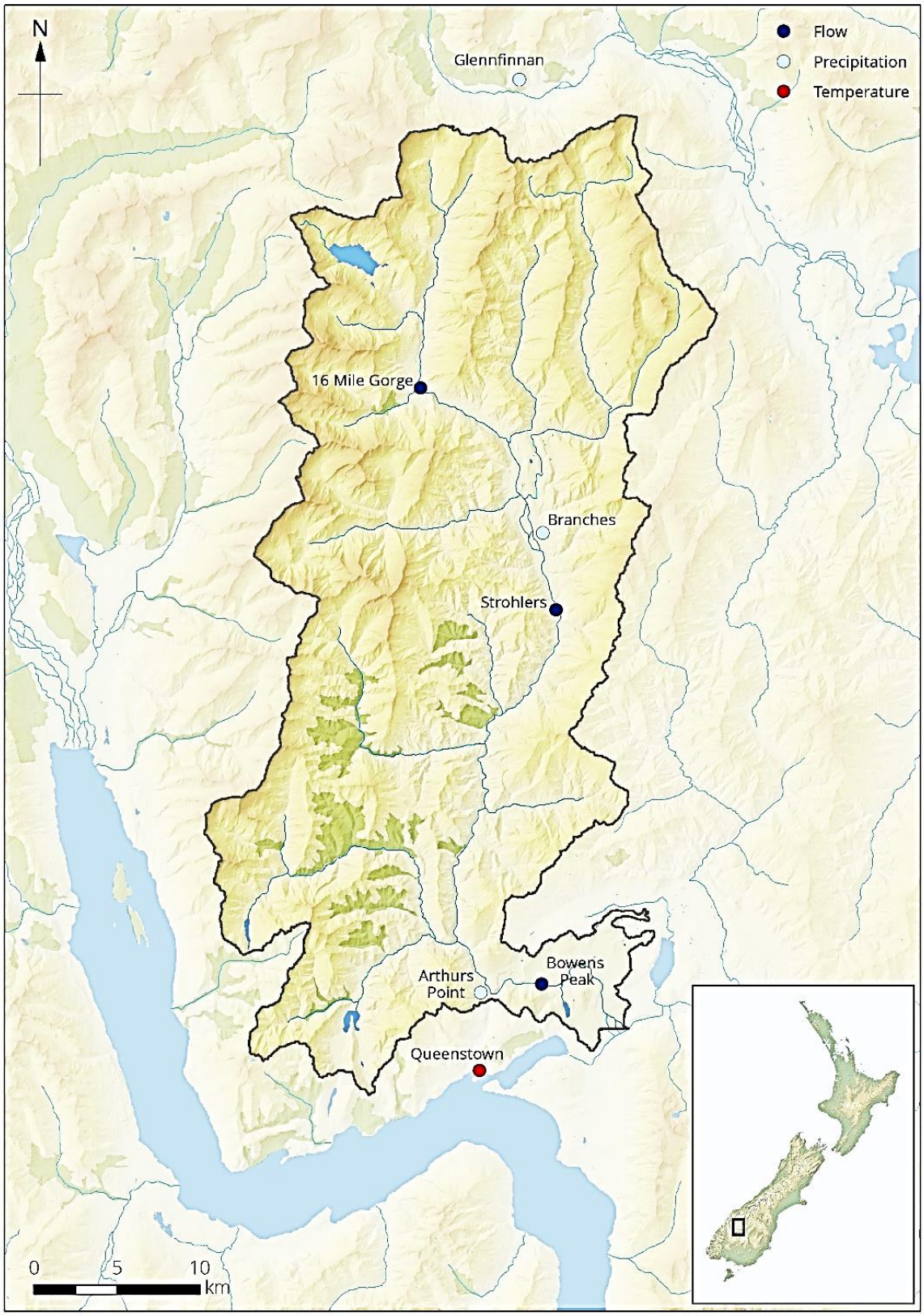

Figure 3.1: *Map detailing the Shotover Catchment, near Queenstown, New Zealand. Listed on the map are possible climate stations that were and could have been used to construct an observed climate time series with which to run the HBV-Light hydrological model.*

3.2 Soil

The general soil trend (Fig. 3.2) from the bottom of the catchment (southeast) to the top (northwest) transitions from yellow-grey earths, through to yellow-brown earths, and higher up in the catchment to podzolized yellow-brown earths (Soil Bureau Bulletin 27 1968). Yellow-grey earths are associated with low elevation areas prone to drought (450–650 mm^{-yr}) with average temperatures of 6–8.8 ˚C, whereas yellow-brown earths are thought to be more acclimatised to cooler (4.5–6 ˚C), wetter climates (600–900 mm^{-yr}) observed at higher elevations (Brash and Beecroft 1987). Above 1800 m, scree slopes, bare rock and small areas of alpine soil occupy 13.4% of the catchment as slope steepness prevents hillside accumulation of vegetation, and exposed rock is weathered by intense frost action (McCraw 1956; 1966), fuelling scree aggregation. The majority of soils in the Shotover catchment comprise of upland and high-country yellow-brown earths, in the form of Moonlight and Dunstan steepland soils which are predisposed to erosion. Such soils are generally considered loose and friable as they are developed on slopes of more than 30˚, and once lost, are very difficult to replenish (McCraw 1966). The lower reaches including Branches, Moonlight, Skippers and Sixteen Mile Creek areas are comprised of yellow-grey earths like Nevis and Teviot soils, similar to the properties of the yellow-brown Moonlight and Dunstan soils, however are less exposed to erosion as these catchments are flatter, e.g. terraces and rolling hills (McCraw 1966).

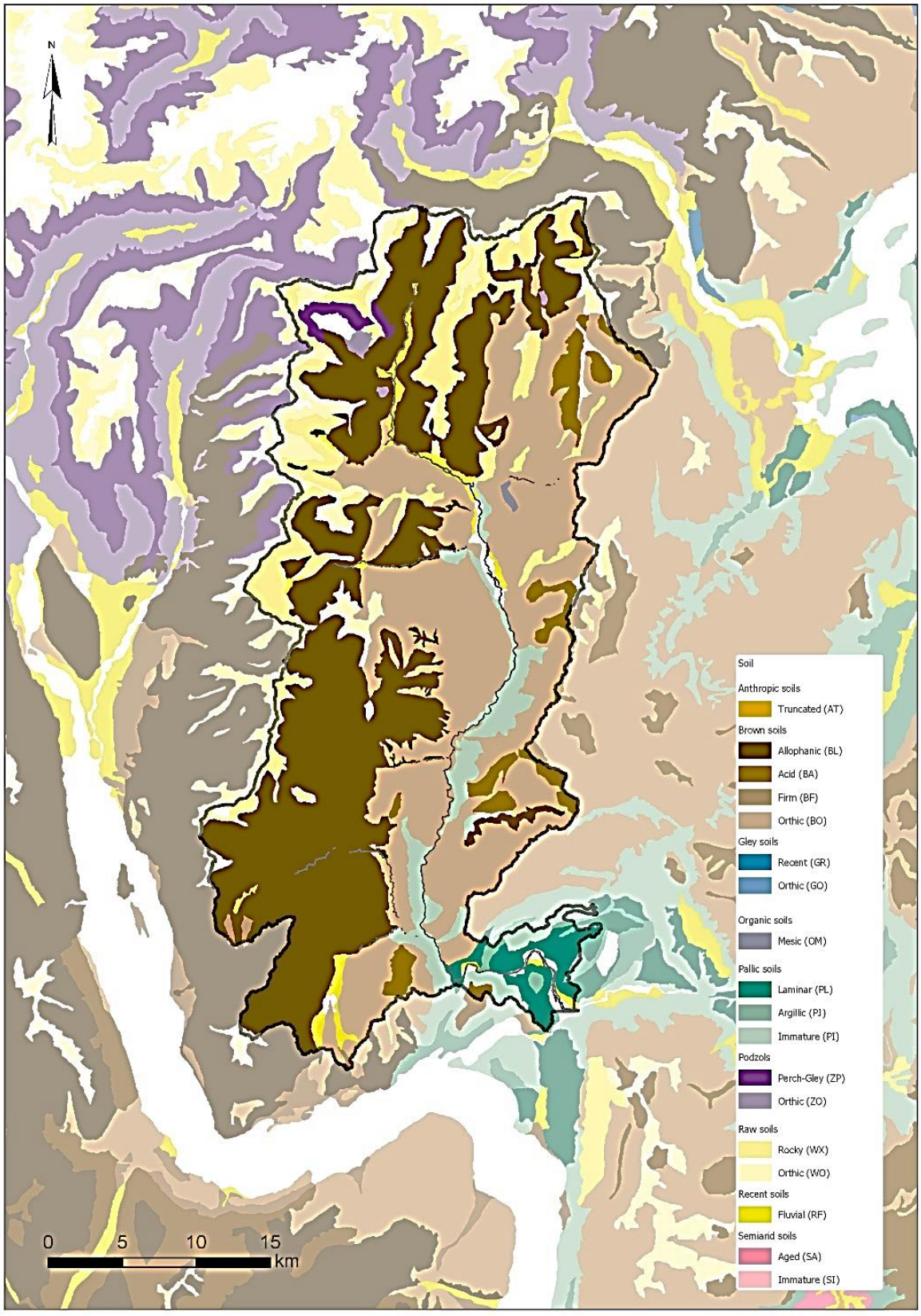

Figure 3.2: *Soil map of the Shotover Catchment, New Zealand.*

3.3 Land cover

The dominant vegetation types of the Shotover Catchment (Fig. 3.3) are grassland, subalpine scrub and scattered distributions of mountain beech forest (*Nothofagus solandri var. cliffortioides*) up to 1000 m with an extreme limit of 1200 m. There are three main types of grassland present in the Shotover; snow tussock, low grassland tussock and sward grassland. Higher up in the catchment snow tussock (*Chionochloa rigida*) is completely dominant between 900 and 1800 m, but in some cases down to 600 m in the shady northwest side (Biggs *et al.* 1990). Manuka shrubland (*Leptospermum scoparium*) was also dominant below 900 m during the early 1960s, however, now occupies a considerably smaller portion of the mid to lower catchment though to be due to the introduction of manuka blight between 1961 and 1975. Through to the present, mainly due to burning and grazing lower down in the catchment (< 900 m), low tussock grasslands have taken over, predominantly in the form of hard tussock (*Festuca novae-zelandiae*), however, blue tussock (*Poa colensoi*) is thought to dominate in small areas where conditions are favourable, anywhere up to 1700 m. Subalpine shrub in the dominant form of *Dracophyllum uniflorum* also occurs up to 1700 m on the northern side, mainly in the shady aspects of the catchment (McCraw 1956). In the lower parts of the catchment sward grasslands in the form of browntop (*Agrostis tenuis*) replace low tussock grassland, predominantly from the Flood Burn and Shotover confluence (< 600 m) and lower (McCraw, 1966).

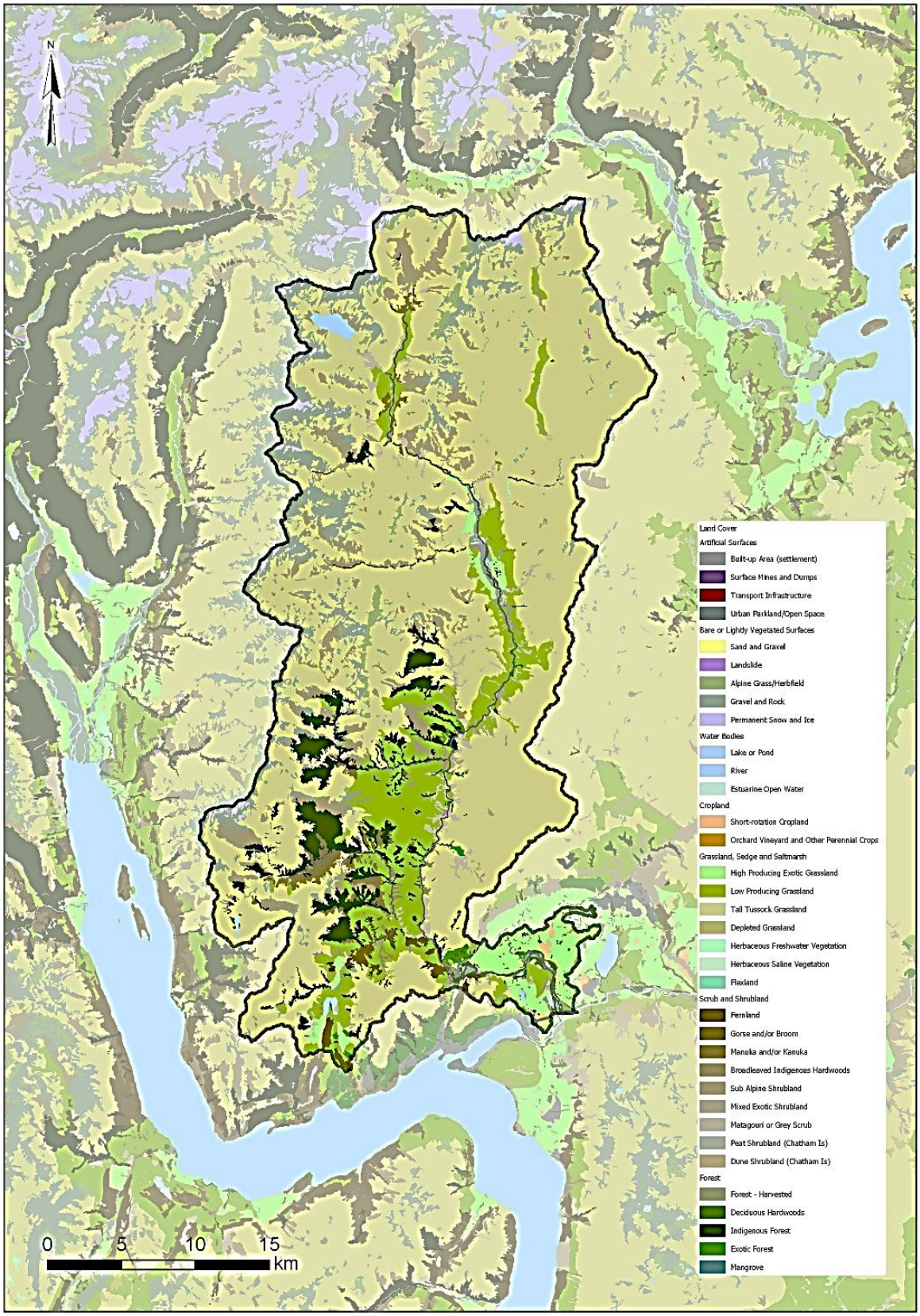

Figure 3.3: *Land cover map of the Shotover Catchment, New Zealand.*

3.4 Climate and Hydrology

Due to moisture laden north-westerly trade winds, in conjunction with orographic uplift, parts of the Shotover (mainly the north-west) can receive an average annual rainfall of 7500 mm/yr-1 in the upper reaches of the catchment (Tait *et al*. 2006). The lower catchment to the east of the main Southern Alps divide receives around 500 mm/yr^{-1} in the mid-lower reaches, however, some estimates for the north-east of the Shotover catchment suggest an annual average in excess of 5100 mm/yr^{-1}, thought to be associated with a spill over effect (Fitzharris 2004). The 20-year (1980 to 1999) monthly average for precipitation ranges from 67.3 mm in September to 93.7 mm in October, however precipitation is relatively constant throughout the entire year (Fig. 3.4). The 20-year average for monthly temperature ranges from 1.7°C in July to 14.1°C in January, with temperatures uniformly decreasing from January through to mid-winter in July and then continually increasing through to January again (Fig. 3.4). The 20-year average for monthly runoff depicts July having lowest with 62.9 mm and October to have the highest runoff with 136.7 mm (Fig. 3.4).

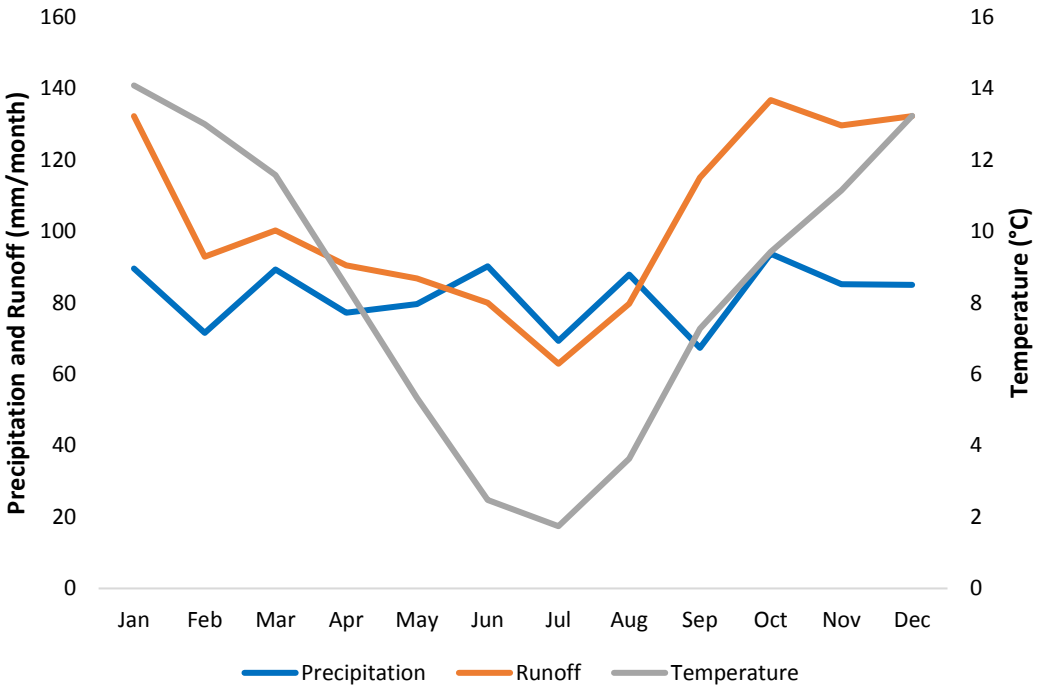

Figure 3.4: *Average monthly observed data (1980 to 1999) for precipitation, runoff and temperature from within the Shotover Catchment, Queenstown, New Zealand.*

3.5 Input data

The majority of hydrology based climate change impact assessment research typically uses models that have been calibrated based on 20-years (1980-1999) of observed data (e.g., Poyck *et al.* 2011; Srinivasan *et al*. 2011; Gawith *et al.* 2012). The challenge of establishing sufficient meteorological and hydrological data sets that coincide with each other over an extended period of time can be difficult (Table 3.1). Accurate overlapping physical records of precipitation, discharge and temperature in mountainous areas such as the Shotover are hard to establish, as the logistics and maintenance of recording and therefore quantifying such material is complicated, requiring considerable resource. A continuous data set between 01/01/1972 and 31/12/1997 (26 years) was compiled for daily precipitation, catchment discharge, temperature and PET. Precipitation and discharge were measured in the Shotover catchment at Arthurs Point and Bowens Peak respectively (Fig. 3.1). The mean minimum and maximum temperatures were obtained from the NIWA climate station at Queenstown, about two kilometres outside of the Shotover catchment. PET was calculated by the Hargreaves method using daily records of the climate variables precipitation, from Arthurs Point, and minimum and maximum temperature from the Queenstown record.

Table 3.1: Locations and recordable variables used as input data to run the HBV-Light hydrological model.

	Network Number	***Variable***	***Operating length***	***Station Operator***	***Latitude***	***Longitude***
Queenstown	I58061	Mean, Max and Min Temperature (˚C)	01/01/1972-Current	N.I.W.A.	-45.034	168.663
Bowens Peak	75276	Runoff (mm/day)	29/06/1967-Current	O.R.C.	-44.996	168.639
Arthur's Point	I48961	Precipitation (mm/day)	01/03/1966-31/10/2011	N.I.W.A.	-44.992	168.667

3.5.1 Potential Evapotranspiration

For the Shotover Catchment, insufficient meteorological data was available to calculate PET using the Penman-Monteith equation as there is no record of daily radiation, which is the preferred technique in climate modelling. Therefore, simplified empirical methods that require fewer input values for parameters can be used, depending on the type of land use, soil composition, elevation and latitude of the study site in question (Lu *et al.* 2005). For the Shotover catchment, the Hargreaves PET method (Hargreaves and Samani 1985) was used as the method is based on mean, minimum and maximum temperatures (Allen *et al*. 1998) that

are relatively easy to obtain. Hargreaves PET (mm/d^{-1}) was calculated using the daily mean, minimum and maximum temperatures (˚C) from the Queenstown climate station (Station ID I58061) for the period between 01/01/1972 to 31/12/1997.

3.5.2 Data Quality and Error

The three stations chosen to represent hydrometric and meteorological variables within the Shotover catchment (Table 3.1) had an overlapping time-series of 36 years (01/01/1972 to 31/10/2011). The decision to run HBV for 26 of 36 available years was due to missing data from the Arthurs Point precipitation record. When constructing the continuous daily time-step required to run HBV-Light, it was noted that for the years 2000–01 and 2003–08, that December was missing large periods of precipitation data, with some December months missing up to 15 days, due to the sampling officer being away (NIWA, personal communication).

When using hydrological models, precision of input precipitation is the largest form of uncertainty (Seibert 1997). Therefore, as there is uncertainty as to what the precipitation is at Arthurs Point at certain periods in time between 1998 and 2008, the data was deemed insufficient for the validity of this research, leaving 26 years to be split into two 13-year periods as described in Klemes (1986) split-sample approach, one for calibration purposes (1972-1984) and the other for validation (1985-1997). The model uses a warm up period to allow the initial model conditions to settle out (Seibert 2005). One year (Seibert and Vis 2012) is considered appropriate for a warm up period (1972 for calibration and 1985 for validation), leaving two 12-year periods to run the model with. The Bowens Peak discharge station was missing 4.03% (189 days) of the 26-year record, and temperature was missing 0.01% (two days). The process for remedying missing discharge days was to fill those days with the monthly average for that particular month, as HBV-Light requires continuous input data in order to run. The difference between doing this for discharge and doing it for precipitation is that, discharge in the Shotover is above zero m^{-3} s^{-1} all year round, therefore river flow is constant and backfilling weeks at a time is not advisable. Conversely, there may be long periods with no rainfall, and therefore using the average of a specific month to fill those gaps would give periods (some periods up to two weeks) constant rainfall which is unrealistic, especially in the peak of summer.

3.5.3 TopNet Input Data

The input data used to run TopNet is different from that used to run HBV-Light. Temperature and precipitation data used to run TopNet was obtained from the Virtual Climate Station Network (VCSN) (Cichota *et al.* 2008; Tait *et al.* 2006; Tait and Turner, 2005), while the

Priestley-Taylor method was used to calculate PET also using VCSN data, as the method is not dependant of actual observations of temperature (Clark *et al.* 2008). VCSN data are estimates of daily rainfall, potential evapotranspiration, air and vapour pressure, maximum and minimum air temperature, soil temperature, relative humidity, solar radiation, wind speed and soil moisture on a regular 5 km grid covering the whole of New Zealand since 1972. Finally, the observed discharge used to run TopNet was acquired from the National River Water Quality Network (NRWQN) that is administered by NIWA and the ORC, which is the only input data from the same source as used by HBV-Light.

3.6 Climate Change Data and Method of Use

Climate data and the source of climate change projections can have an effect on the runoff outputs between different models, or when the same model is run with different climate projections. Therefore, it is necessary to detail the source and suitability of the climate change data used in any climate change impact assessment research. The current research used runoff projections from an A1B-forced ensemble of 12 individual CMIP-3 GCMs (MfE 2008) for two future time periods (2030-49 & 2080-99) within the Shotover Catchment to assess the uncertainty associated between individual GCMs and a mean GCM ensemble projection of runoff between HBV-Light and TopNet.

The 23 GCMs outlined in the IPCC (2007) Fourth Assessment report have greater spatial resolution than what was prepared for the Third Assessment (2001), however the resolution when simulating New Zealand climate patterns was still too coarse. Of those 23 GCMs developed by different research institutes in different countries, not all are suitable as viable estimates of any given locations climate. To account for the uncertainty associated with individual GCMs an ensemble of 12 were chosen from a group of 17 deemed by the MfE (2008) to be substantially more accurate when simulating observed climate records in New Zealand. The grid point spacing for the 12 GCMs chosen for downscaling varied between 1.125° to 3.75° in longitude, and 0.56° to 2.5° in latitude at the equator. The 5 models rejected from the original 17 had coarser resolutions with 3 of them having grid spacing up to 5° in longitude.

Due to the large degree of spacing between the grid points of the 12 GCMs, it was necessary to downscale them to incorporate the complexity of New Zealand's topography. Statistical downscaling was applied to the 12 GCMs as described in Mullan *et al.* (2001) as a two-stage

process. First, the relationships between local climate variables are established, e.g. temperature and rainfall on the smaller catchment scale, and atmospheric pressure patterns and spatially averaged temperature on the larger scale. Secondly, the relationships established are applied to predicted GCM outputs allowing simulations of the local climate characteristics. The statistical downscaling algorithm was applied to all of New Zealand at a resolution of 0.05° latitude–longitude boxes, equating to 11,500 grid points over the entirety of the country, indicating the downscaling method is more precise than previous Ministry for the Environment (2004) observational dataset of just 58 temperature sites and 92 rainfall sites.

Table 3.2: The 12 GCMs deemed suitable in representing climate aspects within the New Zealand context. Source: MfE (2008).

Model	Country	Global change from 1990 to 2090-2099 (°C)	Change to 2030–49		Change to 2080-99	
			Global Avg (°C)	NZ Avg (°C)	Global Avg(°C)	NZ Avg (°C)
cccma_cgcm3	(Canada)	3.1	1.47	1.27	2.99	2.69
cnrm_cm3	(France)	2.75	1.3	0.87	2.6	1.83
csiro_mk30	(Australia)	1.98	0.65	0.54	1.84	1.13
gfdl_cm20	(USA)	2.9	1.29	0.82	2.83	1.96
gfdl_cm21	(USA)	2.53	1.31	1.22	2.44	2.16
miroc32_hires	(Japan)	4.34	2	1.35	4.15	3.44
miub_echog	(Germany/Korea)	2.86	1.19	1.12	2.76	2.23
mpi_echam5	(Germany)	3.31	1.09	0.33	3.15	1.75
mri_cgcm232	(Japan)	2.2	0.97	0.71	2.16	2.07
ncar_ccsm30	(USA)	2.71	1.57	1.19	2.63	2.11
ukmo_hadcm3	(UK)	2.9	1.24	0.66	2.79	1.56
ukmo_hadgem1	(UK)	3.36	1.35	1.14	3.22	2.21

The downscaled ensemble of 12 GCMs appear relatively consistent between 1990 and 2090 in their respective changes in temperature (Table 3.2). One group of individual GCMs (gfdl_cm20, miroc32_hires, mpi_echam5, mri_cgcm232) project that the North Island will see faster increases in temperature compared to the South Island. Another group of GCMs (cccma_cgcm3, csiro_mk30, ncar_ccsm30, ukmo_hadgem1) suggest higher temperature increases in the South Island. Another group of GCMs show slightly less agreement to the rest, with two models (csiro_mk30, mpi_echam5) projecting less warming with little to no north-south temperature gradient, while one GCM (miroc32_hires) suggests higher temperature increases across both the North and South Islands.

Once the GCMs are decided upon and downscaled it is then necessary to establish a future emissions scenario to project how the climate will change, according to how the world adapts to energy use and how that impacts the amount of emissions trapping sunlight in the atmosphere, essentially increasing global air temperatures. The IPCC Working Group III (2000) developed a set of 6 climate emissions projections (A1FI, A1T, A1B, A2, B1, B2) known as the IPCC 'SRES scenarios' named after the report (*Special Report on Emissions Scenarios).* The 6 scenarios are based on how technology and energy use could evolve over the next 100 years (1999 to 2099), including the economic growth, global population and technological changes that future development could bring (MfE 2008).

The A1 scenario is developed with rapid economic growth in mind and peak population growth occurring in the middle of the century which declines thereafter, where rapid economic growth is thought to be coupled with rapid technological advances in energy production, and a decrease in regional disparities of income per capita (IPCC 2007). The A1 'family' contains three separate scenarios (A1F1, A1T, A1B) that are based on the worlds potential direction of change to its energy system. The A1F1 scenario describes a future that is still dependant of fossil fuels, and therefore higher emissions. A1T describes an energy system with no fossil fuel use, and therefore potentially no emissions are introduced to the atmosphere other than what is already there. The A1B scenario focuses on a balance between fossil fuels and renewable energy, or potentially an emissions free energy that hasn't been discovered yet.

The A1B scenario is considered a 'middle of the road' emissions scenario (Lopez *et al.* 2011), and therefore is chosen for this research as it encompasses a balanced, albeit realistic outlook on what the worlds energy system could look like in 100 years. Under the A1B emissions scenario the average surface temperature change is projected to increase between 2.0°C and 4.3°C globally from 1999 to 2099, with a best estimate of 2.8°C rise in temperature for the 12 GCMs deemed suitable for the New Zealand context (MfE 2008). The use of an ensemble of 12 GCMs deemed suitable for representing climate aspects in New Zealand's diverse topography in conjunction with the IPCC SRES A1B climate change scenario chosen for this research follows previous standard practice also undertaken by other New Zealand climate change impact assessment studies e.g. Gawith *et al.* (2012) and Poyck *et al.* (2011).

3.7 The Hydrologiska Bryans Vattenavdelning (HBV) model

The semi-distributed HBV (Fig. 3.5) hydrological model can allow the diversification of a catchment into separate elevation and vegetation zones, and between separate sub-catchments (Lindstrom *et al.* 1997). The HBV model (Eqn. 1) began development in the 1970's (Bergstrom 1976) at the Swedish Meteorological and Hydrological Institute (SMHI), where the name HBV was derived from the Hydrologiska Bryans Vattenavdelning unit, originally designed to simulate discharge and pollution for use in Scandinavia (Bergstrom 1995). The original HBV model has since been used on most continents and over a wide range of catchments (Bergstrom 1995), being used for various applications in more than 30 countries, however, its use has mainly occurred in the Nordic countries (Vehvilainen and Lohvansuu 1991; Vehvilainen and Huttunen 1997; Saelthun *et al.* 1998, 1999; Graham 2000).

$$\mathbf{P - E - Q = d/dt\ (SP + SM + UZ + LZ + Lakes)} \qquad \mathbf{(Eqn\ 1)}$$

Where:

P = precipitation
E = evapotranspiration
Q = runoff
SP = snow pack
SM = soil moisture
UZ = upper groundwater zone
LZ = lower groundwater zone
Lakes = lake volume

Since its conception, the model exists in several versions, but the HBV-light model is widely used in education, and was developed at the Uppsala University of Sweden, in 1993 (Seibert and Vis 2012). HBV-Light was created in the hopes of providing a simple Microsoft Windows version for research and education, with only two changes to the original equation of HBV (Seibert 2005). The routing parameter MAXBAS seen in Figure 3.5 as the last routing function before runoff is calculated, has been modified to allow values other than integers, which potentially aides precision of the time it takes runoff to move through the catchment and out to the end point. Secondly, the HBV-Light model uses a warming up period instead of initial states for parameter values. The range of values for HBV-Lights input parameters, and the values settled upon for this research can be seen in Table 3.3.

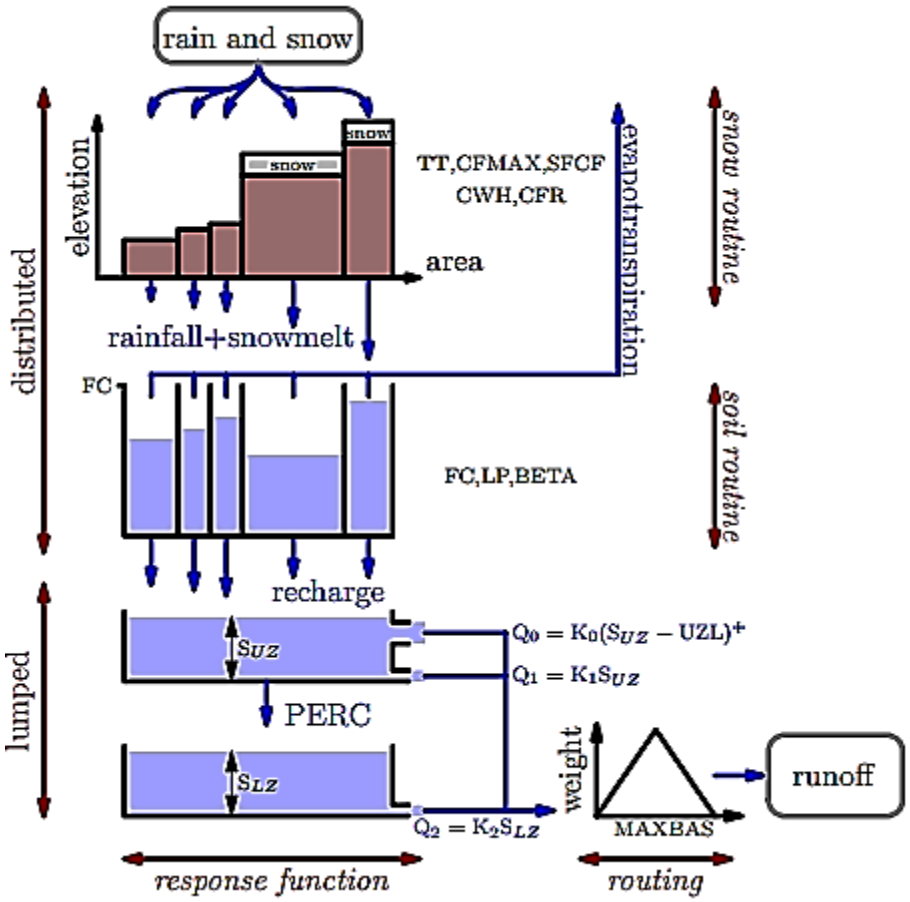

Figure 3.5: *Visualised representation of the HBV-Light hydrological model, sourced from Driessen et al. (2010).*

HBV-Light has the ability to simulate run-off scenarios using observed meteorological time series data which could possibly be used for hazard analysis such as flood warnings for settlements, dam safety, reservoir operation, for data quality control, investigating potential catchment changes, for simulating discharge of ungauged catchments and the effects climate change might have on freshwater catchments (Seibert *et al.* 2005). The HBV-Light model simulates catchment discharge using a daily time step, derived from precipitation and air temperature time series, estimates of continuous potential evaporation rates on a daily time scale, although has the ability to use longer term monthly potential evapotranspiration (PET). The model can also account for snow, soil, groundwater and routing routines (Seibert and Vis 2012).

The HBV model, and therefore by extension HBV-Light, was originally designed to calculate PET using the Penman method described in Penman (1948) as the data can be adjusted for

temperature anomalies such as warm and cold periods associated with the El Niño-Southern Oscillation (ENSO) cycle (Lindstrom and Bergstrom 1992). However, it has been proposed that many different methods for PET can be used, depending on the type of land use, soil composition, elevation and latitude of the study site in question (Allen 1998). Precipitation that does not reach the soil and therefore would not be counted in PET equations can be calculated using the interception routine. The interception routine in a hydrological model accounts for the percentage of water intercepted and stored on the leaves and branches of trees, plants, and the forest floor (Johansson and Seuna 1994). For hydrological models that do not have an interception routine, which includes HBV-Light, PET is assumed as different constants depending on the canopy type (Herbst 2008), e.g., estimates between 10 % and 35% have been found for precipitation interception in broadleaved forests (Rutter *et al.* 1975; Rowe 1983), and 25 to 50% in coniferous forests (Gash *et al.* 1980; Johnson 1990). PET is a combination of air temperature, vegetation, elevation and precipitation, all of which depend largely on seasonal variation and is therefore difficult to estimate, and more so in models like HBV-Light as canopy interception is not calculated, and therefore creating further model uncertainty.

Table 3.3: Set of adjustable parameters able to be calibrated in HBV-Light, along with the parameter values settled upon for this current research. Table adapted from Driessen *et al.* (2010).

Parameter	Symbol	Units	Minimum Value (in HBV-Light)	Maximum Value (in HBV-Light)	Study Value
Threshold Temperature	TT	C*	-infinity	infinity	0.4
Degree-day factor	CFMAX	mm*C-1d-1	0	infinity	3.6
Snowfall correction factor	SFCF	-	0	infinity	1.3
Refreezing coefficient	CFR	-	0	infinity	0.05
Water holding capacity	CWH	-	0	infinity	0.1
Maximum of soil moisture zone	FC	mm	50	500	100
Threshold for evaporation reduction	LP	-	0.3	1	0.5
Shape coefficient	BETA	-	0.01	6	0.01
Correction factor for pot. evapotrans.	CET	C-1	0	0.3	0.01
Recession coefficient (upper stor.)	K0	d-1	0.05	0.5	0.2
Recession coefficient (upper stor.)	K1	d-1	0.01	0.4	0.14
Recession coefficient (lower stor.)	K2	d-1	0.001	0.15	0.055
Routing parameter	MAXBAS	d	1	7	1
Maximum percolation	PERC	mm d-1	0	3	12
Threshold for K0 to become K1	UZL	mm	0	100	5

The main control of catchment runoff within the HBV-Light model is the soil routine. Modification of the Bucket Theory is used to characterise the pathways between infiltration

and evaporation. Originally developed by Manabe (1969), the soil water balance bucket model (BM) is a lumped model that accounts for a single soil layer, which collects infiltration water until the storage capacity is full, essentially like a bucket holding water. The soil routine is based on three parameters: BETA, LP and FC. BETA is the parameter that determines the relative contribution to runoff from each millimetre of rain or snowmelt. LP is a soil moisture value above which ET reaches its potential value when water is continuously available, expressed as a fraction of FC, where FC is the maximum soil moisture storage possible in the model (Seibert 2005). The response routine is what transfers excess water from the soil moisture zone into catchment runoff. The response function accounts for both the upper surface runoff, and lower base-flow components that make up the hydrograph, essential in the response routine, where runoff is calculated as a function of water storage based on a percentage release from K1 and K2 at each time step (Seibert and Vis 2012).

Snow accumulation of any hydrological model is a key component in simulating runoff as snow storage can hold or release large volumes of water during different times of the years, and is particularly relevant in catchments such as the Shotover due to its alpine setting. Precipitation that falls when air temperature (T) is below threshold temperature (PTT) will accumulate as snow, but needs to be multiplied by a snow correction factor (SFCF) to account for uncertainties such as poor catch efficiency of the rain gage, snow depth estimation and snowmelt volumes (Seibert 2005). Systematic errors associated with modelling sublimation of the snow pack and in the snowfall estimation can be accounted for using a PSCF (Seibert and Vis 2012). For all the routines in HBV-Light (snow storage, soil storage, upper and lower groundwater boxes), a warm up period is used to get the initial stores to values that appropriately reflect the current meteorological conditions, the parameters themselves however remain fixed, with one year is found to be sufficient time to do so (Seibert and Vis 2012).

3.8 TopNet

The fully distributed hydrological model TopNet (Clark *et al.* 2008) was developed by applying a kinematic wave routing algorithm (Goring 1994) to a pre-existing hydrological model (TOPMODEL). Originally designed for small watersheds (<1000 km^2) by Beven and Kirkby (1979) and Beven *et al.* (1995), Clark *et al.* (2008) produced a modelling system capable for application in large water sheds (>1000 km^2). The key difference between the older version TOPMODEL and TopNet is that TopNet uses smaller sub-basins within a large

watershed as model elements (Bandaragoda *et al.* 2004). There are two fundamental components of the distributed hydrological model TopNet: (1) the ability to simulate water balance over a number of sub-catchments in a river basin, (2) and the ability to route stream flow from each sub-catchment to the basin outlet (Clark *et al.* 2008). The main TopNet parameters that need single point values to run are PET, canopy interception, soil component, saturated zone, routing component and precipitation interpolation data (Table 3.4, Fig. 3.6). Other parameters do not necessarily need a single value to run appropriately, but values for a series of parameters are required.

Table 3.4: Parameters of the basin model component of TopNet. New Zealand River Environment Classification (REC), the New Zealand Land Resource Inventory (LRI) and the New Zealand Land Cover Database (LCDB). Sourced from Clark *et al.* (2008).

Parameter	Symbol (units)	Description	Default value	Data source
Albedo	χ		-	LCDB[C]
Atmospheric lapse rate	γ (Km^{-1})		0.0065	Uniform
Wetness index (frequency distribution)	K_1		-	REC[A]
Stream distance (frequency distribution)	X_1		-	REC[A]
Saturated store sensitivity	m (m)	Describes exponential decrease of conductivity with depth	0.08	Uniform
Saturated hydraulic conductivity	K_0 ($m\ s^{-1}$)		0.01	Uniform
Drainable soil water	θ_{dr}	Describes between saturation and field capacity	-	LRI[B]
Plant-available soil water	θ_{pa}	Range between field capacity and wilting point	-	LRI[B]
Depth of soil	Z_r		-	LRI[B]
Exponent in drainage function	c	Describes drainage into saturated zone	-	LRI[B]
Wetting front suction	Ψ (m)	Parameter of Green-Ampt infiltration capacity	0.3	Uniform
Overland flow velocity	V ($m\ s^{-1}$)		0.1	Uniform
Canopy capacity	C_C (m)		-	LCB[C]
Evaporation enhancement	C_r	Increasing evaporation losses from interception	-	LCB[C]

The water balance module of TopNet is based on the original TOPMODEL concepts, where saturation excess surface flow and baseflow are both controlled by the subsurface storage component (Beven and Kirkby 1979). TOPMODEL, like TopNet, calculates the saturated surface area based on the assumption that water table depth no matter the location, relates to

the wetness index a/tan b, where a is the upstream area and tan b is the local slope. Baseflow is calculated as an exponential function of the spatial average of the depth to water table (McMillan *et al.* 2016). Other water balance module components represented are canopy interception and storage, snowpack and the soil zone. The three influences of canopy storage are simulated changes to rainfall, throughfall and canopy evaporation. The wetted leaf area is a function of canopy throughfall and evaporation. The inclusion of the three influences on canopy storage is important as the degree of precision in estimating the amount of rainfall to the runoff outlet that is intercepted is greater than other models (HBV-Light), but also provides another benefit. The third influence on canopy storage, the canopy evaporation, also provides greater precision in the amount of rainfall that is available for evaporation via AET processes and subsequently PET which can provide more in-depth analysis of real-world processes within a catchment. Snowfall and snow melt are tracked through the snowpack module through a simple degree day melt formulation. The soil zone module simulates evapotranspiration, drainage and infiltration, all of which are power functions of the soil water fraction (McMillan *et al.* 2016). Through a kinematic channel routing model, TopNet then combines all the stated variables that are associated with water balance for each sub-catchment into one routed streamflow, where it enters the basin outlet (Fig. 3.6).

TopNet has two major components, namely a basin module and a flow routing module. To simulate unresolved stream channel mechanics such as the linkage and integration of hydrological processes at different scales (Bloschl and Sivapalan 1995), the runoff for each basin has a time delay. The time delay is simulated using the empirical frequency distribution of flow path lengths to calculate a conceptual store of residence time (McMillan *et al* 2016). The second component, the flow routine module, uses a one-dimensional Lagrangian kinematic scheme for resolved channel network variables, where the runoff is viewed as individual parcels propagating through an empirical drainage network (McMillan *et al* 2016), where each parcel is then calculated into kinematic wave channel flow (Fig. 3.6).

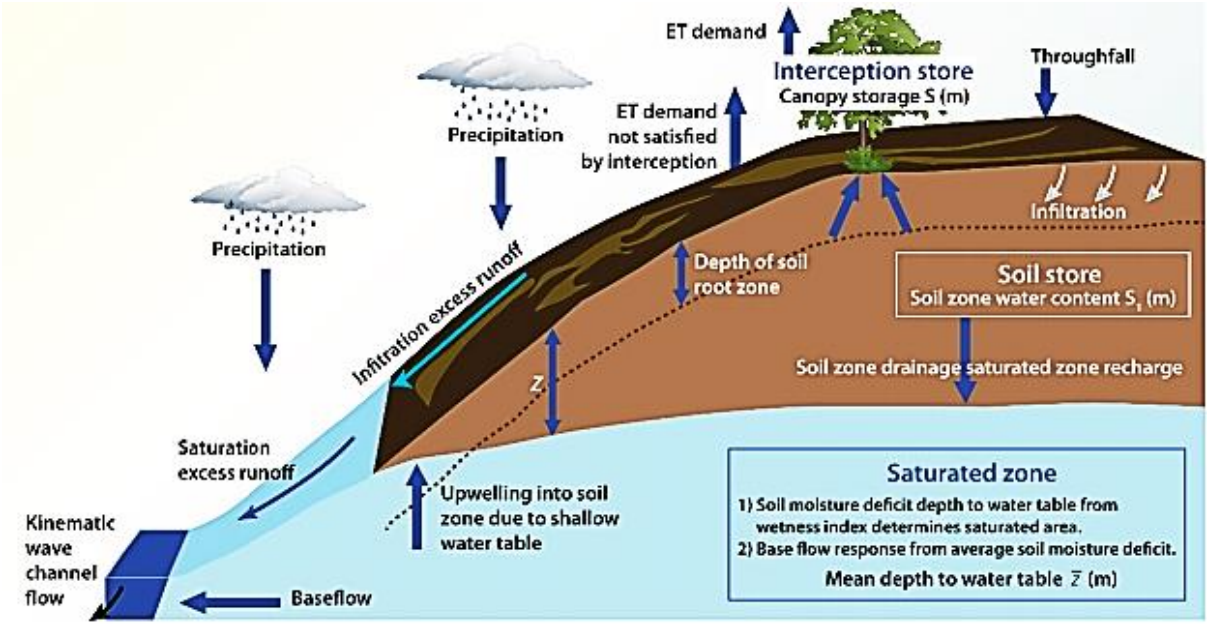

Figure 3.6: *Schematic of how the hydrological model TopNet represents a catchment, sourced from Bandaragoda et al. (2004).*

3.8.1 Basis for TopNet as a model comparison

Hydrological models operating in New Zealand catchments have been thought to require a comprehensive description of the hydro-climate landscapes, and diverse hydrological influences present. The use of TopNet in New Zealand as a tool for hydrological modelling has been justified as it includes vegetation and snow modules, infiltration-excess and saturation-excess runoff, while also simulating the complex interactions between the water table and soil zones, with the ability to cover a wide range of river basins (Clark *et al.* 2008). TopNets comprehensive coverage of catchment variables (Table 3.4) allow for use in snow-influenced catchments, as it can simulate the effects of infiltration-excess and saturation-excess flow, and influences of catchments with different vegetation types, using a single model structure, which are reasonable justifications for use in New Zealand as a whole (McMillan *et al.* 2016). Another justification for the use of TopNet in New Zealand is the fact that the TopNet model was developed and is used by the National Institute of Water and Atmospheric Research (NIWA) as the primary component in flood forecasting for the whole of New Zealand (Clark *et al.* 2007). The models modular structure makes it easy to apply new capabilities, and any new capabilities can be passed straight onto NIWA to aid and improve the models flood forecasting abilities (Clark *et al.* 2008). Furthermore, the use of TopNet to model the impacts that future climate change could have on freshwater availability was shown to be of success in Gawith *et*

al. (2012), Poyck *et al.* (2011) and Srinivasan *et al.* (2011) (Section 2.6) and is the basis for why TopNet was chosen as the comparison model for HBV-Light.

The two main limitations of TopNet are the size of the model and obtaining access to use it. TopNet requires a large set of input data to fill the model parameters needed to successfully run the model, all of which have to be calibrated and validated against actual data measurements which can be incredibly time consuming and costly. As the model was developed by NIWA, access to it can be difficult and not always granted (Clark *et al.* 2008). Other limitations are noted by McMillan *et al.* (2011), such as, the use of a single groundwater store for each catchment and sub-catchment, and therefore not accounting for possible recession behaviours, no idealised account for possible subsurface flow between sub-catchments through deep groundwater movement, and the lack of a glacier component. An unpublished groundwater assessment study by the Otago Regional Council (ORC 2003) found that the Shotover Catchment had significant groundwater resources with which a highly transmissive connection is shared with Lake Wakatipu, Kawarau River and the Frankton Flats Aquifer. The lack of a deep groundwater component may limit the effectiveness of TopNets ability to satisfactorily replicate an observed data set within the Shotover Catchment.

3.9 Calibration techniques

For HBV-Light, the agreement between simulated and observed data sets for the calibration period was assessed using a monthly Nash-Sutcliffe Efficiency number (NSE), ranging from negative infinity to 1. The basic idea of a NSE value of 1 being a perfect fit of the observed and simulated flow (Nash and Sutcliffe 1970) and 0 or less indicating that using the mean observed runoff as the predictor is just as reliable as using the model, meaning the model is poor. The squaring of differences in observed and predicted flows is a limitation of an NSE value because it allows overestimation of large flows which neglects low flows, and thus presents the limitation of underestimating performance in low flows, and overestimates model performance in peak flows (Legates and McCabe 1999). Coupled with NSE values, visual comparison of the observed and simulated runoff's timing and magnitude was undertaken, where an acceptable (visual) replication of the observed runoff was settled upon during the calibration process.

It is noted that although calibration techniques were undertaken to try and justify the use of a hydrological model for future climate change impact assessment, there is further introduction

of uncertainty. Errors in model structure or input data can sometimes be compensated for by unrealistic parameter values (McMillan *et al.* 2016). For the most sensitive parameters (TT, CFMAX and SFCF) in HBV-Light a realistic range was determined based on prior knowledge of the catchment and values reported in other literature. Other parameters within the HBV-Light model were altered to match the timing and volume of measured river runoff. The research in question used manual calibration techniques as opposed to the automatic Monte Carlo simulation provided by the HBV-Light software. The rationale behind this was because even though automatic calibration through a Monte Carlo approach provided higher NSE values, the daily and monthly simulated runoff were not as replicable visually as the observed runoff hydrograph. Therefore, a combination of statistical and visual aids was used to assess the effectiveness of HBV-Light in simulating an observed runoff data set during the calibration and validation process, where model performance was deemed satisfactory once a balance between the NSE and graphical outputs was achieved.

3.9.1 TopNets Calibration

TopNet is used in this research as a comparison model for HBV-Light, where the version of TopNet used is the same as the one seen in Poyck *et al.* (2011) and Gawith *et al.* (2012). TopNet was set up and calibrated for the Clutha Catchment as a whole using observed flow data from the Clutha Catchment itself and two smaller sub-catchments, the Matukituki and the Lindis. Therefore, it is important to note that the version of TopNet used in this research was not calibrated for the Shotover Catchment specifically. However, as TopNet was validated in both a relatively wet sub-catchment (Matukituki) and a relatively dry sub-catchment (Lindis), the model is considered a viable option for modelling all 2343 of the Clutha, including the Shotover. No other calibration procedures we undertaken in regards to TopNet in this research. Furthermore, the runoff data modelled by TopNet that is used for comparison to HBV-Light is the only part of the TopNet model that was provided by NIWA for this research and has not been altered in any way.

The TopNet model was set up and calibrated against measured discharge from the Clutha Catchment as a whole using streamflow data from the Clutha (at Balclutha), and two sub catchments: the Matukituki and the Lindis. Initially, the spatial parameters, e.g. elevation distribution, wetness index, soil hydraulic conductivity, infiltration capacity, overland flow velocity were run using New Zealand River Environment Classification (REC), the New Zealand Land Resource Inventory (LRI) and New Zealand Land Cover Database (LCDB)

estimates. However, the estimated parameter values used from the REC, LRI and LCDB did not produce accurate simulations of observed river flow and therefore needed calibration.

Calibration was undertaken by semi-automatically generating 5000 parameter sets for each of the three catchments (Clutha, Matukituki and the Lindis) that were restricted by plausible spatial and temporal values for the hydrological parameters, which were run from 01/09/1993 to 31/12/1994 to account for high flow recordings in the beginning of 1994. For each of the three catchments, the 20 top performing parameter sets were used to run the model over a 20-year period (1980-1999) where visual inspection between observed and simulated runoff outputs were undertaken for best fit. The size of the Clutha Catchment that TopNet was originally calibrated for meant that dimensionality of the model was limited by adjusting the spatial distribution of parameters uniformly, applying the settled upon parameter multipliers to all 2,343 sub-catchments in the Clutha, including the Shotover. Model evaluation of the 60 parameter sets and resultant runoff outputs were assessed statistically through hourly NSE values of observed verse simulated runoff, a 20-year average of weekly observed verse simulated runoff that allowed for visual inspection of seasonal flow patterns and snow melt timing, and cumulative modelled verse observed runoff and rainfall plots that allow for an estimation of modelled actual evapotranspiration and an assessment of total volume of streamflow.

3.10 Summary

The Shotover Catchment was chosen as the field site for which to assess HBV-Lights ability to simulate an observed runoff data set due in part to its unique alpine setting close to the main divide of the Southern Alps which makes the climate and hydrology more complex than other catchments, and is a good challenge for testing HBV-Light. The hydrological model chosen for comparison, TopNet, has performed well in similar catchments to the Shotover, such as the Matukituki, while also performing well in catchments much larger like the Clutha, and much drier like the Lindis. Lastly, the Shotover catchment has many hydrometric and climate stations with which over-lapping continues data sets were able to be generated.

The daily observed data used to construct a continuous 26-year timeline (1972 to 1997) for precipitation, temperature, discharge and PET was cut down from 38 years due to inaccuracies in the discharge collection data, where 26 years was deemed to be long enough for model calibration (1972 to 1984) and validation (1985 to 1997). An important point of this chapter is

differences between the input data used to run HBV-Light and TopNet (Section 3.5.3), and stems from the use of VCSN data which is based on the spatial interpolation of actual data observations, compared to single point data. TopNet was run using VSCN data for temperature and precipitation, while the Priestly-Taylor method used to calculate PET was also derived from VSCN data.

Another important point of this chapter (Section 3.9.1) is that TopNet was not specifically calibrated for the Shotover Catchment like HBV-Light was. As the model is owned and operated by NIWA, it was kindly run for the Shotover Catchment for the purposes of this research. TopNet was calibrated for the Clutha Catchment in its entirety (21,960 km^2), and used flow data from the Matukituki (799 km^2) and Lindis (1045 km^2) sub-catchments to validate the use of the model for all 2343 sub-catchments of the Clutha, including the Shotover. Through the use of statistical analysis such as NSE, PBIAS, RMSE and RSR values, and with the help of graphical aides like monthly runoff hydrographs and flow duration curves, HBV-Light calibration methods detailed in Section 3.9 will be validated in Chapter Four.

Chapter Four

Model Performance

In this Chapter, the analysis of model performance will be presented through a combination of graphical and statistical analysis. The two most common forms of graphical analysis are hydrographs and percent exceedance probability graphs (Moriasi *et al.* 2007), more commonly referred to as a flow duration curve (FDC). Graphical analysis is considered an essential method of appropriate model evaluation (Legates and McCabe 1999), and therefore monthly discharge outputs (hydrographs) and FDCs will be investigated. Included in the graphical analysis, scatter plots will also be examined, accompanied by statistical analysis of the model output versus the observed data. Firstly, the comparison of river runoff between the observed runoff data and the simulated output for all three analysis periods; calibration (1972 to 1984), validation (1985 to 1997) and the combined data set referred to as the 'all data years' period (1972 to 1997), will be displayed and commented on (Section 4.1). The second method used to analyse model performance will be through the FDCs of all three data periods, as FDCs give an indication of how the model reacts to sudden changes in extreme discharge (Section 4.2). Thirdly, regression analysis was performed on three output periods to determine if a relationship exists between the observed and simulated variables (Section 4.3). Finally, the statistical evaluation techniques of monthly Nash-Sutcliffe Efficiency (NSE) values, percent bias (PBIAS) of the simulated data, root mean square error (RMSE) and the RMSE-observations standard deviation ratio (RSR) are used to make inferences about the appropriateness of the simulated model output in relation to the observed catchment runoff (Section 4.4). Through the use of daily and monthly hydrographs, FDCs, NSE, RMSE, PBIAS and RSR values, a case will be made which will be the basis on which the hydrological model HBV-Light is argued to be acceptable to run for future climate scenarios within the Shotover Catchment in New Zealand.

4.1 Discharge Comparison

Hydrographs are useful as they provide a visual representation of the simulated versus observed discharge as a time series plot over the intended study period, where both calibration and validation periods can be analysed separately (Moriasi *et al.* 2007). The importance of hydrographs is they allow identification of periods where there is a difference in the timing and magnitude of peak flows between the simulated and observed discharge (ASCE, 1993). For the purpose of this research, monthly hydrographs will be analysed to assess how individual months compare over the data set as a whole, however examples of where an individual year displays a strong NSE versus a poor NSE will be analysed in terms of their daily discharge hydrographs (Fig. 4.2 & 4.3).

4.1.1 Average Monthly Discharge

The average monthly hydrographs for the calibration, validation and total combined data years (Fig. 4.1 A, B & C) display good agreement between the simulated and observed data for the majority of the averaged months. What is a noticeable pattern between all three model runs however, is the simulated discharges slight inability to replicate peak observed discharge in October. All three runs display the same pattern in mid to late spring, where the model under-simulates runoff by around 20-30 mm/month, most notably in the month of November in the validation data set (Fig. 4.1 B). Visually, the calibration data set (Fig. 4.1 A) appears the best fit, as the simulated output resembles the observed closely for the months of January to June, only slightly overestimating discharge. The calibration period also has the least difference in discharge out of the three model runs for October, November and December. The calibration data set does however under simulate river flow in July and August to a higher degree than the validation period. The combined overall data set (Fig. 4.1 C) displays good agreement for monthly simulated versus observed discharge, as the simulated replicates the trends of the observed data for the majority of the year (January to early October), however fails to simulate the magnitude of peak discharge for October and November, but December is good. Overall, the modelled runoff most closely matches the overserved runoff during the calibration period, but matches the validation and all year's period as well. Thus, the three data periods and their simulations indicate model stability as the simulation runoff has not over-fitted the observed data, showing the HBV-Light model has provided a realistic simulation of runoff flow outside of the calibration period.

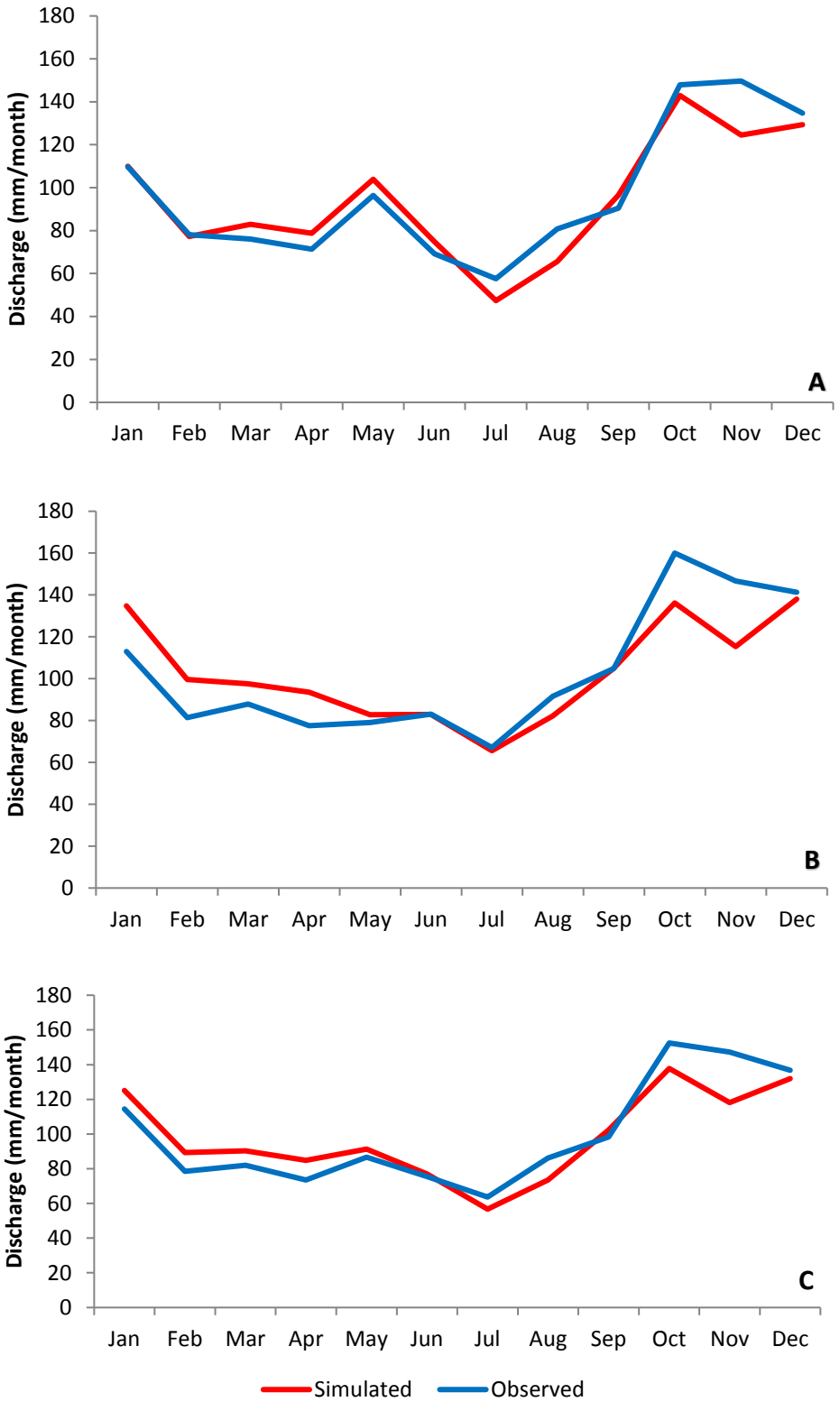

Figure 4.1: *Simulated versus the observed runoff comparisons between the calibration period (A), validation period (B), and the All Years data sets (C).*

4.1.2 Average Daily Discharge

The average daily observed and simulated time series for discharge can give an indication as to how well the simulated discharge replicates the observed discharge for a given year, or the entire time period. The daily NSE value for the calibration period (1973 to 1984) is 0.5638 which is "satisfactory", and for the whole-time period (1973 to 1998) is 0.4791, indicating the simulated versus observed data display a "satisfactory" relationship. Unlike monthly NSE that gives an indication of model fit over periods of time through smoothed averages of NSE, daily NSE allows the assessment of how the simulated runoff responds to individual meteorological forcing events. When representing NSE values for small periods of time (e.g. one year), monthly NSE produces 12 data points per year, and can be difficult to interpret as the 365 variations of daily discharge are smoothed out into 12 monthly points. The extent of extra data points when looking at daily NSE allows individual days with high runoff to be more influential on NSE, where the monthly NSE smooths the higher than normal flow events. Therefore, it is beneficial to assess how the daily discharge can fluctuate within a single year, as daily data can provide a higher resolution of simulated versus observed runoff to assess how changes to parameter values during the calibrating period effects the peaks in runoff.

The daily hydrographs of two individual years; 1982 (Fig. 4.2) and 1993 (Fig. 4.3), were selected for representation as they display the largest range of daily NSE between all of the single data years used in this research. The variation of NSE values were evenly distributed with 14 daily NSE values deemed 'satisfactory' and 12 deemed 'poor', with a range of 0.6693 to -0.6416. The daily time series for 1982 (01/01/1982 to 31/12/1982) had a daily NSE of 0.6693 which is considered 'good' (Moriasi *et al.* 2007), while 1993 (01/01/1993 to 31/12/1993) displayed an 'unsatisfactory' NSE of (-0.6416). The 1982 time-series (Fig. 4.2) displays how the simulated runoff replicates the observed peaks in runoff to a good standard, whereby, most if not all observed peaks are matched by an increase in the simulated runoff. Also of note, is that after a peak in the simulated discharge, the output drops back down to base flow in relatively the same time frame as the observed runoff. In contrast, the 1993-time series output (Fig. 4.3) displays a simulated discharge output that overestimates the majority of the observed discharge peaks by upwards of 5 mm/day. Unlike 1982, the simulated baseflow fails to replicate the observed, whereby the simulated runoff takes more time to return to baseflow, and during some periods fails to return to observed altogether.

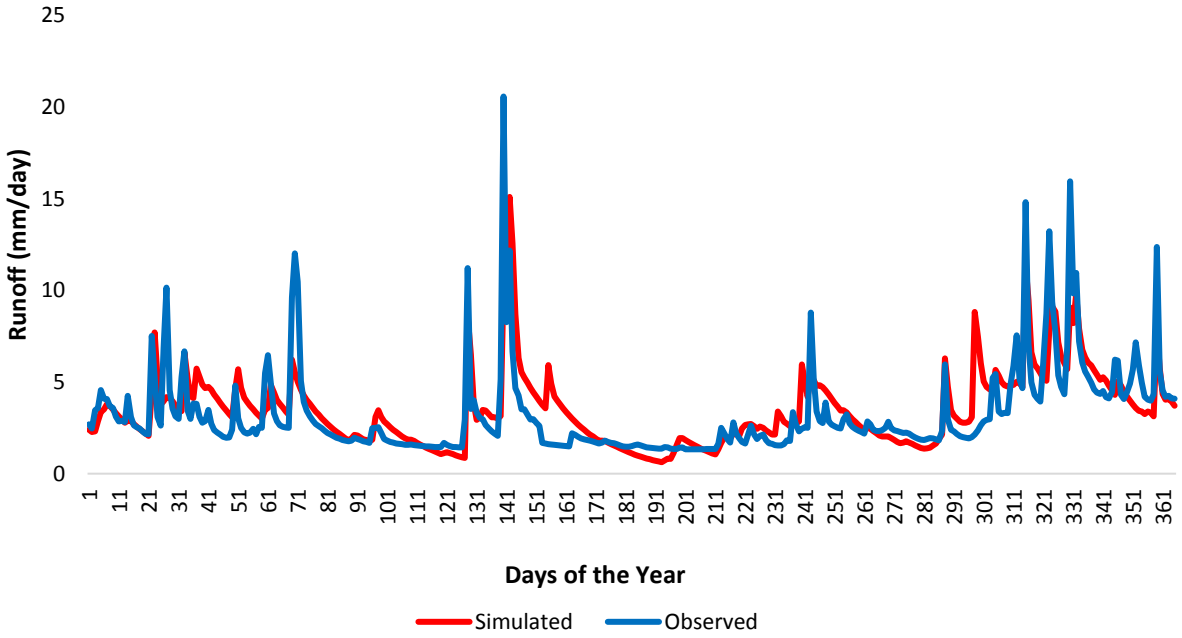

Figure 4.2: *Daily time series hydrograph of a single year (1982).*

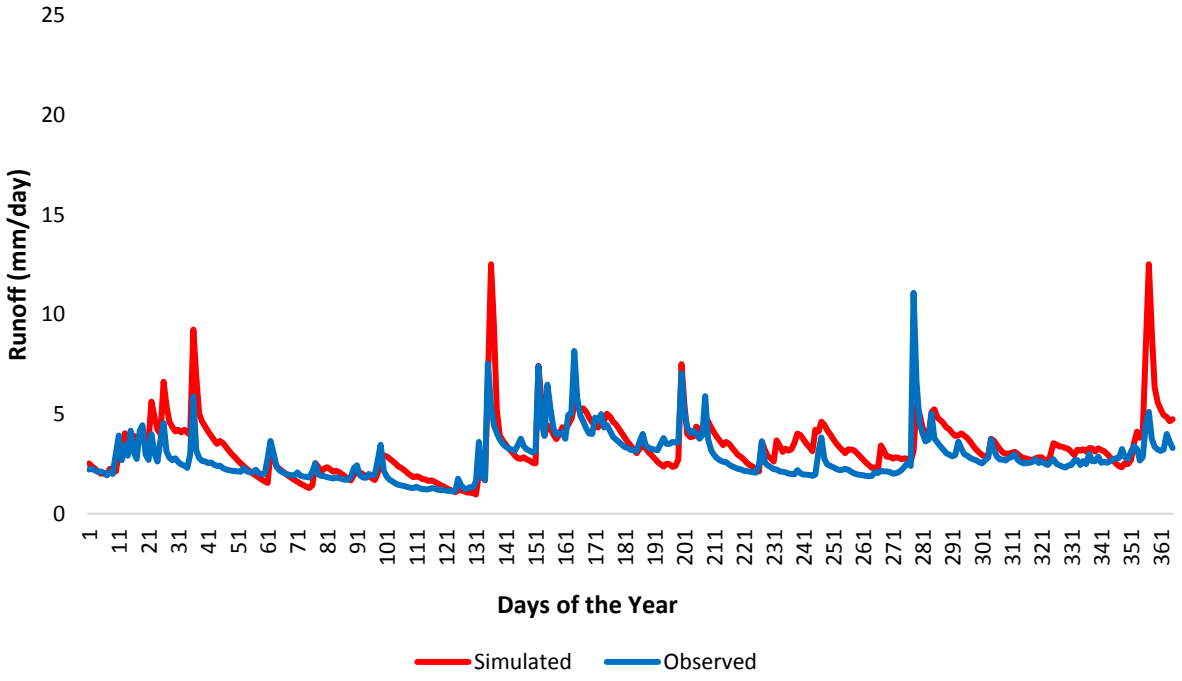

Figure 4.3: *Daily time series hydrograph of a single year (1993).*

Differences in climate between 1982 and 1993 could be an important cause of variation in model performance noticed in the daily NSE outputs between the simulated and observed runoff. The 1982 year had slightly higher total rainfall (1042 mm) compared to 1993 (1003 mm), only 3.9 %, and therefore not a likely cause of disparity between NSE variation. Further analysis of climate conditions between the two years shows that 1982 shows that 1982 has 34

days where the temperature was below 0°C compared to 17 days in 1993. Over the period of 34 days in 1982 there was 31.6 mm of precipitation compared to 17.5 mm over the 17 days in 1993, suggesting more snow was accumulated in 1982. The differences in temperature variation between the two years could have influenced the snowmelt leaving the catchment as discharge too. The days that HBV-Light simulated snowmelt to occur were similar, with 268 days in 1982 and 282 days in 1993, however, there is a large disparity between the simulated snowmelt volumes. In 1982 HBV-Light simulated there was 13902 mm of total snowmelt compared to 18121 mm in 1993. The large variation in snowmelt between the two years indicate that HBV-Light may be overstimulating the actual snowmelt occurring in the 1993 catchment and therefore unable to replicate the amount of discharge occurring which is why the model is returning an extremely poor NSE value. Due to the unpredictable nature of yearly atmospheric change and the inability of models to incorporate accurate knowledge of catchment climate and hydrological relationships, there is a need to strike a balance between acceptable NSE values and somewhat equal visual symmetry between observed and simulated runoff to have a viable acceptance of the model's efficiency.

4.2 Flow Duration Curves

A flow duration curve (FDC) displays the percentage that a known discharge (observed) was under or overestimated by another stream flow record (simulated) over a period of time, and is a useful visual tool to analyse the relationship between magnitude and frequency of monthly discharge (Vogel and Fennessey 1995). The calibration period (Fig. 4.4 A) shows that the lower percentile (0-25 %) consistently underestimates the observed data in the order of 10-60 mm/month, and overestimates observed by 5-10 mm/month between 40 and 65 %. Flow duration curves for the validation period (Fig. 4.4 B) and All Year's (Fig. 4.4 C) model runs show good agreement of peak flows between the simulated and observed data sets. The validation period between 15 and 100 % show good agreement, with a minor deviation away from the observed between 80 and 90 %, in the order of 5 mm/month. Between 0 and 15 % there is more pronounced deviation away from the observed, in the order of 10-50 mm/month. The All Year's simulated data set shows good agreement with the observed between 20 and 100 %, and between 0 and 20 % the modelled discharge under simulates the observed by 5 mm/month consistently, however, visually is a very good fit. Compared to the validation and All Year's FDC, the calibration period under simulates discharge within the last 10 % (90-

100%), indicating the models simulated base flow is lower than that of the observed, but general overall output is good.

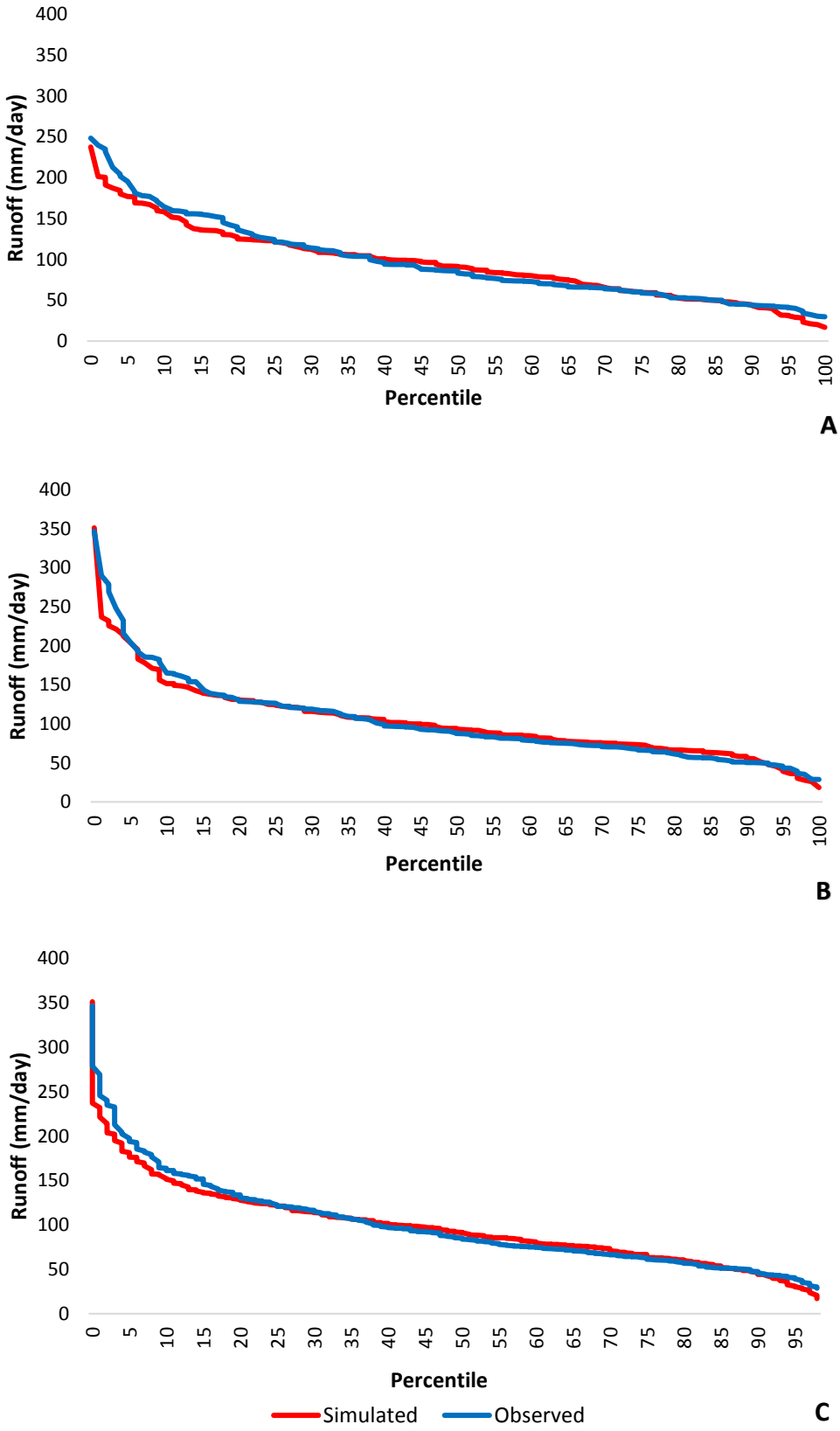

Figure 4.4: *Flow duration curve outputs between the observed and simulated runoff for the calibration period (A), validation period (B), and for both data sets combined (C).*

4.3 Regression Analysis

The output from the HBV-Light model can also be compared to the observed runoff by monthly scatter plots, to assess the strength of the relationship if present. A coefficient of correlation (r-value) can determine how strong the relationship between the independent (X= observed) and dependent variables (Y= simulated) if one exists. Figure (4.5 A) indicates through an r-value of 0.7203 a strong relationship between the observed and simulated data sets for the calibration period. Visually, the spread of data points suggests a linear relationship with the months of higher discharge having more of a dispersed spread. The validation data set (Fig. 4.5 B) also displays a strong r-value of 0.6125. However, with a difference □0.1 less than the calibration periods r-value, is due to the increased dispersion of data points as the monthly discharge increases. The overall monthly observed versus simulated monthly discharge (Fig. 4.5 C) displays a strong r-value of 0.6512, as it is a combination of both the calibration and validation data sets.

The greater spread of data points and difference in r-values presented in Figure 4.5 B compared to Figure 4.5 A suggests that the higher monthly discharge values seen in the validation data set is influencing the calibration confidence compared to the calibration period, due to a wider range of hydrological variation that is occurring in the validation period (Fig. 4.5 B). Limiting the validation periods observed runoff to that of the calibration period of 250 mm/month or less, which removes the four largest runoff values, returns an R-value of 0.5486, which is quite a lot less (0.0639). The validation period has one simulated outlier of 350 mm/month compared to an observed runoff around 200 mm/month and when removed from the data returns an increased R-value of 0.6449, thus suggesting model performance is highly receptive to outliers. The observation can be made that the HBV-Light model performs better with higher observed runoff magnitudes, meaning more water in the system as suggested by (McMillan *et al*. 2016). Even though the calibration period had lower runoff magnitudes and a higher NSE value, that particular period was targeted for calibration which influenced parameter values to give a greater NSE/model performance.

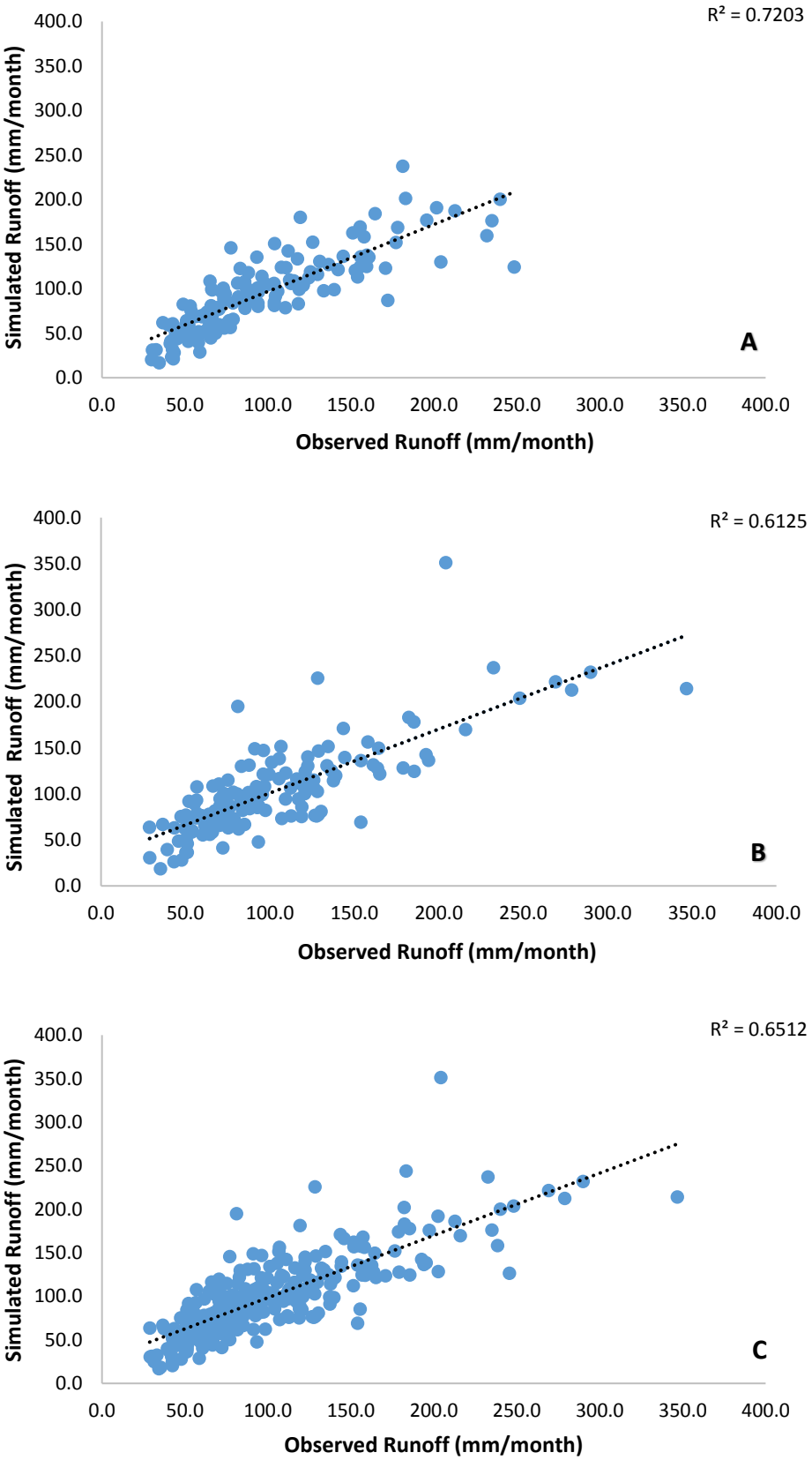

Figure 4.5: *Monthly observed versus simulated runoff scatterplots for the calibration period (1972 to 1984) (A), validation period (1985 to 1997) (B), and the All Years period (1972 to 1997) (C).*

4.4 Statistical Analysis

Validation of a rainfall-runoff model is typically assessed through graphical analysis, however, can further be subject to analysis through statistical outputs (Table 4.1). Moriasi *et al.* (2007) suggest there are four common statistical methods of assessing a hydrological model's ability to simulate discharge. These are a Nash-Sutcliffe Efficiency (NSE), a percent bias (PBIAS) of the simulated data, the root mean square error (RMSE) and the RMSE-observations standard deviation ratio (RSR).

Table 4.1: NSE, RSR, PBIAS and RMSE output for the calibration (1973-1984), validation (1986-1997), and combined data sets (1973-1997).

	NSE (monthly)	PBIAS (%)	RMSE (mm/month)	RSR (monthly)
Calibration	0.717	2.4	26.15	0.53
Validation	0.601	0	34.02	0.63
All Years	0.644	1.49	30.46	0.59

Monthly NSE (Nash and Sutcliffe 1970) is considered 'good' (0.65< NSE <0.75) for the calibration period, and 'satisfactory' (0.50 < NSE <0.65), for the validation and All Years data periods (Moriasi *et al*. 2007). The calibration period returns a monthly NSE value of 0.717, suggesting the model has a simulated output more representative of the observed data than the validation period, indicating a NSE of 0.601. The All Year's data set shows the combination of the calibration and validation data sets as one continuous record, where the model simulated overall discharge with a NSE of 0.644 (satisfactory). PBIAS quantifies the magnitude to which the simulated data over or underestimates the observed output (Gupta *et al.* 1999). The lower the magnitude is to 0, the greater accuracy of the simulated data, where a negative PBIAS indicates overestimation, and positive values indicate underestimation (Gupta *et al*. 1999; Moriasi *et al.* 2007). The calibration period appears to have the highest PBIAS (2.4) indicating that the model under simulates the observed discharge by 2.4 %, however, is still a good result as anything below 10 % is considered a 'very good' fit (Donigian *et al.* 1983; Moriasi *et al.* 2007). The validation period has a PBIAS of 0, indicating that the model is predicting the observed runoff. The combined data set has a PBIAS of 1.49 %, indicating that overall the model underestimates the observed runoff by a low-magnitude.

Analysis of and RMSE and RSR values are commonly used to assess model error statistics (Chu and Shirmohammadi 2004; Singh *et al.* 2004), where a lower RMSE is considered more acceptable (Moriasi *et al.* 2007). RSR standardizes RMSE using the observations standard

deviation (Legates and McCabe, 1999). The calibration period displays the lowest RMSE at 26.15 mm/month, indicating the least magnitude of difference between simulated and observed monthly discharge. The validation period indicated the highest RMSE (34.02 mm/month), with a difference of more than 7 compared to the calibration period. Overall, the total data set returned an RMSE of 30.46 (mm/month). All three RMSE values are considered 'very poor' (Henriksen *et al.* 2008), as all model run periods show RMSE's greater than 10. The RSR values calculated show the same pattern as the NSE and RMSE values, where the calibration period returns the best value (0.53), the validation value being less desired (0.63) and the All Year's period being somewhere in the middle of the two values (0.59). According to Moriasi *et al.* (2007), the calibration and All Years RSR can be considered 'good' ($0.50 < RSR < 0.60$), while the validation period is 'satisfactory' ($0.60 < RSR < 0.70$), where 0 is considered perfect.

4.5 Calibration Comparisons of Other Studies

The NSE values settled upon during the calibration can be compared to other impact assessment of climate change research that used the hydrological models HBV-Light and TopNet from within New Zealand (Table 4.2). The use of HBV-Light in the Shotover Catchment for this research had an NSE value (0.7) higher than Koedyk and Kingston (2016) who also used HBV-Light and is the only other published example of HBV-Light in New Zealand. Although Koedyk and Kingston (2016) used a catchment considered less Alpine and more highlands, is still research conducted using HBV-Light within New Zealand. Also of note is Gawith *et al.* (2012) who used TopNet in sub-catchments (Matukituki and Lindis) of the Clutha similar to the Shotover, which performed slightly lower than HBV-Light (0.68 & 0.69), while Poyck *et al.* (2011) for the same catchments (Matukituki & Lindis) also using TopNet, published NSE values of 0.86 and 0.81 respectively. However, Poyck *et al.* (2011) used a 20-year average of weekly discharge, whereas the current research, Koedyk and Kingston (2016), and Gawith *et al.* (2012) all used monthly NSE average, and therefore using smoothed data could explain why Poyck *et al.* (2011) have higher NSE values.

Table 4.2: comparisons of model complexity and calibrated NSE values for similar research within the Southern Alps, New Zealand.

Research Paper	Model	Complexity	Catchment	Calibration NSE (monthly)
Koedyk and Kingston (2016)	HBV-Light	Semi	Waikaia	0.6
Gawith *et al.* (2012)	TopNet	Fully	Matukituki	0.68
			Lindis	0.69
Poyck *et al.* (2011)	TopNet	Fully	Balclutha	0.9
			Lindis	0.81
			Matukituki	0.86

4.6 TopNets Simulation of Observed Data

Although TopNet has not been calibrated for the Shotover Catchment specifically, it is still important to know how realistically the model simulates catchment runoff, so that comparisons of runoff between the two models can be made with greater insight. On a monthly scale TopNet simulates spring melt runoff in the Shotover accurately for the month of October (Fig. 4.6). Leading up to peak runoff, May, June, July, August and September all simulate runoff relatively accurately to the observed. The warmer months month of the year, January, February, March, April, November and December all under simulate the observed runoff, with a maximum under simulation of 60 mm/month (42 %) in December. Over the 20-year baseline period (1980-1999) TopNet under simulates the observed Shotover runoff for almost all of the years except 1980 and 1999 (Fig. 4.7). From 1981 to 1998 there is a consistent margin between the observed and simulated runoffs, with the greatest under simulation of 440 mm in 1987. Interestingly, statistical analysis of TopNets simulation of observed catchment data returns a monthly NSE value of 0.71 for the 1980 to 1999 baseline period.

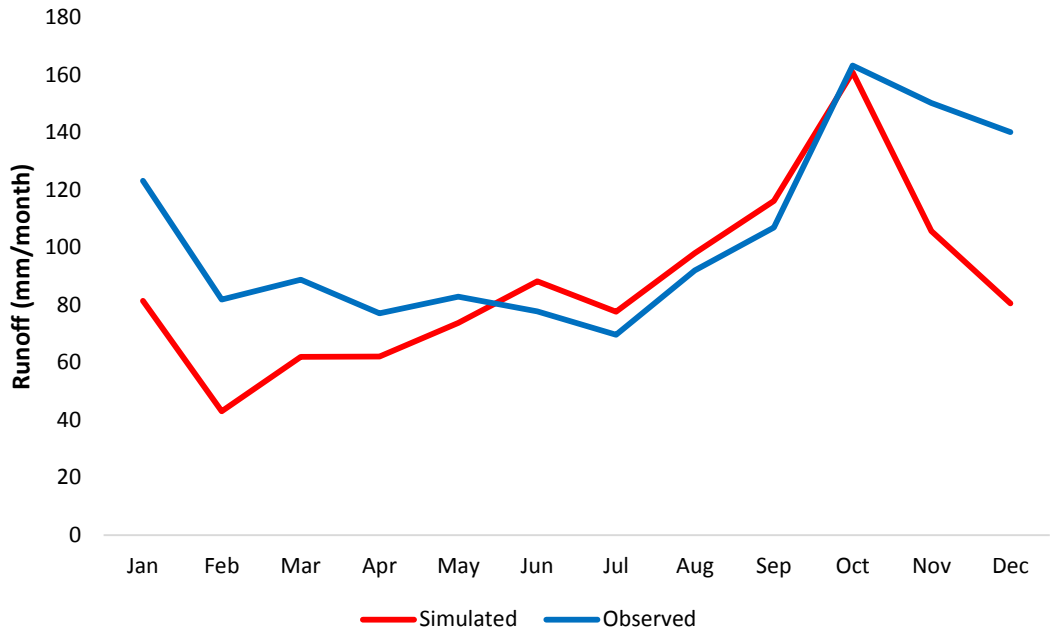

Figure 4.6: *TopNets simulated 20-year (1980-1999) monthly average runoff verse observed data from within the Shotover Catchment, New Zealand.*

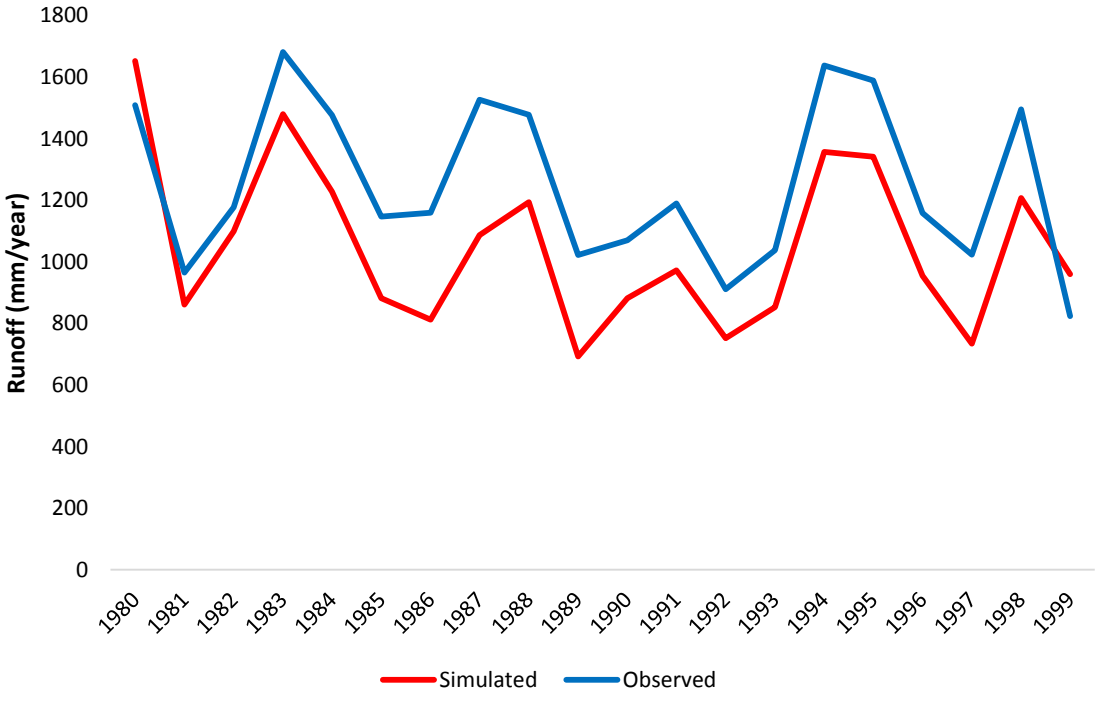

Figure 4.7: *TopNets simulated 20-year (1980-1999) average runoff verse observed data from within the Shotover Catchment, New Zealand.*

4.7 Summary

Most literature agrees that the common practice for analysing a rainfall-runoff models ability to represent a known period of discharge is through the combined use of graphical and statistical techniques (Legates and McCabe 1999; Singh *et al.* 2004; Moriasi *et al*. 2007). Through the use of graphical aids (daily & monthly hydrographs, FDCs and scatterplots), the calibration and validation periods have been shown to visually represent the observed data sets to a good standard. The overall data set of 24 continuous years (1972-1997) show good overall visual comparison between the simulated and observed monthly discharge. The statistical analysis of the calibration and validation periods also suggest the HBV-Light model is justified to replicate a known observed discharge over a period of time within the Shotover Catchment of New Zealand. The NSE outputs were described as 'good' for calibration (0.72) and 'satisfactory' for the validation (0.61) and All Years data sets. The PBIAS for all three data sets are described as 'very good'. Lastly, the RSR for the calibration and All Years data sets was described as 'good' and the validation data set described as 'satisfactory'. The three statistical tools NSE, PBIAS, and RSR were described based on the work of Moriasi *et al.* (2007), and RMSE as described by Henriksen *et al*. (2008). The suitability of using TopNet to simulate an observed data set from within the Shotover Catchment was also assessed, bearing in mind the model was not specifically calibrated for the Shotover. TopNet returned a 'good' monthly NSE (0.71), although under-estimated the warmer months, some by an extreme of 60 mm (December). TopNet did however simulate the colder months very well, suggesting the model works better when more water is in the system.

Chapter Five

Results

In this section, there are two main lines of enquiry. Firstly, the potential impacts that future climate change may have on the Shotover Catchment as modelled by HBV-Light are presented (Section 5.1). Secondly, HBV-Lights scenario output variables are compared to that of TopNet, to make assumptions about HBV-Lights suitability for assessing the impact of climate change compared to a fully distributed hydrological model (Section 5.2). As previously stated (Section 3.6), the climate change input data used to run HBV-Light and TopNet for the future scenario periods are the same, as provided by NIWA, where a "middle of the road" emissions scenario (A1B) was used, utilising a warming period with a magnitude of 2˚C. The difference being however, is in the way in which the respective models use the same input data sets. All 2040 and 2090 scenario output data is shown using the average of the 12 suitable GCMS for the New Zealand context, when describing the potential impacts climate change could have on the Shotover Catchment, except for Figures 5.12 and 5.13 that show individual GCM outputs to assess GCM related uncertainty.

The previous chapter (Chapter Four) used a calibration period of 1973-1997 labelled the 'All Years' period as it was the longest period of good quality data. As shown in Section 4.1.2, Figure 4.2, there are periods within the calibration timeframe that display lower or greater fit than the overall 26-year data period. The use of the 'All Years' data period helped the research to accomplish the first aim, which was to assess the suitability of HBV-Light to model an observed runoff data set within the Shotover Catchment. To accomplish the second aim of the research, HBV-Light was run with a 'baseline' data set from 1980-1999 to compare the runoff data provided by NIWA as modelled by TopNet for the same timeframe. In doing so, the current research is in line with other climate change impact assessment studies that compare changes from a baseline (1980-99) to two future periods (2030-49 & 2080-99).

To assess the potential impacts of climate change as modelled through HBV-Light, Section 5.1 will include the projected change suggested through the 20-year average of monthly runoff for all three scenario periods; 1990 (1980 – 1999), 2040 (2030 – 2049) and 2090 (2080 – 2099) using the GCM ensemble average (Fig. 5.1). The monthly change in runoff will then be

quantified as a percent change, as such analysis gives better visual representation of the potential change (Fig. 5.2). To better understand which variables are influencing runoff, precipitation and runoff will be compared to gain a sense of how precipitation increase contributes to runoff in both 2040 (Fig. 5.3) and 2090 (Fig. 5.4). Section 5.2 will present HBV-Lights projected changes in future runoff compared to TopNets (Fig. 5.10 & 5.11), how each model simulates the GCM ensemble (Fig. 5.12 & 5.13), and some key outputs of the two models' components, namely, soil moisture (Fig. 5.14) the snowpack (Fig. 5.15) and AET (Fig. 5.16). Finally, a summary of HBV-Lights suggested impacts of climate change on basin characteristics will be concluded.

5.1 Changes in Monthly and Annual Runoff

The HBV-Light model suggests there are differences in runoff between the 2040 and 2090 scenario periods compared to the 1990 baseline, within the Shotover Catchment. The predicted 2040 and 2090 runoff scenarios are presented through a 20-year monthly average of a 12 GCM ensemble suitable for the New Zealand climate (Fig. 5.1). HBV-Light suggests both 2040 and 2090 will have an increased runoff period for February to August, where January and September appear to show a small increase in runoff. October and November have clear increases in runoff, however, of a smaller magnitude to that of the rest of the aforementioned months. An increase in runoff in 2090 compared to 2040 is also observed for the months of May, June, July and August.

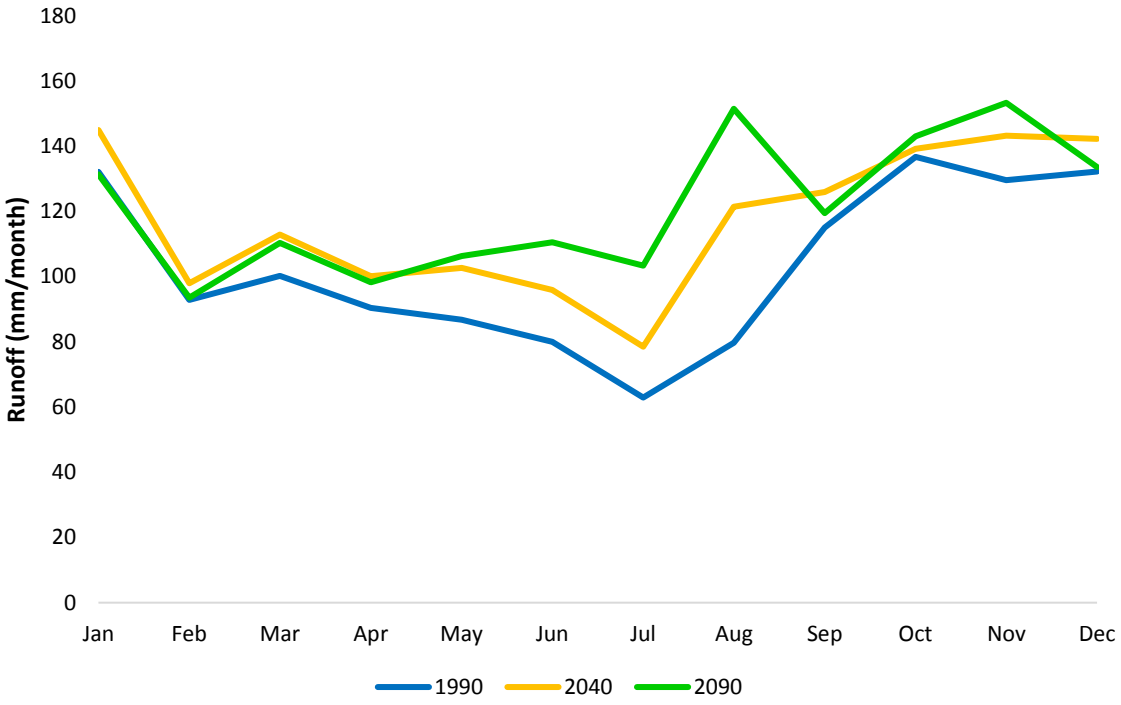

Figure 5.1: *HBV-Light's baseline and future scenario runoff comparisons using the GCM ensemble means for 2040 and 2090.*

The 20-year monthly average from the baseline to the two respective future scenarios (2040 and 2090) can be quantified as a percentage increase (Fig. 5.2). The spring and summer months show the least amount of increase, with an increase in runoff between 1.8 % and 12 % in 2040. The winter months June, July and August, along with the last month of autumn (May) display the greatest increase in surface runoff with a range between 18 and 52 %. The 2090-time period displays the same characteristics as 2040, where the winter months display a continuing

increase in runoff from May to August, until the beginning of spring, where potential runoff decreases almost to the same level as the 1990 baseline. The range of increasing runoff in 2090 however is almost double that of 2040, where at its peak in August, the potential increase in runoff reaches 90 %. The spring and summer months however show a smaller increase in runoff compared to 2040, where in January, HBV-Light suggests runoff will decrease slightly (-0.6 %). These results therefore suggest that the amplification of seasonal increases and decreases in runoff will be more extreme in 2090 than that of 2040.

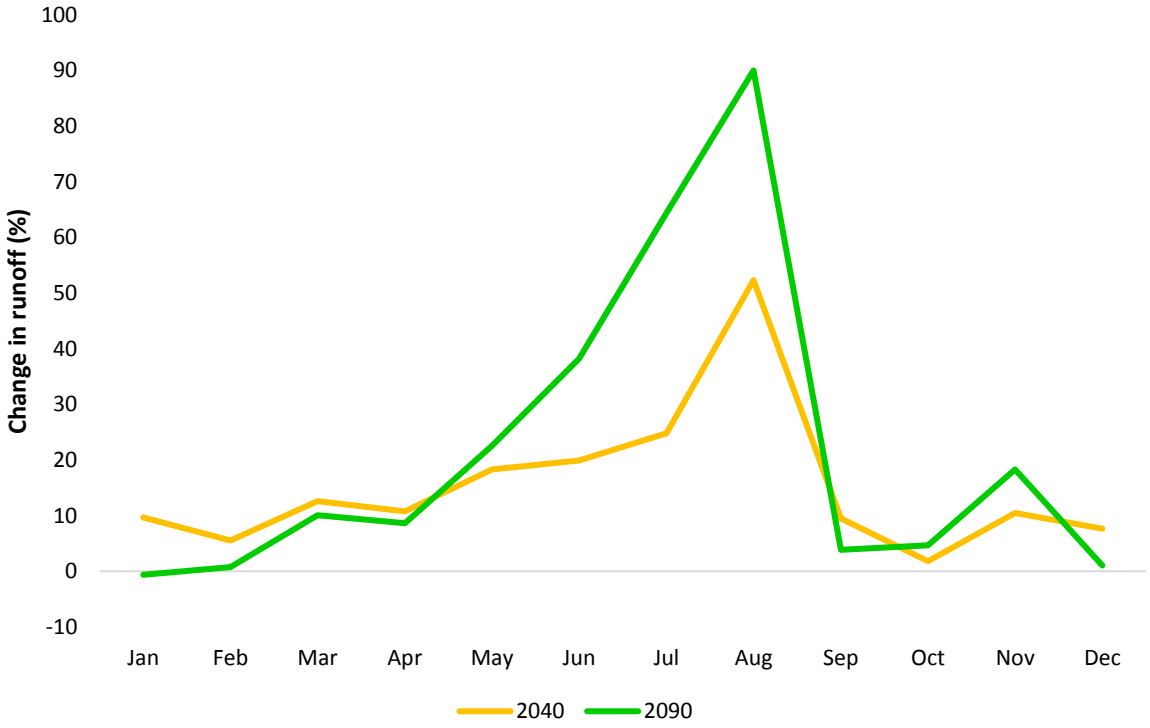

Figure 5.2: *Monthly percentage changes in HBV-Lights predicted future runoff scenarios from the observed baseline.*

5.1.1 Precipitation and Temperature influences on Runoff

The comparison of seasonal runoff changes and projected changes in precipitation can help identify water balance factors that may be influencing such changes to catchment runoff. The projection of precipitation and runoff for both 2040 and 2090 suggests that it is not just changes in precipitation driving increased runoff (Fig. 5.3 & 5.4). Both 2040 and 2090 display similarities in their respective precipitation and runoff for the summer and autumn seasons, but differs significantly during the winter and spring months. Runoff increases in July and August by a greater magnitude than precipitation in both 2040 and 2090, and decreases in September.

Therefore, it is suggested that other water balance components than just precipitation are influencing the projected changes during winter and spring.

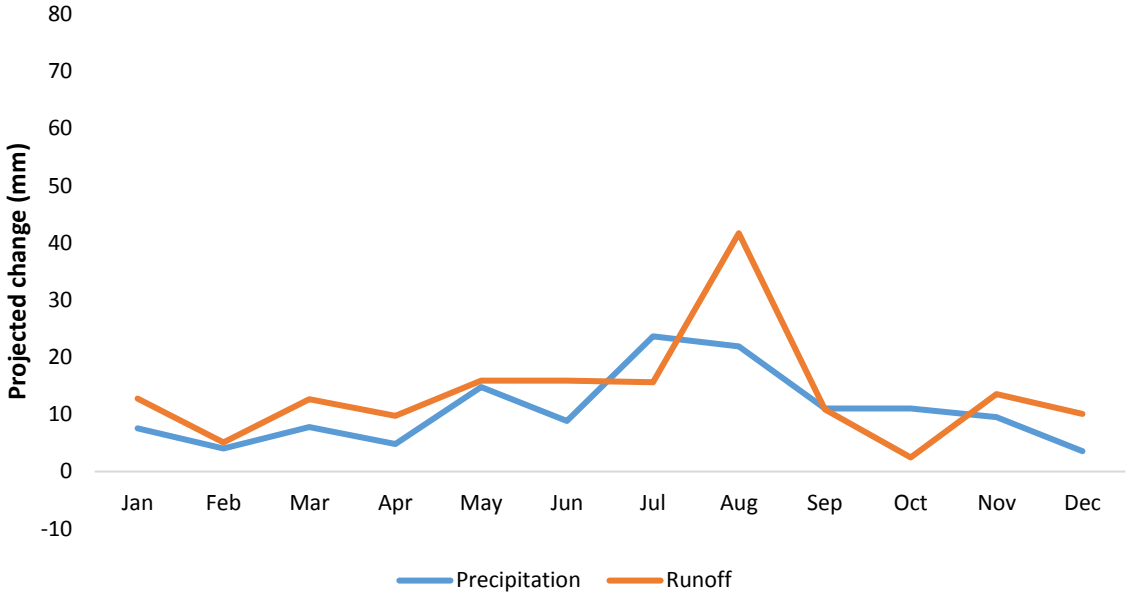

Figure 5.3: *Comparison of predicted future changes to precipitation (modelled by NIWA) and runoff (modelled by HBV-Light) in 2040.*

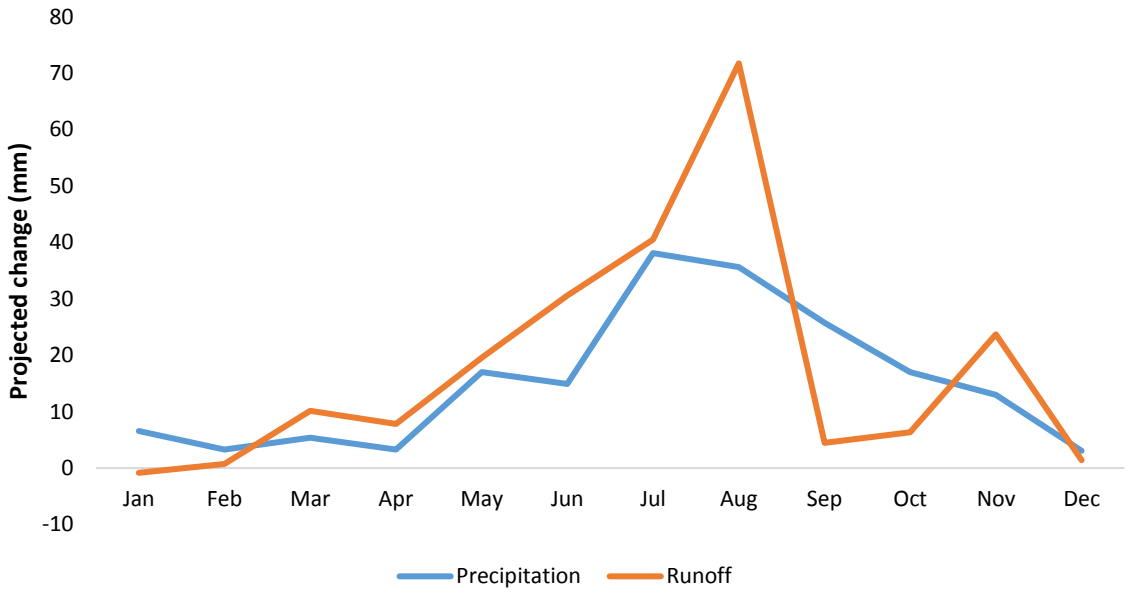

Figure 5.4: *Comparison of predicted future changes to precipitation (modelled by NIWA) and runoff (modelled by HBV-Light) in 2090.*

Changes to precipitation are evident in Figures 5.3 & 5.4, however the amount of change is important. The increase in magnitude of precipitation for the top five percent of rainfall events

used as input data to run HBV-Light (Fig. 5.5) shows how the ensemble of GCMs predict larger rainfall events. The differences between the largest precipitation event of 1990 and 2040 is 20 mm, and 77 mm for 2090. The highest two percent of precipitation days appears to be of a higher magnitude in the future periods compared to the baseline.

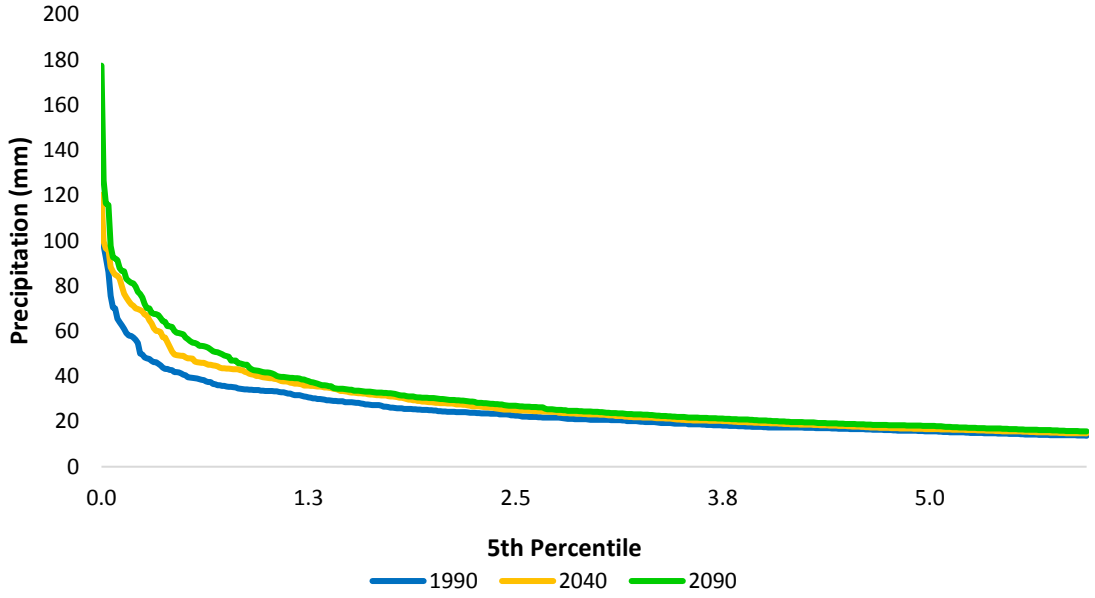

Figure 5.5: *Comparison of changes to the top 5th percentile of precipitation between the observed baseline and the simulated 2040 and 2090-time periods.*

Temperature and precipitation increases are expected in New Zealand over the next 100 years (IPCC 2000, 2007; MfE 2008). Figure 5.6 displays how temperature is expected to rise within the Shotover Catchment on average by 2˚C warmer in 2090 than the 1990 average of 8.4℃. There appears to be no change to the temperature in spring between 1990 and 2040 when most of the snowpack would be expected to melt. The expected increase in precipitation is most pronounced from April through to December (Fig. 5.7). The greatest monthly increase between 1990 and 2090 is in July, not during the peaks of both time periods that occur in August. The amount of precipitation increase appears to be larger between 1990 and 2040 compared from 2040 to 2090, suggesting the rate of precipitation increase declines over the 100-year simulation period.

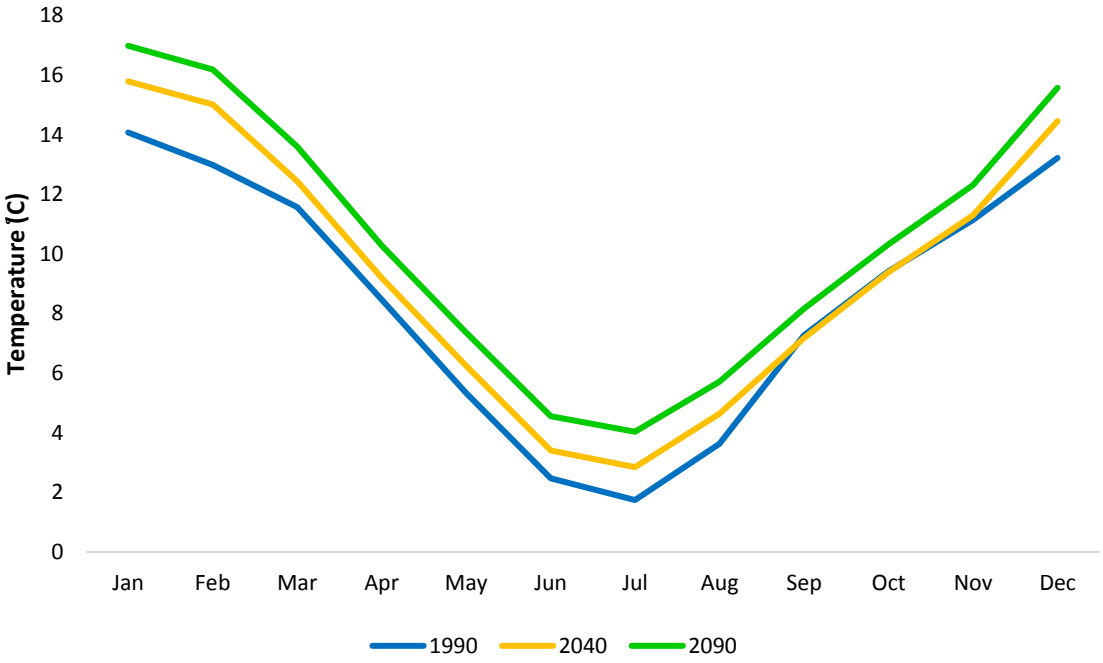

Figure 5.6: *Expected changes to average monthly temperature from the observed baseline period to the predicted future 2040 and 2090-time periods.*

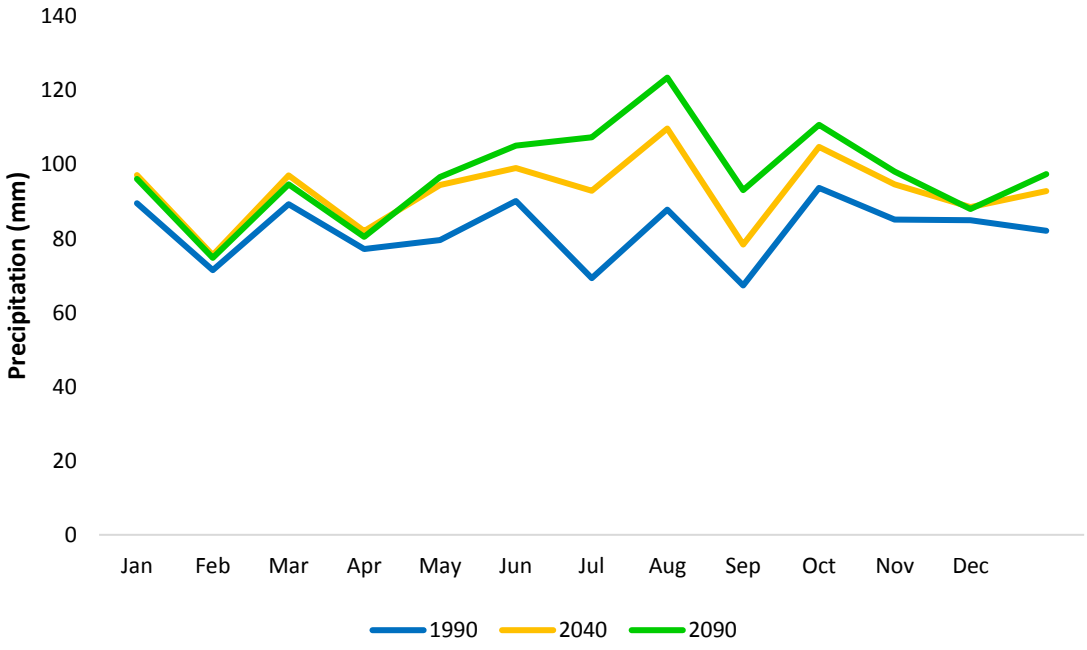

Figure 5.7: *Expected changes to precipitation from the observed baseline period to the future predicted 2040 and 2090-time periods.*

5.1.2 Changes in Intermediate Model Variables

The snowpack output for 2040 and 2090 shows a decrease (Fig. 5.8) from the baseline. The 2040 scenario shows a slight decrease in the amount of snow stored in the catchment for August and September, where from October to December, and January until March, the suggested rate of snow melt is equivalent to that of the 1990 baseline. There is a large decrease in snowpack for 2090 compared to both 1990 and 2040. The snowpack for the second half of the 2090 scenario (June to December) is significantly less, and appears to flatten out over winter without reaching a sharp peak in August like that of 2040 and 1990. The yearly snowmelt contributing to runoff in 2090 compared to 1990 decreases by 41.7 %.

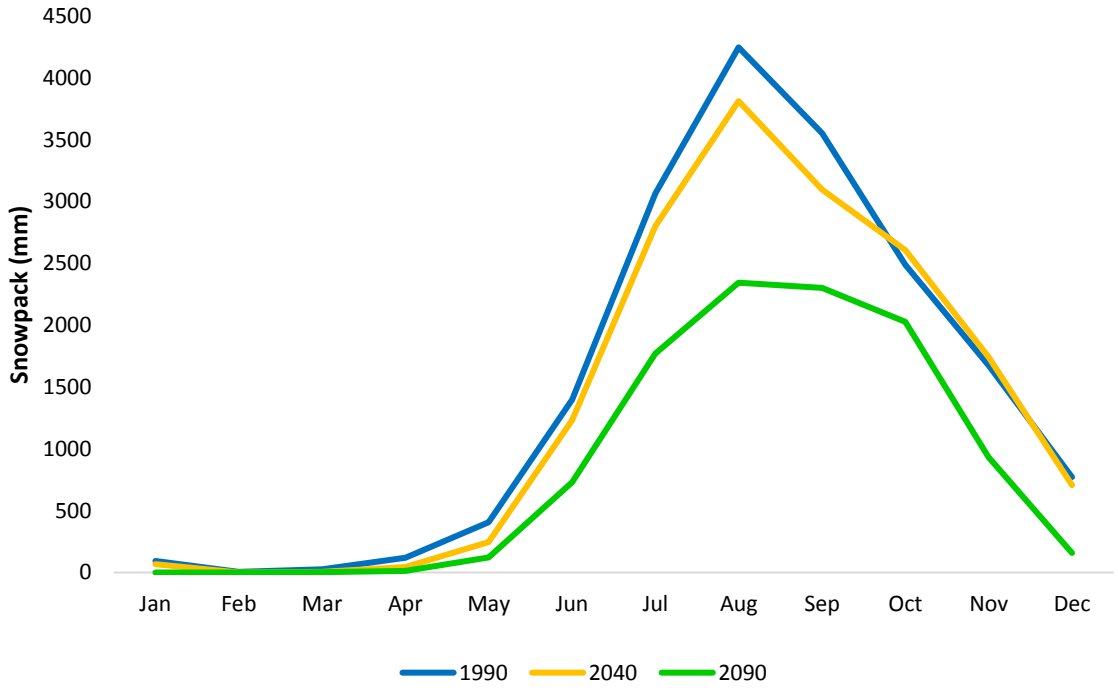

Figure 5.8: *Modelled changes to the snowpack as predicted through HBV-Light from the baseline period to the future 2040 and 2090-time periods.*

The QSTZ variable in HBV-Light is the contribution to runoff controlled by the K0 parameter. Therefore, it is reasonable to infer that QSTZ corresponds approximately to infiltration excess runoff (IER) in other hydrological models, like TopNet. The (IER) can help show how much of a precipitation event is channelled through the system when the soil infiltration capacity is reached. The IER is shown to increase in both the 2040 and 2090 scenarios under HBV-Light. In comparison to the baseline, August is where IER peaks in 2040 and 2090, unlike 1990 which peaks in November, and has a similar magnitude of IER in March. 2040 also a peak in

November that is the same height as August, while 2090 shows the same November peak but however, is not to the same magnitude as in August. The IER for both future scenarios are concentrated around the late winter early spring months (Fig. 5.9), the same months where there is a maximum increase in precipitation (Fig. 5.3 & 5.4).

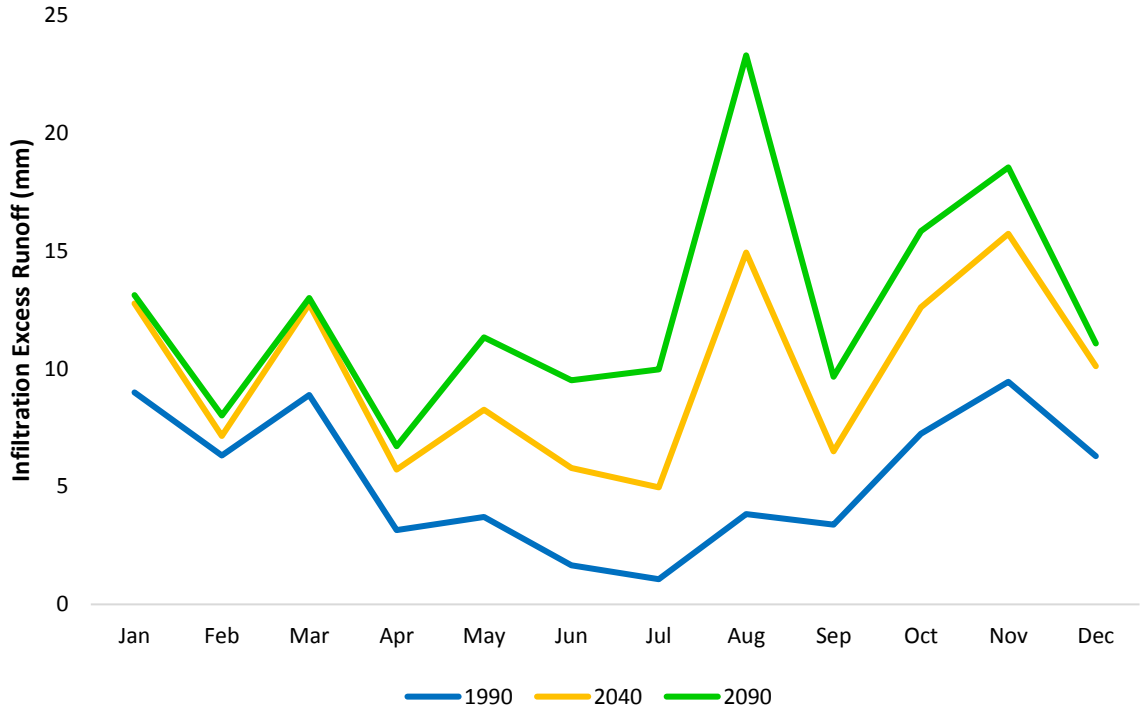

Figure 5.9: *Comparison of changes to infiltration excess runoff (IER) between the baseline period and future 2040 and 2090-time periods as modelled by HBV-Light.*

The IER as a percentage of runoff increases from 5.2 % in 1990 to 8.4 % in 2040 and 10.3 % in 2090 (Table 5.1). The IER as a percentage of runoff effectively doubles from 1990 to 2090, while at the same time the snowpack for 2090 is half that of 1990 (Fig. 5.8). The 20-year mean runoff average for each time period are also be numerically summarised in Table 5.1, clearly showing a larger increase in runoff between 1990 and 2040 (a 13.4% increase), than that of 2040 and 2090 (an extra 4% increase).

Table 5.1: Comparison of projected changes to mean annual runoff and infiltration excess runoff (IER) as modelled by HBV-Light, between the 1990 baseline period and future 2040 and 2090-time periods.

Year	Runoff (mm)	Runoff increase (mm)	Runoff increase (%)	IER (mm)	IER (%)
1990	1238.4	-	-	64.0	5.2
2040	1404.7	166.3	13.4	117.3	8.4
2090	1454.3	216.0	17.4	150.1	10.3

5.2 Comparison of HBV-Light and TopNet

Understanding and quantifying the potential effects that future climate change could have on available freshwater resources are of great importance, especially in New Zealand, where agriculture and human consumption is heavily dependent on the freshwater resource. Streamflow represents the integrated response of almost all catchment characteristics, and is essential to quantify such changes to runoff as any variation in flow could result from impacts associated with hydrologic inputs from the surrounding catchment area (Jiang *et al.* 2007). As climate change is expected to influence all aspects of catchment hydrology and not just runoff, this study will compare the outputs of soil moisture, snow, AET and IER between HBV-Light and TopNet.

The variation of 12 individual GCM runoff projections for 2040 (Fig. 5.12) and 2090 (Fig. 5.13) will also be displayed as a percentage increase from the 1990 baseline scenario. All other comparisons are expressed as actual projected change from HBV-Light and TopNets respective baselines. Comparisons between hydrological response variables of 20-year monthly average runoff (Fig. 5.10 & 5.11), soil moisture (Fig. 5.14), snowpack (Fig. 5.15) and AET (Fig. 5.16) for outputs from both HBV-Light and TopNet will be made for the 2090-time period, as it is the most uncertain period due to the potential increased variation of climatological conditions from the present.

5.2.1 Comparison of Projected Change in Annual Runoff

For the 2040 scenario period (Fig. 5.10), HBV-Light simulates higher runoff compared to TopNet. The average of the 12 GCMs differs from a runoff increase of 13.4% for HBV-Light and 10.3% for TopNet, a difference of 3.1%. HBV-Light has a smaller range of GCM runoff projections from 7.9% to 21% (13.2%) while TopNet has a GCM output range of 2.3% to 23.8% (21.5%). Only GCM 6 predicts a higher runoff increase by TopNet than HBV-Light in 2040. In comparison, the 2090 scenario (Fig. 5.11) shows TopNet has a higher increase in

potential runoff. The average of the 12 GCMs suggest that TopNet projects an increase in runoff at 18.9%, and HBV-Light an increase of 17.3%, a difference of just 1.7%. Like 2040, HBV-Light has a smaller range (6.1 to 29.1%) of projected GCM runoff outputs compared to TopNet (1.4 to 37.9%), with ranges of 23% and 36.6% respectively. Unlike 2040, the GCM projections show HBV-Light to simulate less runoff in 9 of TopNets 12 projected GCM outputs, where the three GCMs that simulate higher runoff (GCMs 2, 7 & 10) are all less than 10%.

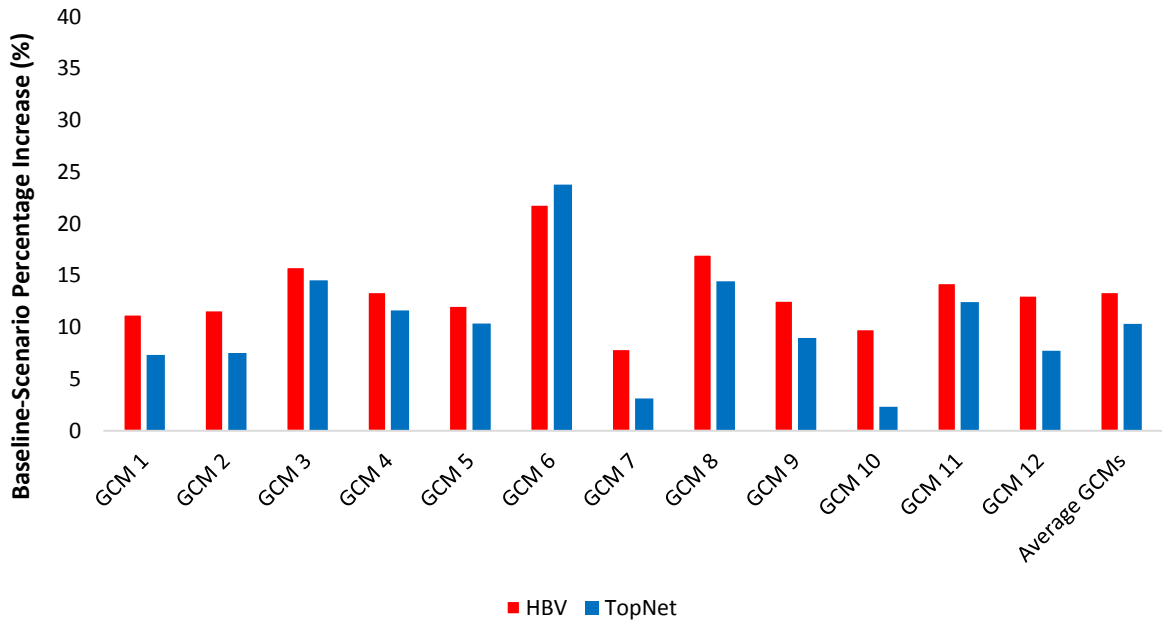

Figure 5.10: *Comparison of the changes to runoff for 12 individual GCMs and the average GCM mean ensemble as modelled by HBV-Light and TopNet for the 2040-time period.*

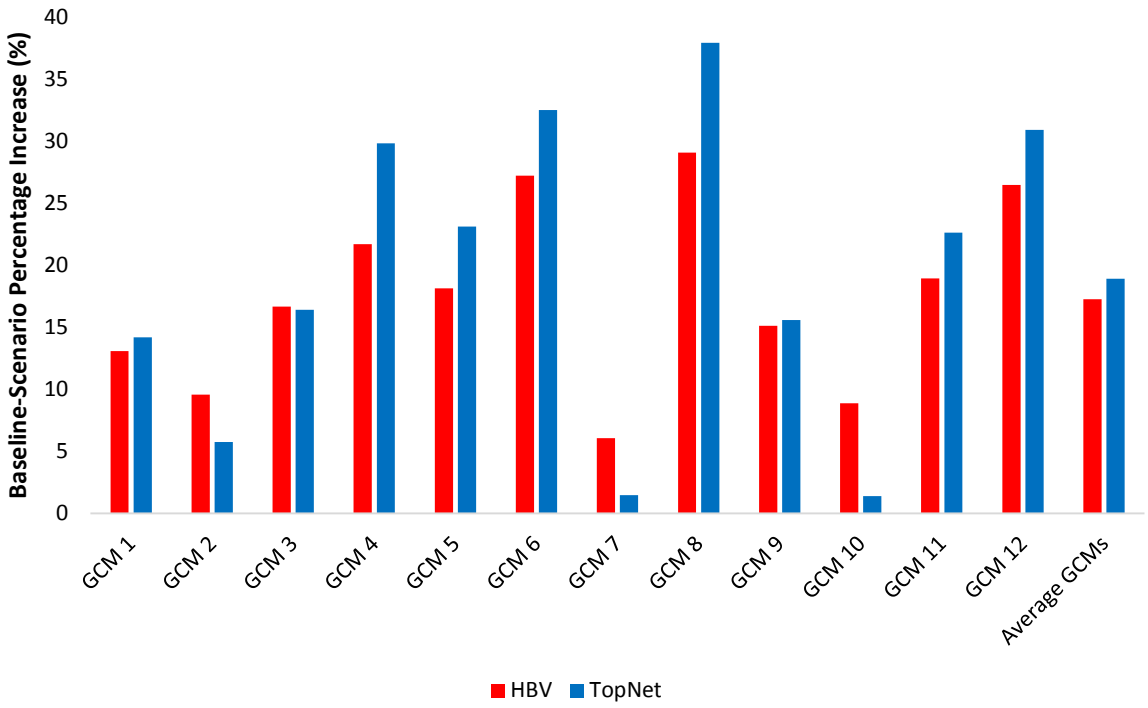

Figure 5.11: *Comparison of the changes to runoff for 12 individual GCMs and the average GCM mean ensemble as modelled by HBV-Light and TopNet for the 2090-time period.*

5.2.2 Comparison of Projected Change in Monthly Runoff

Figures 5.12 and 5.13 show projected change in monthly Shotover Catchment runoff for the 2040 and 2090 future scenario periods, using individual GCM forcing as well as the ensemble mean and 1990 baseline mean. HBV-Light's GCM spread is wider than TopNets for the 2040-time period. The months from January to July show a slight increase in mean runoff in HBV-Light compared to TopNet that shows none. For July and August HBV-Light projects an increase in runoff for all 12 GCMs scenarios, two months earlier than TopNet, which suggests the expected increase in runoff begins in the spring time months of September and October.

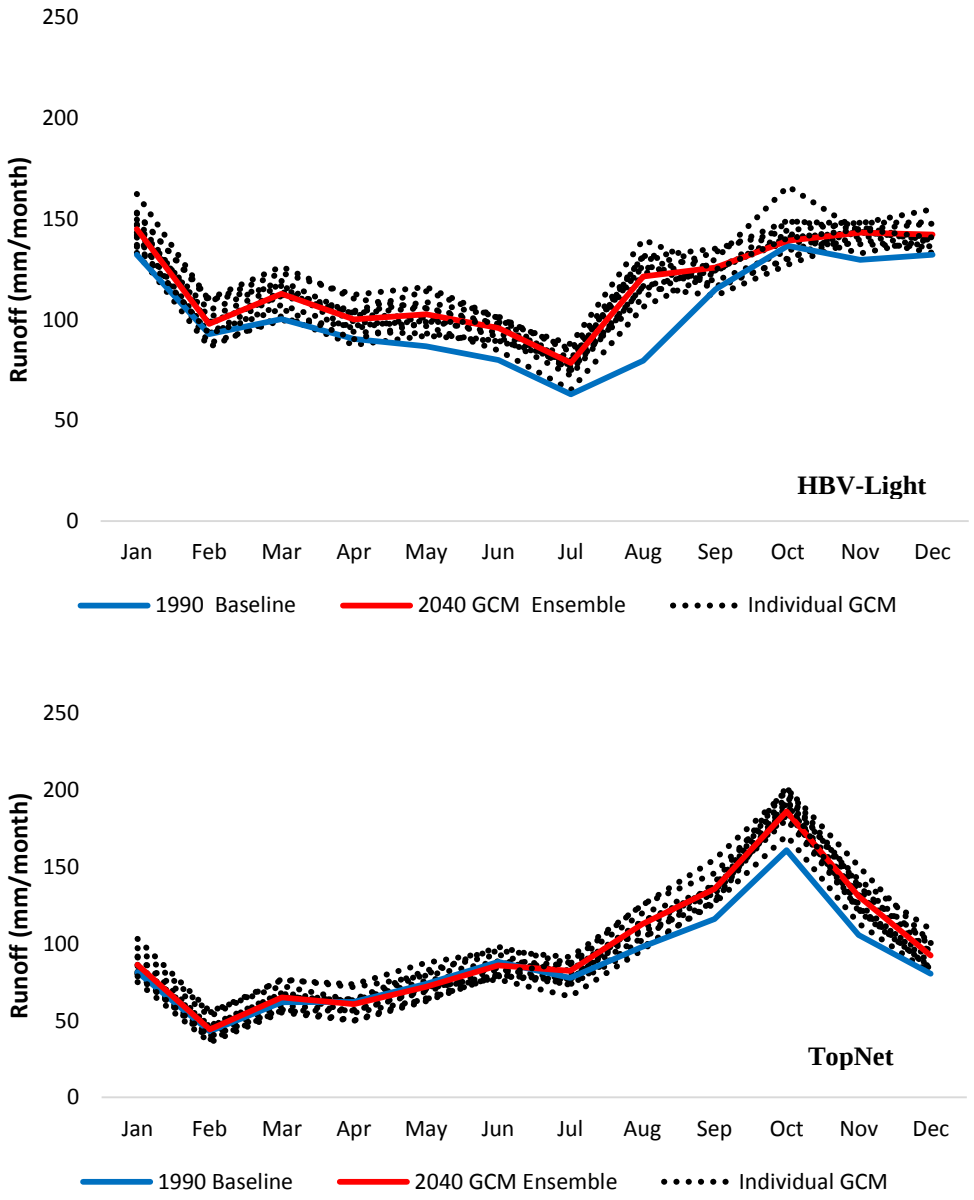

Figure 5.12: *Representation of the spread in monthly runoff for the 12 individual GCMs, and the GCM ensemble mean.*

The 2090 model outputs (Fig. 5.13) have a wider degree of variation compared to 2040 for both hydrological models. HBV-Light's mean ensemble begins to deviate from the baseline as early as March (autumn), whereas TopNets mean ensemble begins later in autumn, May and June. The majority of TopNet GCMs (10) suggests an increase in early spring runoff, where HBV-Light shows no increase in spring runoff. The baseline scenarios of HBV-Light and TopNet differ slightly as well. HBV-Lights baseline decreases from March through to July, whereas TopNet increase steadily from February until June, and increases again from July

through to October. The summer time GCM spread for HBV-Light is more varied than that of TopNets, suggesting more uncertainty in the higher runoff flow of HBV-Light.

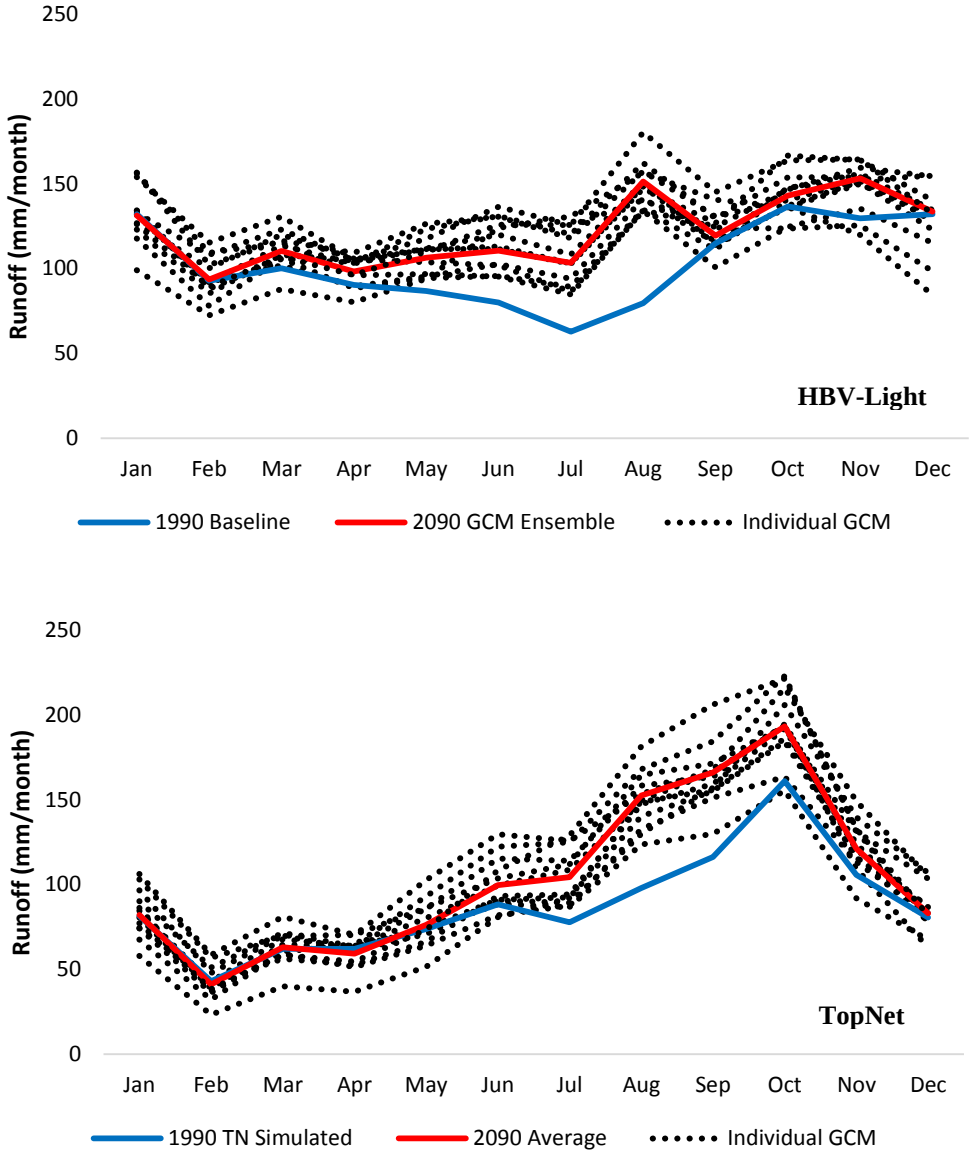

Figure 5.13: *Representation of the spread in monthly runoff for the 12 individual GCMs, and the GCM ensemble mean.*

5.2.3 Comparison of Water Balance Components

The soil moisture comparisons for 2090 between the two models appear the same (Fig. 5.14). Both models display an increasing soil moisture content from February through to June, where HBV-Light decreases slightly for the winter month of June, and then peaks in August, almost in exact replication of TopNet. From spring, through to early summer HBV-Light simulates soil moisture to the same level as TopNet visually. Quantitatively however, HBV-Light under-

estimates TopNet soil moisture by 300 mm/yr^{-1}. The range of monthly soil moisture values differs greatly. TopNet has a maximum of 832 mm/month for August, and a minimum of 183 mm/month for February. HBV-Light like TopNet has a maximum soil moisture content in August, and minimum in February, however as stated, is under-estimated significantly, with a maximum content of 267 mm/month and minimum of 36 mm/month.

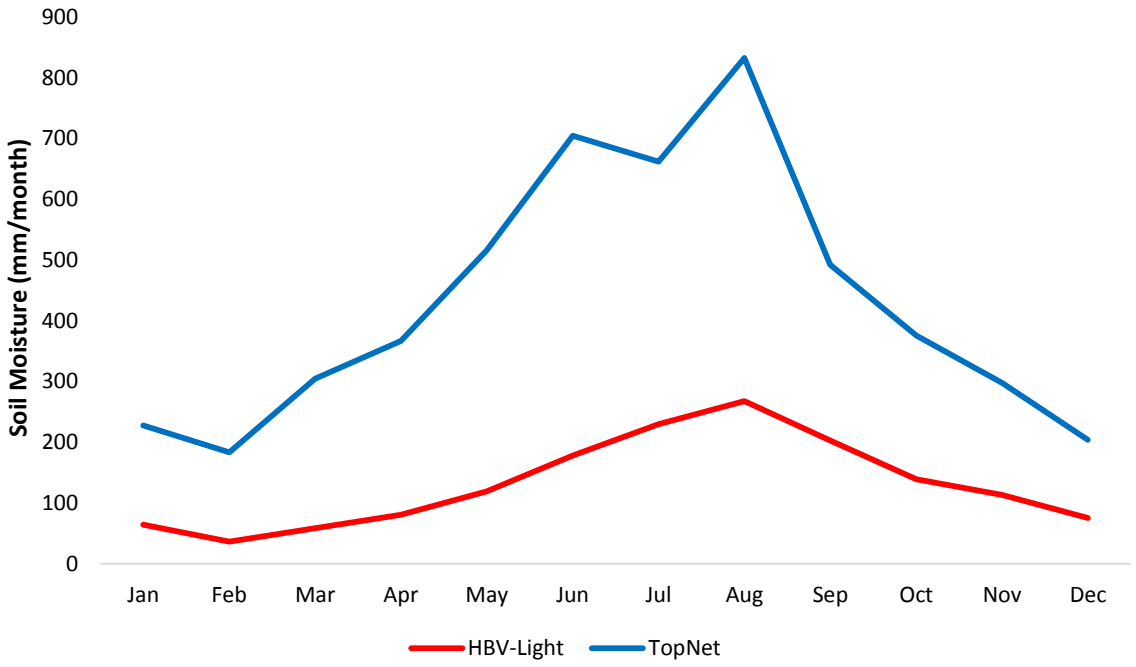

Figure 5.14: *Comparison of the amount of soil moisture present within the Shotover Catchment for the 2090-time period as projected by HBV-Light and TopNet.*

The amount of snow in a system is quantified differently between HBV-Light and TopNet. HBV-Light measures snow as the amount of frozen water (mm) stored in the catchment, whereas TopNet works out the amount of snowmelt that is contributing to runoff (kg/m^2). Therefore, it is beneficial to analysis both model's estimation of snow in the catchment on separate axis, and comment on the observable monthly changes (Fig. 5.15). HBV-Light follows a standard rate of freezing and melting cycle, where late autumn (April and May) the temperature in the catchment is cold enough to store snow, and melt time begins in late winter (August), as previously stated earlier. TopNet, even though is displaying the amount of snowmelt to contribute to runoff, suggests that once warmer temperatures in spring are present, the rate of melt water contributing to runoff steadily decreases.

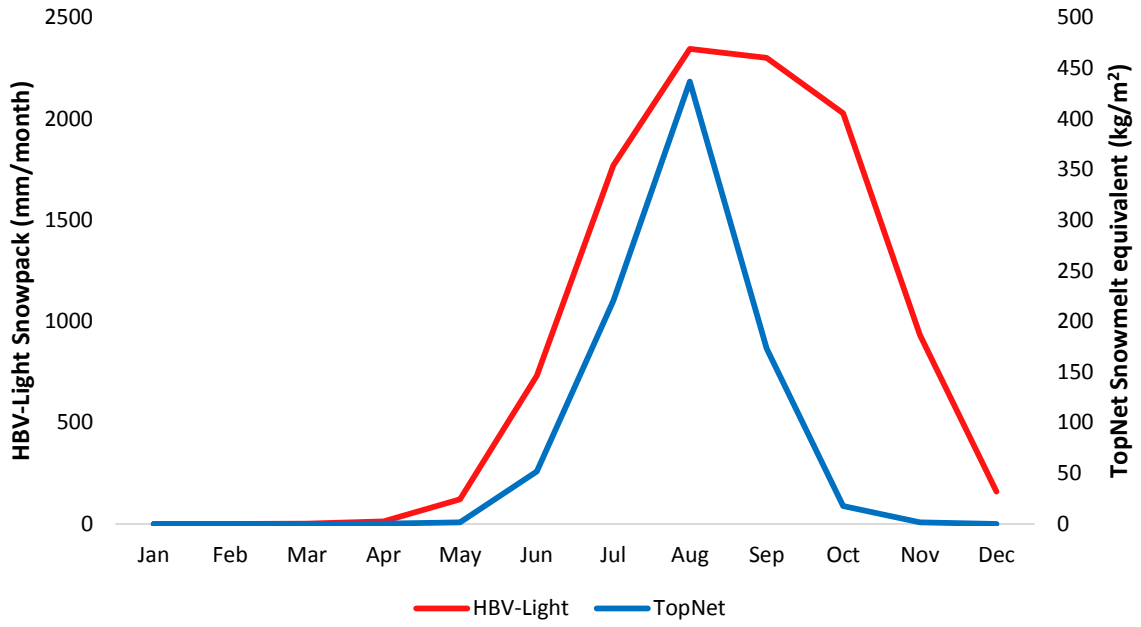

Figure 5.15: *Comparison of snow storage within the Shotover Catchment as projected by HBV-Light and TopNet for the future 2090-time period.*

Actual evapotranspiration (AET) is similar to soil moisture in that the visual similarity between HBV-Light and TopNets output is good (Fig. 5.16). HBV-Light simulates AET to decrease from March to June, then begins increasing in August, until AET peaks in the beginning of September. TopNet however, projects AET increases from July to the peak in October. HBV-Lights AET increases from November to December where as TopNet decreases continuously from October, however, in January HBV-Light suggests AET will decrease at a steeper rate than that of TopNets simulated AET.

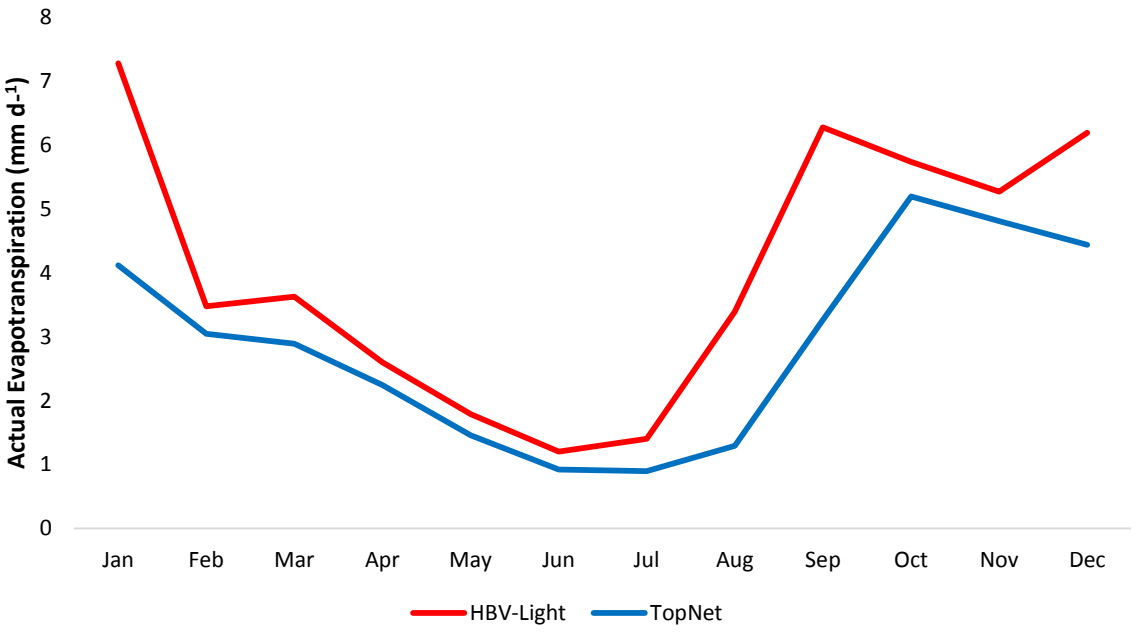

Figure 5.16: *Comparison of the actual evapotranspiration as projected by HBV-Light and TopNet for the future 2090-time period.*

5.3 Summary

In this Chapter, the potential changes to catchment hydrology and their water balance variables under future climate forcing, as simulated through the HBV-Light hydrological model were analysed (Section 5.1), which were then compared to the possible impacts as modelled by TopNet (Section 5.2). Future monthly runoff is suggested to increase in both 2040 and 2090 as simulated by HBV-Light, with 2090 expected to increase its monthly runoff for August by double that of the baseline period (a 90 % increase). Actual changes to precipitation were plotted against runoff for both future scenarios, where the inference was made that precipitation alone was not responsible for the increase in runoff later winter, as runoff increased by a greater magnitude than precipitation during the winter and spring months. The amount of precipitation stored in the catchment as the snowpack was then analysed. It was suggested that the snowpack, and therefore contribution of snowmelt to runoff, is set to decrease by almost half from the baseline period to the 2090 scenario (41.7 %), but snowpack from the baseline to 2040 only decreases by 8.3 %, while all three periods continue to show signs of melt from early spring (September). Finally, the impact on infiltration excess runoff (IER) was analysed to better understand how high precipitation events would behave when moving through the catchment. HBV-Light suggests that excess runoff as a percentage of runoff will increase by roughly 50%

from 1990 (5.2 % of runoff) to 2040 (8.4 % of runoff), and again from 2040 to 2090 (10.3 % of runoff).

Table 5.2: Summary table for key changes to yearly variables from 1990 to 2040 and 2090 as simulated by HBV-Light.

Time period	Precipitation (%)	Temperature (°C)	Yearly (%)	Snowmelt (%)	Soil moisture (%)	AET (%)	IER (%)
2040	13	1	13.4	-8.30	28.10	11.20	8.40
2090	18.6	2	17.4	-41.7	16.8	17.0	10.3

The second section of the chapter (Section 5.2) focused on the comparisons between HBV-Light and TopNets runoff, soil moisture and AET outputs for the 2090-time period in order to gain a sense of how realistic HBV-Light reproduces the impacts that climate change could have on freshwater compared to an already proven, albeit more complex hydrological model. The 20-year average for an ensemble of 12 GCMs suggests in 2040 that HBV-Light over-estimates the percentage increase as modelled by TopNet. All bar one GCM (GCM 6) showed HBV-Light to over-simulate TopNet. In contrast, the GCM ensemble suggests HBV-Light underestimates the increase in runoff modelled by TopNet, where 3 out of the 12 GCMs (2, 7 & 10) showed HBV-Light to overestimate TopNets runoff. The monthly spread of GCMs for 2040 shows an earlier increase in runoff as modelled by HBV-Light (July & August), than that of TopNet (September and October). The 2090 GCM spread suggests a much earlier increase in runoff from May to August as modelled by HBV-Light, whereas the TopNet models an increase in runoff for July and September only. The soil moisture contents of both models show similar monthly variation, however the quantification of HBV-Lights soil moisture consistently under-estimates that of TopNet by 300 mm/yr^{-1}. Finally, the visual comparison of AET suggests HBV-Light increases earlier from July to September, whereas TopNet suggests a similar increase in AET although beginning later in August, through to a peak in September.

Chapter Six
Discussion

The ability to understand future climatic changes to precipitation and temperature, and the associated changes to catchment processes such as storage, evapotranspiration, soil moisture, snow melt and infiltration allows for more robust analysis of the future impacts climate change could have on New Zealand's freshwater catchments. Understanding such changes also requires detailed knowledge of the surrounding uncertainty of input data, model structure, calibration and the uncertainty surrounding the outputs, before any conclusions are drawn on overall runoff output. Despite the acknowledged limitations of distributed conceptual hydrological models, researchers continue to use and refine such models for climate change impact assessments, due to their relatively cheap and time efficient calibration advantage that otherwise would be introduced through physically based field work calibration.

The comparison of simulated runoff between models of differing complexity could yield benefits for any research that is economically, temporally quantitatively challenged, and wishes to substitute a fully-distributed hydrological model for a semi-distributed hydrological model such as HBV-Light. The aim of this research was firstly to determine whether a relatively simple hydrological model can realistically simulate an observed flow in an alpine catchment in New Zealand. Secondly, if a simple model can realistically simulate an alpine flow, compare projected future climate change impacts on river flow between the simple hydrological model and that of a complex model. On that basis, the following chapter is divided into three parts. Firstly, in section 6.1, the results of HBV-Lights impact assessment of future climate change under the A1B scenario, and the possible reasons for changes to catchment runoff and processes are discussed. Section 6.2 highlights key differences between the two hydrological models that could contribute to the respective assessments made surrounding future climate forcing and the impact to catchment hydrology. The differences in model outputs of catchment processes such as snowmelt, soil moisture and actual evapotranspiration (AET) are evaluated and commented on in Section 6.3. Section 6.4 attempts to evaluate the key differences between the two models and justify which model is more suitable within the New Zealand context. Section 6.5 details the uncertainty of hydrological modelling and limitations surrounding the research in question

are reviewed, where possible improvements to model performance is discussed, followed by a summer of the chapter in Section 6.6.

6.1 HBV-Lights Simulation of Climate Change

HBV-Lights validation period indicated the model was sufficient in representing an observed river flow within the Shotover Catchment (Section 4). Therefore, the next step in this research was to run the model with climate forcing data, to gauge what would happen to water balance components under an increase in annual temperature of 1 ˚C (2040) and 2 ˚C (2090) under the A1B scenario (MfE 2008) for two future time periods; 2030 to 2049 and 2080 to 2099 respectively. In the Shotover catchment, HBV-Light suggests through the GCM ensemble mean that both time periods would see an increase in monthly runoff (Fig. 5.1), with the largest increase occurring in winter (Fig. 5.2). Thus, through the use of monthly runoff figures (Fig. 5.1) and percentage change of future runoff (Fig. 5.2) as modelled by HBV-Light, it is evident that climate change will increase the amount of runoff, but reduce the range of runoff between the highest and lowest months in 2090 compared to the baseline within the Shotover Catchment.

6.1.1 Annual changes in runoff

The seasonal changes identified for the 2040 and 2090 time periods also suggest climate change will have an impact on annual runoff within the Shotover Catchment (Table 5.1). It is predicted that in 2040 runoff per year will increase by 13 % (166.34 mm) and 17 % (215.99 mm) in 2090. Poyck *et al.* (2011) predicted streamflow for the Clutha catchment using the same ensemble of 12 GCMs as this current research, and found that there would be an increase of around 6 % in 2040, and 10 % in 2090, lower than that of HBV-Lights prediction. Gawith *et al.* (2012) suggested that runoff in the Matukituki Catchment would increase by 7 % in 2040 and 13 % in 2090, while for the Lindis Catchment, increases of 10 % and 20 % were recorded for 2040 and 2090 respectively. The spread of annual average increases in runoff seem to be relatively consistent between all of the Clutha sub-catchments studied, with the relatively minor differences of 3−7% explained by either change in catchment specific precipitation or model assumptions between HBV-Light (Shotover) and TopNet (Matukituki and Lindis). In regard to the projections of annual runoff increase as suggested by HBV-Light, the model appears to be in line with current research for annual runoff increase in the surrounding catchments (Gawith *et al.* 2012). The ability to reproduce annual changes to runoff under climate change gives credibility to the overarching research question of whether or not HBV-Light is complex

enough to produce potential climate change impacts on future river flow to the same standard as TopNet, detailed more in Section 6.2.

6.1.2 Seasonal changes in runoff

The extent of autumn and winter runoff change as modelled by HBV-Light (Fig. 5.2) where autumn and winter is expected to see a large increase in runoff, as high as 90 % in August, is somewhat different to previous studies of climate change impact assessment conducted within the same Catchment, the Clutha, and two of its tributaries, the Matukituki and the Lindis sub-catchments. A climate change impact assessment study similar to the present research was carried out on the Matukituki (799 km^2) and Lindis (1045 km^2) catchments, sub-basins of the Clutha Catchment (21,960 km^2), the same catchment that the Shotover (1078 km^2) is a sub-catchment of. Gawith *et al.* (2012), using TopNet, suggested that the largest increase in runoff for the 2090 Matukituki Catchment will occur close to the lowest monthly baseline flow, in August, the same timing as seen with HBV-Light for the Shotover (Fig. 5.2). For the second catchment studied by Gawith *et al.* (2012), the Lindis, the highest suggested 2090 monthly runoff increase occurs in August, the same month as suggested for the Matukituki and by HBV-Light for the Shotover. The difference being however, that in the Lindis, the largest runoff increase occurs during the highest baseline flow which is August, where in contrast HBV-Light displays October having the highest monthly baseline flow, the same as the Matukituki.

The observed differences in peak flow within the baselines of the Matukituki, Lindis and Shotover rivers respectively can be attributed to the different physical environments, and could be why the 2090-time period displays runoff peaks that vary between the three rivers. The Matukituki and Shotover Catchments are closer to the main divide of the Southern Alps and therefore receive more precipitation, up to 5000 and 7500 mm/year respectively in the headwaters, whereas the Lindis is further east in more of a potential rain shadow, only receiving between 500-1000 mm/year. Due to the elevation of the Matukituki (300-3000 masl) and Shotover Catchments (300-2525 masl) being considerably higher than the Lindis (220-1925 masl), there are lower temperatures and more snow accumulation which contributes to snowmelt and hence more runoff during the warmer spring months. As there are no glaciers in the Lindis Catchment the overall influence of snow storage and consequential melt is small, as only seasonal snow melt contributes to runoff which in comparison to the Shotover and Matukituki Catchments is small, and is why the Lindis catchment experiences low flows in summer (Poyck *et al.* 2011).

The similarities between the physical environments of the Matukituki and the Shotover catchments compared to the Lindis Catchment provides the basis for interpretation of the results. As there are similarities between the results of HBV-Lights climate change impact assessment of the Shotover and TopNets representation of the Matukituki Catchment, and that there are similarities between the catchment characteristics of the two, it is highlighted that HBV-Light appears to provide physically realistic simulations of future climate change impacts. The difference in characteristics between the Shotover and the Lindis Catchments, and the respective differences in peak runoff results also suggest HBV-Light responds well in representing the impacts that climate change could have on freshwater resources in the Southern Alps.

Running HBV-Light with the GCM ensemble for runoff shows an increase of up to 50 % in 2040 and 90 % in 2090 for August (Fig. 5.2). The magnitude in runoff changes as modelled by HBV-Light from the baseline is somewhat unexpected as other studies suggest smaller increases in 2090 for August of around 50% in the Lindis, 46% in the Matukituki (Gawith *et al.* 2012), and 37 % for the Clutha (Poyck *et al.* 2011). Furthermore, the timing of seasonal change is different between the Clutha and some of its sub-catchments. The Shotover Catchment shows increases in runoff using the GCM ensemble mean from February through to December for 2090 (Fig. 5.2), April to October for the Matukituki and May through to October for the Lindis (Gawith *et al.* 2012). For the Clutha, seasonal changes to runoff only see increases for June to early October (Poyck *et al.* 2011), but the three smaller sub-catchments of the Clutha (Shotover, Matukituki and Lindis) see similar periods of increased runoff, or at least see increases earlier in the year compared to the Clutha.

The result of studies by Poyck *et al.* (2011), Gawith *et al.* (2012) and this current one can indicate how the location and the scale of a catchment influences changes in runoff and potentially how different catchments will respond to climate change, as all three of the respective research methods are very similar. Although the research by Poyck *et al.* (2011) was conducted in the Clutha Catchment as a whole, the runoff output was focussed near the catchment outlet close to Balclutha. Runoff at the outlet for the Clutha Catchment is dominated by what happens in the headwaters such as the Shotover, Matukituki and Lindis Catchments, however the size of the catchment, roughly 22,000 km^2, which dampens the variability of high flow events in the upper catchment. For catchments such as the Shotover, Matukituki and the Lindis, all of which are considerably smaller than the Clutha will show high precipitation

events corresponding with a greater or more pronounced runoff response, as a smaller volume of water takes less input to register change (McGlynn *et al.* 2004). For the same magnitude of seasonal runoff change to be seen in the Clutha outlet point, more of the Clutha's tributaries upstream must undergo changes to seasonal runoff as the volume of the Clutha is so large. For all of the tributaries to undergo pronounced runoff increases large enough to influence a runoff response in the Clutha, to the same magnitude and frequency as the smaller tributaries can experience, there would need to be a relatively large-scale climate event. The location of all the tributaries means that very rarely all the tributaries will receive precipitation at once, indicating the scale of the Clutha is so large that the locations of the tributaries play a significant role in its runoff, as not all tributaries receive the same changes to precipitation. Therefore, for the impacts of climate change to influence the Clutha in the same magnitude as the smaller Matukituki, Lindis and Shotover tributaries, a large majority of the tributaries will need to be impacted by climate change and receive relatively the same increases or decreases in precipitation.

The extra months that see increases in runoff for sub-basins of the Clutha (Shotover, Matukituki and Lindis), and how the Clutha does not, could be attributed to a lagging effect. As the distance from the headwater catchments to the Clutha outlet is so large, the extra increase in runoff could be lost to storage processes such as evaporation, groundwater, or consumption uses like irrigation and drinking supply for towns. Therefore, any noticeable increase in runoff at the Clutha end due to the length of the river and its volume could require a gradual build-up of increases to runoff in the sub-catchments further inland, like the Shotover. Hydrological modelling of mesoscale catchments is often adversely affected by a lack of adequate information about specific site conditions (Montzka *et al.* 2008). The amount of lag present in the Clutha catchment is currently unknown to the authors, and quantifying a time frame that takes into account all the sources that could contribute to a lag effect, and therefore lack of information, can still be a large source of uncertainty (McGlynn *et al.* 2004).

Comparison of Koedyk and Kingston (2016) to this current research is useful as it is some of the only literature to use HBV-Light for impact assessment of climate change in New Zealand, Koedyk and Kingston (2016) reported increases of monthly runoff highest in July (around 50 % increase), with a continuous decline in increased runoff from August through to October using HBV-Light, however the magnitude of increase in 2090 was half that of this research conducted in the Shotover. Koedyk and Kingston (2016) used the Waikaia Catchment in

Southland, New Zealand, a tributary of the larger Mataura River. The Waikaia is considered to be more of a 'natural flow regime' as water abstraction and land use changes are negligible (Koedyk and Kingston 2016) rather than a steep alpine river, and is much further east of the main divide, receiving higher mean annual rainfall of 950 mm in the lower catchment compared to the Shotover (500 mm). There are reports however of catchment precipitation in the headwaters of the Shotover range up to 7500 mm (Tait et al. 2006), whereas areas such as Old Mans Range which is on the north-east boundary of the Waikaia receives between 1500 and 2600 mm annually (McGlone *et al.* 1997).

The scenarios used in Koedyk and Kingston (2016) were different than those used in this research. The authors opting to use QUEST-GSI (Todd *et al.* 2011) which presents a different magnitude of climate change, and used 5 GCM ensemble instead of 12, which can decrease the representation of GCM related uncertainty and associated range of potential runoff outcomes that 12 GCMs may display. Four of the 5 GCMs used however were the same as the current research (CCCMA-CGCM31, MPI-ECHAM5, NCAR-CCSM30, and UKMOHadCM3). As suggested previously, differences between catchment characteristics such as physical environments (size, rainfall, location) and the use of climate change scenarios (QUEST-GSI verse SRES IPCC) could contribute to the observed range in runoff increases. The importance of the Koedyk and Kingston (2016) study is that the same model was used as this research, however, in different physical environments, with different GCM ensembles, but still the results relatively reflect the same responses to future climate change. Such increases in winter runoff as modelled by HBV-Light in this research and Koedyk and Kingston (2016), and other researchers using TopNet (Poyck *et al.* 2011; Gawith *et al.* 2012) all suggest an agreement that future climate change will lead to a dampening of the winter seasonal runoff cycle. The winter low flow is expected to increase and spring high flow expected to decrease as there is reduced snow storage and reduced spring melt related peaks in and around the Southern Alps. The ability that HBV-Light has demonstrated in producing future climate change impact results in the same vicinity as other published research gives some credibility to answering the second research question, that HBV-Light can reproduce similar outcomes of future climate change impacts to freshwater as more complex hydrological models in the New Zealand context.

6.1.3 Influence of precipitation uncertainty

Quantifying changes in future precipitation are one of the most uncertain aspects surrounding climate change impact studies (IPCC 2007). Such uncertainty surrounding precipitation input

data used to drive hydrological models can affect the models ability to accurately predict runoff. Advances in hydrological modelling techniques and model structures to improve the analysis of future runoff are continually challenged by sampling errors and data quality of the precipitation used to run hydrological models (McMillan *et al.* 2011). The quality and reliability of precipitation data used to run models for observed data however, is not the only source of precipitation uncertainty researchers may have to face. Although climate change is thought to affect precipitation across the majority of the Southern Alps, the current spatial diversity within singular catchments could either increase, decrease or remain as constant as the present into the future as increased precipitation events occur.

Climate change scenario modelling for New Zealand as identified by other researchers (Woods *et al*. 2008; Poyck *et al.* 2011; Srinivasan *et al.* 2011, Gawith *et al.* 2012) suggest a reduction in the return periods of heavy rainfall events, but an increase in the amount of precipitation occurring. An increase in precipitation intensification is seen in the top 5 percent of precipitation events (Fig. 5.5) for the Shotover Catchment, and a reduction in return periods of precipitation days, with 2040 seeing 55 rainfall days fewer and 2090 seeing 153 fewer than 1990. The suggestion of a decrease in the number of rainfall days, coupled with greater precipitation intensity in the Shotover have been projected by others in the Canterbury (Woods *et al.* 2008; Srinivasan *et al.* 2011) and Central Otago regions (Poyck *et al.* 2011; Gawith *et al.* 2012).

The precipitation input data used to run HBV-Light for future scenarios were provided by NIWA following the method described in the Ministry for the Environment guidance manual for local government (MfE 2008), that uses an ensemble of 12 GCMs suitable under New Zealand's diverse climate. Therefore, for the Shotover catchment, the data suggest the same pattern of precipitation change occurring for the 2040 and 2090-time periods exemplified in Woods *et al.* (2008), Srinivasan *et al.* (2011), Poyck *et al.* (2011) and Gawith *et al.* (2012), who all used the 12 GCM ensemble recommended by MfE (2008). Such patterns of rainfall projection as noted in other research (Poyck *et al.* 2011; Srinivasan *et al.* 2011, Gawith *et al.* 2012) suggests aspects of impact studies like precipitation will be affected by climate change across the Southern Alps at different magnitudes regionally. However, spatial diversity of precipitation is much greater within the catchment scale, and can also be as diverse as other water balance components (runoff, soil moisture, infiltration excess runoff and snowpack) that are catchment specific. Currently, the Shotover at its outlet in Queenstown receives roughly

500 mm/yr^{-1} of rainfall, and some estimates in the headwaters of around 7500 mm/yr^{-1} (Tait *et al.* 2006). As precipitation is already one of the greatest sources of uncertainty surrounding reliable impact assessment studies using hydrological models (McMillan *et al.* 2011), increasing precipitation is most likely going to exacerbate the magnitude of uncertainty which will further hamper efforts to reliably assess future changes to runoff.

6.1.4 Influence of temperature on snow storage

The comparison of precipitation and the corresponding changes in seasonal runoff suggests it is not just precipitation influencing changes in runoff. Both the 2040 (Fig. 5.3) and 2090 (Fig. 5.4) time periods exhibit the same timing of increases and decreases in runoff for the winter and spring months respectively, albeit differing magnitudes, the patterns are similar. The comparison of seasonal precipitation and runoff show patterns similar to those exemplified in other research (Gawith *et al.* 2012). However, the increase in runoff compared to precipitation for the winter months (July and August) could suggest that other components of the water balance cycle are contributing to the increase in winter runoff, i.e., higher rates of snowmelt.

Coupled with a projected increase in precipitation for 2040 and 2090, climate change models suggest an increase in global air temperature (IPCC 2000). It has been suggested that with an increased temperature (Fig. 5.6), there will be a marked increase in precipitation entering the catchment as rainfall instead of being stored in the snowpack (Srinivasan *et al.* 2011). An increased temperature also means a higher rate of snowmelt will occur, meaning any snow that does fall will melt faster (Srinivasan *et al.* 2011).

Seasonal snowfall for New Zealand in 2040 and 2090 has been simulated by Hendrikx *et al.* (2009), where it was concluded that there would be more precipitation occurring as rainfall and decreases in snowfall that could be responsible for a shift in many of New Zealand's flow regimes. HBV-Light appears to replicate such a shift (Fig. 5.1). Such assessments of future snow storage support that of HBV-Light, as the modelled snowpack for both 2040 and 2090 is less than that of the baseline period, and for 2090 in particular, storage is about half that of 1990 (Fig. 5.8). During July and August when runoff is at its peak, an increase in temperature within the Shotover Catchment (Fig. 5.6) could cause the snow to rain ratio to change, leading to more rain than snow and potentially indicating why there is a greater increase in runoff compared to the increase in precipitation (Fig. 5.3 & 5.4). As stated, precipitation increases, and the snowpack decreases for the Shotover Catchment in 2040 and 2090 (Fig. 5.8).

Therefore, any precipitation is more likely to pass through the system and out to the end point as runoff and is not stored in the snowpack, where such inferences have also been suggested by Gawith *et al.* (2012) for the Matukituki and Lindis Catchments. Poyck *et al.* (2011) also agrees with HBV-Lights assessment of snowmelt, suggesting that in a much larger scale, the Clutha Catchment, the contribution of snowmelt to runoff decreased significantly for both 2040 and 2090-time periods.

With higher temperatures (+2°C in 2090, Fig. 5.6) reducing the amount of snowfall occurring, it will also influence the snow that does accumulate as storage. Snow within the catchment is projected to decrease by 42 % in 2090 compared to the 1990 baseline period, but the timing of snow accumulation and snowmelt will remain the same (Fig. 5.8). Reduced snow storage will lessen the influence that meltwater usually has on runoff, which is evident in spring (September & October), when the majority of seasonal snowpack would melt during the baseline period, ultimately contributing to runoff. Therefore, it could be assumed that for the future scenarios, spring time runoff should start to decrease earlier than the baseline, as there is less snowmelt to propagate runoff, however, this is not the case. Spring time runoff is higher in 2040 (7 %) and 2090 (9 %) compared to 1990 (Fig. 5.1). It has been suggested by Poyck *et al.* (2011), who found similar results, that despite reduced snow storage in the future scenarios, and therefore less continued snowmelt, runoff is not affected due to the offset from slightly higher rainfall within the colder months (July & August). As well as higher winter rainfall and less snow storage, an increase in precipitation (22 %) for the warmer months of September, October and November (Fig. 5.7) would help explain why there is no decrease in runoff (Fig. 5.1 & 5.2) as would be expected with decreased snow storage.

6.1.5 Infiltration excess runoff

It has already been suggested by many researchers (Poyck *et al.* 2011, Srinivasan *et al.* 2011, Gawith *et al.* 2012) that the recurrence of precipitation events will decrease but the magnitude of such events will increase. The future precipitation and temperature data provided by NIWA for the Shotover Catchment supports this suggestion (Fig. 5.5), and therefore there could be an increased potential for flooding. One of the ways hydrological models assess the impact of surface flooding is through outputs usually labelled infiltration excess runoff data (IER). When the rate of rainfall exceeds the soils capacity to permeate water through the surface, IER is initiated which leads to large storm flows and less soil moisture storage because there is less soil infiltration (Srinivasan *et al.* 2011). Therefore, IER is an important tool for analysing flood

events (Gawith *et al.* 2012). In HBV-Light, the equivalent parameter is labelled QSTZ, however, for the purpose of this research QSTZ will be referred to as IER to limit confusion when comparisons are made between this research and others (Poyck *et al.* 2011; Gawith *et al.* 2012). Unfortunately, the research in question was not able to obtain the IER outputs for TopNet within the Shotover Catchment specifically and hence why will only be compared with IER outputs using TopNet from similar catchments.

The occurrence of IER is suggested to increase for both 2040 and 2090-time periods (Fig. 5.9), and is also projected to increase as a proportion of total runoff (Table 5.1). The HBV-Light conceptual representation of IER increases between July and August for both 2040 and 2090 compared to the baseline, with increases of a slightly lower magnitude in early spring (Table 5.1 & Fig. 5.9). IER appears to increase as a proportion of total yearly runoff as well, increasing by 8 % in 2040 and 10 % in 2090 (Table 5.1). These findings are consistent with other studies such as Lill (2003), who suggested there will be late winter and spring floods of greater magnitude likely by the 2080s, where the late winter and spring floods almost double in peak volume under the 2080 period (2070-2089) for the Rangitata catchment. Gawith *et al.* (2012) found that for the Matukituki, IER also increased in winter and early spring, although the magnitude of increase was not as high as this current research. Gawith *et al.* (2012) suggested that the changing occurrence of snow storage in the Matukituki Catchment was the driving force behind the sharp increase in IER for the winter months (Fig. 5.9). Given that the snow storage in the Shotover Catchment displays signs of extreme decline (Fig. 5.8), snow storage could be the reason for HBV-Lights assessment of sharply increased IER for the winter and early spring months. The proportion of precipitation that enters the catchment as rain instead of snow in July and August, as previously discussed, could also be a possible reason for an increased IER, as Gawith *et al.* (2012) showed that the higher percentage of precipitation occurring as runoff would contribute to the increased IER for July and August, just like HBV-Light suggests.

IER could increase beyond what is simulated by HBV-Light, as some catchment variables are not characterized by the model, such as the influence of a frozen ground. Although there is projected to be an increase in precipitation occurring as rainfall instead of snowfall due to warmer air temperatures, parts of the catchment will still remain below 0˚C in the winter months, meaning parts of the catchment will still have ground frozen solid (Gawith *et al.* 2012). The occurrence of excess runoff increases when rain falls on snow-covered or frozen ground

because there is no capacity for soil infiltration. The decreased ability for rain to infiltrate the soil because parts of the catchment have frozen over increases rainfall transportation (IER) to the river channel, increasing the risk of flooding, especially over the winter months of July and August. Such inferences of increased IER due to rain on snow or frozen ground have been suggested to become more common under climate change (Gawith *et al.* 2012).

6.2 HBV-Light and TopNet Comparison

The second part of the research aim was to investigate to what magnitude HBV-Light simulates the potential impacts of climate change on freshwater resources in comparison to TopNet within the Shotover Catchment specifically. It is clear from Figures 5.10, 5.11 and 5.12 that the simulated influence a 'middle of the road' climate change scenario could have on the same hydrological catchment is different when run by HBV-Light and TopNet. HBV-Lights GCM ensemble mean simulates a higher percentage change for annual runoff in 2040 with 11 of the 12 GCMs simulating higher runoff (Fig. 5.10), and a lower GCM ensemble mean runoff for 2090, with 9 out of 12 GCM's simulating lower runoff change compared to TopNet (Fig. 5.11).

The comparison of individual GCM runoff simulations between both hydrological models also exhibits differences. Visually, HBV-Light projects a relatively uniformed spread in individual GCM runoff projections for 2040 (Fig. 5.12), however, the GCM spread is greater in the spring months of September and October than the other months, with one GCM (micro3_2_hires) spiking a lot higher than the rest. The individual GCM simulations for 2090 (Fig. 5.13) display a much greater spread for both models compared to the relative uniformity of 2040. HBV-Light's GCM spread is less during the winter months of July and August compared to the wide ranging GCM projections displayed through TopNet. TopNets GCM simulations for spring months however display greater uniformity than HBV-Lights that appear to scramble from November through to December.

6.2.1 Model inclusivity of precipitation

Precipitation in particular is one of the most uncertain aspects of catchment hydrology. Therefore, understanding how a hydrological model incorporates precipitation can allow the user to assess the level of uncertainty associated with the corresponding runoff output. Although precipitation input data used to run the two models for the future scenarios were the same, the representation of spatial variability in precipitation across the catchment is different.

HBV-Light uses a single precipitation time series (Section 3.5). Whether that corresponds to a weighted average of other stations, unweighted average, or a record from just a single station (like this current research) is up to the user. The more stations there are available the more realistic of the chosen study environment the precipitation average is (this research only used one station point in the catchment). Once an average daily precipitation point has been calculated, the user then can divide the catchment up into elevation zones, where the user can set the correction for precipitation increase or based on the elevation above sea level for each of the specified zones (Seibert 2005). The limitation of using a single precipitation point in the context of this research is that there is limited scope for spatial diversity within the Shotover Catchment. TopNet uses more spatially detailed precipitation inputs. TopNet uses the VCSN network which is a gridded data set at a spatial resolution of 5 km The VCSN is a weighted sum of point precipitation measurements. A GIS based parameterization program, TOPSETUP, is used to facilitate the transformation of spatial datasets into modelling parameters and the calculation of weights associated with point precipitation measurements to provide sub-basin aggregate precipitation. The weighted precipitation points for each sub-basin gauge are created by TOPSETUP during pre-processing, where linear interpolation based on Delauney triangles are used (Bandaragoda *et al.* 2004). Delauney triangulation allows the model to describe precipitation in a watershed as three dimensional. Essentially TopNet uses multiple gauges across a catchment allowing greater in-depth analysis of the precipitation gradient that occurs in most Alpine areas.

The level of precipitation integration in the hydrological model TopNet compared to less complex models like HBV-Light is potentially the most important difference between them, as precipitation is the most uncertain aspect of hydrological modelling (McMillan *et al.* 2011). Within the New Zealand context precipitation varies significantly between the west and east coasts, especially in the South Island due to the Southern Alps. Precise measurements of precipitation, especially in alpine catchments such as the Shotover, are not always available and therefore is already a major source of uncertainty that cannot be controlled by the model. The use of more sophisticated integration of precipitation distribution through TopNet attempts to eliminate some of the associated uncertainties with complex precipitation gradients that are common in most alpine catchments. Therefore, TopNets three-dimensional description of precipitation gradients across a catchment makes it slightly more desirable in New Zealand's complex hydrological environments, such as the Shotover catchment.

6.2.2 Actual and potential evapotranspiration

As mentioned in the background literature (Section 3.8), the possibility of PET being more realistic of catchment values through TopNet for the baseline period, and therefore the resultant AET output, could explain why runoff through the GCM ensembles is different between HBV-Light and TopNet. In addition, a canopy storage component also adds another surface for evapotranspiration to occur within the TopNet model. TopNets inclusivity of more forms of catchment AET allows for a more realistic idealisation of what could be happening in the real-world environment, in comparison to HBV-Light.

Potential Evapotranspiration has been suggested as one of the largest sources of uncertainty on simulations of runoff under climate change (Kingston *et al*. 2009). The PET used for running TopNet was calculated through the Priestley-Taylor method (Priestley-Taylor 1972), considered adequate for most modelling purposes (Pereira and Pruitt 2004), while for this research Hargreaves was used to run HBV-Light due to the limited radiation and temperature data that is needed to run Priestley-Taylor. As well as the quantitatively different AET outputs derived from the two models, the timing of AET peaks between HBV-Light and TopNet is also of interest. AET as modelled by HBV-Light for 2090 peaks in September and consistently under-estimates TopNets projection that peaks in October (Fig. 5.16). Closer analysis of the difference in available water for evaporation between the models' show that the GCM ensemble mean for runoff also peaks in October for TopNet (Fig. 5.13), the same month as peak AET. For HBV-Light however, there is a slight delay in the AET peak seen in September (Fig. 5.16), as runoff peaks in August (Fig. 5.13). Therefore, the inference could be made that since TopNet is more complex as it features an extra component for assessing AET (Canopy storage), the TopNet model is more responsive to changes in available water for AET to occur as evident in the symmetry seen in the runoff (Fig. 5.13) and AET (Fig. 5.16) peaks.

The suggestion that AET (a function of how PET is limited by water availability) is responsible for differences in future runoff has been published in recent research by Koedyk and Kingston (2016). Koedyk and Kingston (2016) who also used HBV-Light to model climate change impacts to the Waikaia River found that differences in PET for 6 different methods were responsible for a fluctuated runoff in the order of only 5 %. Comparing Hargreaves and Priestly-Taylor from Koedyk and Kingston (2016) only, the maximum difference between the methods for 2090 was 2.3 %. For this research, AET was responsible for removing 48.22 mm/year in 2090, around 3.32 % of yearly runoff as modelled by HBV-Light, slightly higher

than Koedyk and Kingston (2016). Overall AET's influence on runoff and predicted changes to AET as projected by HBV-Light, the model performs well, and is consistent with similar research (Koedyk and Kingston 2016). However, in the context of this research, AET was responsible for removing 3.32 % of runoff which is something, the influence of AET on runoff in the Shotover Catchment as modelled by HBV-Light is minimal and not considered a key contributor to overall differences to runoff between HBV-Light and TopNet.

6.3 Modelled Catchment Processes

The ability to understand catchment processes embedded in HBV-Light and TopNet such as storage, evapotranspiration, soil moisture, infiltration and snow melt allows for more in-depth analysis of the future impacts climate change could have on New Zealand's freshwater catchments, and acknowledge the uncertainty in accepting such predictions as guides. Although more aspects of TopNet have a physical basis in comparison to HBV-Light, both models contain parameterisations of real-world processes. Parameter values are set by the user for both models, but the kind of parameterisations used in HBV-Light result in a simpler description of catchment hydrological processes in comparison to TopNet. Simplification of catchment hydrological processes such as water storage, soil moisture, infiltration and snow routines, potentially allows misrepresentation of real world catchment characteristics. Comparing how HBV-Light and TopNet integrates catchment processes (storage components, soil moisture and snowmelt), and the differences between them, could help understand differences in future model runoff projections seen in this research.

6.3.1 Storage Components

Water storage and how runoff is calculated after such stores are filled, is a fundamental component of hydrological modelling, as not all precipitation leaves the catchment as runoff. The role of water storage within each model could be the reason there are discrepancies between the changes in runoff expected under the influence of climate change. As previously stated, HBV-Light essentially consists of three storage components (snow, soil and groundwater) derived from daily time steps of precipitation, air temperature, and PET. Not all of the partitioned precipitation and meltwater left over after the storage routines are filled for a given time step (daily), is assumed to be the only contribution to runoff, some will be retained for release later (depending on parameter values set by the user). Rain and snowmelt is partitioned between the soil box and the upper groundwater box depending on the water content of the soil box, its field capacity (FC), and the BETA parameter. A proportion of the upper

groundwater box is released as runoff through K1 when K0 is reached, if water in the upper box is above the UZL threshold. A proportion of water in the upper box will percolate down to the lower box according to the PERC (maximum percolation) parameter, and a proportion of water in the lower box will also be released as runoff (K0).

TopNet on the other hand has five storage components, three of which describe the same aspects as HBV-Light; snow, soil, groundwater (aquifer) storages, however TopNet has two extras; canopy and surface storages. The canopy storage component quantifies the amount of precipitation stored by the leaf area of trees and shrubs, which also has embedded a component that calculates how much precipitation is occurring as through fall to the catchment when the canopy reaches its capacity. The canopy component adds an extra storage area for incoming precipitation to the catchment, potentially reducing the precipitation available for runoff. The other storage component, surface storage, equates the water that travels as overland flow before entering the river network, and includes hillslopes, transient flow paths and unresolved stream channels (Clark *et al.* 2008). The addition of a surface storage component in a hydrological model like TopNet diverts more water away from runoff, where in HBV-Light more or less water could be transferring into the soil box which continues through the system and is released as runoff. HBV-light does attempt to account for surface storage through the use of the MAXBAS parameter, however does not account for how much water is stored on the leaf area or when the canopy reaches its maximum holding capacity, potentially releasing more or less water as runoff. The two extra storage components within TopNet give the model more realistic analysis of real-world catchments and how the water is stored.

Although HBV-Light simulates slightly higher runoff (1454 mm) in 2090 than TopNet (1242 mm) the percentage increase from the model's respective baselines is lower in HBV-Light, with an increase of 12.5 % compared to an 18.3 % increase by TopNet. One main reason for a higher runoff increase from the baseline in TopNet could be the differences in precipitation input data. As detailed in Section 3.5.3, TopNet was run using VCSN data which is only an interpolation, and therefore could be adding more precipitation into the system than what was observed and used to run HBV-Light. The VCSN precipitation data used to run TopNet over estimates the observed 1990 baseline period by 4.8 mm/year (6 %). The reason for why HBV-Light simulates higher yearly runoff but less baseline change in 2090 could be because of differences in storage components mentioned in the previous paragraph. The extent to which TopNets storage components are based on physical (as opposed to empirical) relationships that

require observed parameter values which are therefore are more precise, retaining more precipitation in storage, and could explain why overall yearly runoff differences show HBV-Light under simulates TopNets runoff projections for the 2090-time period.

6.3.2 Soil Moisture

Before exploring soil moisture components of both models, it is useful to understand how TopNet simulates catchment flows of water compared to HBV-Light. TopNet uses basin geometry, water holding capacity of the vegetation and soil, and the transmissibility of the subsurface in each sub-catchment, allowing the model to describe a catchments geometry. With such descriptions, calculated using a 30 m DEM, the parameters are used for defining sub-catchment variations in the soil water balance, and water routing of runoff to the main stream network (Clark *et al.* 2008). HBV-Light represents the catchment as a lumped model, where the only changes to parameter values is between the vegetation and elevation zones (Seibert 2005), with the maximum number of elevation zones being 20 and 3 vegetation zones. TopNet on the other hand uses value attribute lookup tables from the LCDB to fill each of the 30 m DEM grid scale points across the target catchment with soil texture classes and land cover types, and therefore instead of 3 vegetation zones there is a different zone every 30 m^2, each with its own moisture intake.

Soil moisture is embedded as a storage component in both HBV-Light and TopNet, however the equations that govern the capacity of the soil box is different. The soil moisture content of both models peak in August, however, TopNets peak soil moisture content is twice that of HBV-Lights (Fig. 5.14), indicating the timing of input variables (liquid water and evaporation) is roughly the same, but the level of water input and retention is different. There is evidence to suggest the difference in soil moisture between HBV-Light and TopNet are a function of both the amount of water that is provided as input to the soil, and how soil moisture is simulated. Soil moisture depends on liquid water input (i.e. precipitation as rain, and snow melt), evaporation, and in the case of TopNet, the transfer rate of water from soil to the river and groundwater flow (Woods *et al.* 2008). The amount of liquid water from snow melt is higher in TopNet for the 2090 period (Fig. 5.15), as seasonal snow melts quicker in spring than snowmelt simulated by HBV-Light, and therefore could attribute to higher rates of soil moisture. The other contributing factor could be how soil moisture is calculated. TopNets soil storage capacity is determined by the infiltration rate of water (precipitation and snowmelt) minus the soil evaporation rate, minus the rate of drainage from the soil to the aquifer (Clark

et al. 2008). As detailed in Section 3.7, the soil moisture content in HBV-Light is based on the amount of water entering the system from precipitation and snowmelt, and how three parameters (BETA, LP and FC) calculate what is left in the soil zone.
The use of an infiltration component as a function of the components incorporated to calculate soil moisture, or lack thereof in the case of HBV-Light, could be the main contributing factor to the differences in soil moisture storage (Fig. 5.14). TopNet looks at the infiltration rate of precipitation to the soil box, the soil evapotranspiration rate and the amount of drainage from the soil box to the aquifer. HBV-Light takes the remaining precipitation and snowmelt left over from evapotranspiration, runoff, the rate of percolation from the upper soil box to the lower, and estimates infiltration as the sum of the current water content of the soil box divided by the soil boxes maximum capacity. The addition of an infiltration component allows for a realistic incorporation of how liquid water enters the soil box, and potentially renders TopNet more sensitive to climate scenario changes to soil moisture.

Infiltration is caused by voids in the soil, larger for fined grained soils (clays and small sands), where voids create suction through capillary attraction, and is known as the suction head (millimetres or inches). The infiltration of precipitation into the soil zone in TopNet is more precise than HBV-Light. HBV-Light assumes the soil moisture zone is spatially constant throughout the depth of the zone, whereas TopNet does not. TopNet calculates the soil zone as a vertical gradient, taking into account the wetting front and the soil depth. On top of an extensive view of the soil zone, TopNet uses a Green-Ampt equation. A Green-Ampt equation works on the assumption that infiltrated water primarily enters relatively dry soil that is a sharp wetting front. A sharp wetting front being defined as the region with a rapid downward decrease in water content. Therefore, in theory, the amount of infiltration assumed by TopNet is closer to the true nature of the real world, assuming the input data used to define the infiltration characteristics of the soil are realistic. In contrast, HBV-Light and the simplicity of the soil moisture component could be taking more or less precipitation as storage than what could actually be going on within the Shotover Catchment, ultimately adding uncertainty associated with the estimated runoff. In this case, HBV-Light is receiving less liquid water through infiltration than TopNet, resulting in lower water retention levels in the soil moisture zone (Fig. 5.14) for the beginning of the year (January to May) when there is less precipitation input (Fig. 5.7).

6.3.3 Snowmelt

The snow routines of both models and the respective differences between them are important for analysing monthly trends in surface runoff. Both HBV-Light and TopNet treat snow accumulation in the same manner, i.e. once temperature falls below a certain threshold (user defined), all precipitation will accumulate as snow. Like precipitation, TopNet has a more sophisticated representation of snow accumulation, as the input data (i.e. VSCN) uses a digital elevation model (DEM) to try and highlight the spatial variation that temperature and precipitation can have in catchments, which ultimately results in the same spatial variation in snow accumulation. The use of a DEM provides gridded input data, again giving the model more of a 3D image of the catchments spatial variation. HBV-Light places assumptions on snow accumulation the same way it does precipitation and temperature, where one point in the catchment fits all, with the only variation brought about through specified elevation blocks.

Although snow melt (2090 HBV and TN Snow) for both models' snow melt peaks at the same time (mid-July), HBV-Light appears to store snow for a longer period, releasing snow at a slower rate than that of TopNet, and could be the main reason for GCM ensemble mean differences in runoff for the 2090 period (Fig. 5.13). TopNets runoff peaks in October and sharply decreases through to December, in the same angle of slope as the representation of snow accumulation that starts in mid-July and ends in October. The difference in melt and runoff representation periods is the reverse effect of decreasing snow storage equalling increasing runoff. HBV-Light has a melt rate less pronounced than TopNet, and could be the reason why the 2090 GCM ensemble peaks in August, and then remains relatively constant for the remainder of the spring months, due to a drawn-out melt rate that ends in December, causing higher runoff rates at a shallower slope than TopNet.

The different quantities of snow accumulation the 2090 future catchment could be down to TopNets snow component equation. TopNet calculates the snow pack by subtracting the estimated snow to fall through the canopy by the snow melt rate, which is set through temperatures that vary across the catchment due to the use of DEM's. Therefore, like precipitation, TopNet simulates more detailed spatial and temporal trends of snow accumulation and the resultant melt. HBV-Light uses single temperature and precipitation records from in or around the catchment, corresponding to single points that are then lapsed according to the user-specified elevation range and lapse rate. In the case of this research the elevation was divided into three zones, between 300 m and 800 m (40 % of catchment), 800 m

to 1500 m (50 %), 1500 m and above, roughly 10 % of the catchment. Such a method has the possibility of assuming many parts in a catchment will have equal accumulation and melt rates, and potentially releasing more or less snow for a large portion of the catchment depending on the pre-existing assumption about the catchments degree day melt factor. In the case of this research, it is observed through Figure 5.15 that HBV-Light assumes more snow storage, and therefore a longer melt period, occurring within the Shotover catchment than what is suggested by TopNet. Due to the simplistic idealisation of single point temperature and precipitation assumptions made about the basin in HBV-Light, the snow routine is the greatest influence of the timing in runoff peaks and continued projection throughout spring and early summer compared to TopNets declining runoff for the same months.

6.4 TopNet or HBV-Light within New Zealand?

The general approach and in-depth description of a hydrological catchments components as seen in the TopNet model description of parameters (Table 3.4), is what sets it apart from HBV-Light. TopNet has 31 parameters (Table 3.4), most of which are related to physically based processes, 8 of the 31 parameters are calibrated by the user, where the remaining 23 estimates for the parameter values are constructed using descriptions from New Zealand's topography, land cover and other physical properties (McMillan *et al.* 2016). HBV-Light in comparison has 15 model parameters (Table 3.3) spread over four storage routines, of which three parameters are essentially constant (CFR, CHW and CET).

One of the most important parameters that TopNet uses is an *f* parameter. The *f* parameter, which is the same as TOPMODELS, controls the rate of transmissivity of water through to the water table, and has been estimated for more than 500 New Zealand Rivers through the use of recession curve shape analysis (McMillan *et al.* 2016). A relationship was derived between the recession shapes, geology, soil and climate parameters, in each of 15 defined hydrological regions of New Zealand. The depth of recession shape analysis across New Zealand means that the relationship between recession shape, geology, soil and climate parameters allows TopNet to use a relatively realistic real-world *f* parameter for any catchment or sub-catchment across New Zealand. HBV-Light also has a similar function (PERC) responsible for percolation of water through the upper and lower groundwater boxes, however the PERC parameter is manually calibrated to fit the simulated daily runoff with the observed, and may not necessarily represent values from within the catchment. Essentially, the TopNet approach to estimating soil hydraulic conductivity (infiltration) is a more realistic representation of catchment

processes because of the quantifiable approach taken in calculating the *f* parameter. The physical input values used for the *f* parameter in TopNet is one of the main reasons the model has been suggested as the most preferable to use in New Zealand's landscape (McMillan *et al.* 2016).

On the point of calibration, consider, for instance, the difference between real-world values and values derived from the highest NSE value through a Monte Carlo simulation. TopNet relies heavily on predetermined parameter estimates which describe the current catchment landscape such as the wetness index, stream distance, drainable soil water, depth of soil, overland flow velocity, and canopy capacity (Table 3.4). HBV-Light relies on user defined input values for less complex or in-depth catchment parameters, usually through calibration. Calibration of parameters is necessary to correct or match the runoff response times and magnitudes of the simulated hydrograph to the observed, which are real-world values (observed runoff datasets). In this research, to get the HBV-Light model to a NSE of 0.6 or higher the input values were manually calibrated, however, some tests were run using physical input values used in other research. Take for example threshold temperature, degree day factor and snowfall correction factor. When the model was run with values used in areas adjacent to the Shotover taken from Barringer (1989), hence values more representative of the Alpine area that the Shotover is situated in like the Remarkables, slightly South of Queenstown (although not exact location but the closest observed values to the Shotover), the NSE decreased by more than 0.15 of its final calibrated value (0.72), which in the context of NSE is large. Therefore, the use of real-world values for certain parameters in distributed models like TopNet may not necessarily provide better representation of observed runoff, and hence future change in runoff as HBV-Light produced runoff projections for 2040 and 2090 similar to TopNet (Fig. 5.10 & 5.11) using calibrated catchment values.

Despite the acknowledged differences in model structure and uncertainty associated with the two respective hydrological models, and the noted sophistication of TopNet compared to HBV-Light, the end results were relatively similar. The monthly NSE values for the Shotover using both HBV-Light (0.72) and TopNet (0.71) were almost identical. Similar study sites to the Shotover that were simulated using TopNet, i.e. the Matukituki (0.68) and the Lindis catchments were also very similar to the NSE values recorded in the Shotover (Table 4.1 & 4.2). Seasonally, HBV-Lights projected change is not in line with TopNet, as TopNet peaks in October for both 2040 and 2090, whereas HBV-Light flattens out from July through to December in 2040, and peaks in August and November for 2090. However, the amount of

spread between the 12 individual GCM's (Fig. 5.12 & 5.13) appears consistent between both models, suggesting the same level of uncertainty which is common among hydrological models when simulating runoff 100 years into the future (Poyck *et al.* 2011; Gawith *et al.* 2012). Using an ensemble mean of 12 GCMs, HBV-Light projected higher yearly runoff (3.5 %) in 2040 and lower runoff (1.7 % %) in 2090 compared to TopNet. Therefore, it is suggested through the analysis of future seasonal and yearly (Fig. 5.10 & 5.11) changes to runoff as projected by both models, that HBV-Light can be considered an acceptable alternative to TopNet for the use of assessing future impacts that climate change could have on New Zealand's fresh water resources, and provides further validity in answering the second research question.

6.5 Uncertainty associated with this current research

The most common uncertainty in reliable predictions of future impacts to freshwater resources under climate change conditions in New Zealand is accurate precipitation and temperature data. Recording precipitation and temperature data for the use of climate change impact assessment, especially in New Zealand, is inherently difficult as a result of location and orographic effects brought about by tectonic uplift creating the Southern Alps (Kenny 2010). McMillan *et al.* (2016) highlighted studies by Madden and Kidson (1997) and Madden *et al.* (1999), who indicated for New Zealand, that during any growing season, half of the temperature variability and a third of precipitation was predictable. Given that any growing season is reference to crops that would be situated on flatter ground that is easily accessible by growers, the scale of increasing precipitation and temperature uncertainty in more diverse landscapes unsuitable for cropping like the Shotover, would be more intense.

With the knowledge of climate change impact assessment uncertainty within New Zealand for current climates, the future variation of precipitation and temperature for a "middle-of-the-road" emissions scenario (A1B) can be considered. The amount of variability associated with climate change modelling however, suggests that taking one emissions scenario, or the ideal future emissions scenario as truth, should be avoided. Most impact assessment studies conducted in New Zealand use one emission scenario (A1B), but use 12 GCM scenarios all based on the chosen (A1B) emissions trajectory through time (Gawith *et al.* 2012; Poyck *et al.* 2011, Srinivasan *et al.* 2011). The Ministry for the Environment report (2016) outlines 4 emissions scenarios for New Zealand ranging from 0.7 °C (RCP2.6) to 3.0 °C (RCP8.0), where a comparison between SRES and RCP scenarios places the SRES A1B output closest to

RCP6.0, which indicates 'more than likely' (51-100 %) to exceed a 2 ℃ warming of air temperature by the end of the century. The use of one emission scenario as conducted in this research is not universal, although the most common, does not take into account the other possible increases or decreases in future emissions as highlighted by the MfE (2016) report, however, the use of such practices minimises a key facet of climate change related uncertainty. The use of GCMs within a chosen emissions scenario is typically by far the most important source of climate change related uncertainty when focusing on a single scenario, and should be considered as a range of outcomes, and not individual idealised outcomes depending on what the research is trying to achieve. Therefore, for this research is it highlighted that the projected future changes to runoff in the Shotover Catchment for 2090 as modelled through HBV-Light is only valid if humanity remains on an A1B emissions scenario course.

6.5.1 Shotover characteristics on model performance

A recent study by McMillan *et al.* (2016) highlighted 5 conditions that would aid the performance of a hydrological model. Larger catchments (>1000 km^2) are expected to yield better model performances, as larger areas tend to smooth out irregular variations in flow because such variations become less important due to the scale of water in the catchment. The Shotover is on the smaller side of catchment scale (1088 km^2). Due to the relatively small size of the catchment, irregularities in flow are more pronounced in the observed data, potentially making it more difficult to match simulated flow data and therefore providing a less desirable NSE value. The use of a larger catchment however might smooth out irregular flow patterns and storm events to provide a higher NSE, by may not necessarily provide a greater simulation of real-world hydrological processes.

Precipitation input data is one of the greatest forms of uncertainty. Therefore, model performance would benefit from areas with greater estimates of precipitation depth and more data points spread throughout the catchment. As the precipitation used for this research came from one-point source low down in the outreach of the Shotover Catchment, the lack of spread may have contributed to lowering the final calibrated NSE value.

Catchments that generally receive more rainfall or are "wetter" would perform better as the relationship between falling rain and hillslopes become more entwined, as hillslopes can store surface water. Also, more rainfall would mean catchments are less likely to have intermittent flows, leading to a higher base flow for the model to replicate, making base flow replication easier. For this research, the Shotover Catchments rainfall is quite large (500−7500 mm yr^{-1}),

however, catchments west of the main divide exhibit higher annual rainfall and could potentially model an observed data set with more precision.

Catchments that have less groundwater influence. HBV-Light has a simple conceptual representation of groundwater processes, and potentially could demonstrate poorer performance in catchments with alluvial plains that have more complex groundwater movement. Due to a lack of information and time constraints, real-world estimates of groundwater flow, volume and control mechanisms within the Shotover were not considered. Calibration of K2 and K1 was undertaken however there was no physical data to start the calibration process to verify the final model input values for real-world consistency. Knowing more about the impacts groundwater has on runoff within the Shotover Catchment, either contributing more or less to surface water at various points in the catchment would have allowed for greater understanding of water balance dynamics during the calibration phase of this research, and therefore provided better results.

Hydrological models are less reliable during spring (drying) and autumn (wetting-up periods) because detailed input data for such periods require great understanding of movement and storage of water in the catchment. Due to the Shotover being an Alpine Catchment, there is a strong presence of seasonal variation in precipitation that influences water storage in the spring and autumn periods which could be influencing the results. Therefore, catchments with less seasonal variation than the Shotover might perform better.

6.6 Summary

Analysis of the modelling results found consistency between HBV-Light and TopNet, and expected outcomes of HBV-Light as suggested by other modelling research undertaken in close proximity to the Shotover Catchment were supported. In general HBV-Light performed to an almost equal standard during the calibration period compared to that of TopNet in the Lindis and Matukituki using observed data. Although the calibration periods and catchments were different between the two models, the monthly NSE for each catchment was deemed satisfactory. Representation of the potential future impacts that climate change could have on the Shotover River were also consistent with previous literature, with HBV-Light indicating that runoff will increase for the winter and spring months for both 2040 and 2090. The discussion looked at possible reasons why runoff might increase in 2040 and 2090, and found that although precipitation increased, it was at its peak, only half that of runoff. The influences

to the snowpack as projected by HBV-Light were analysed, where it was suggested that higher rates of snowmelt, set about by higher average monthly temperatures, were responsible for higher rates of runoff. The increased temperature would lessen the storage time and therefore less accumulation of snow will occur throughout the year.

In comparison to TopNets future projection for the Shotover River, HBV-Light performed well, over simulating the 2040-time period by 3.5 %, and under simulating the 2090-time period by 1.65 %. Differences between water balance and catchment parameter equations within each of the respective model structures, contributed to differences in catchment parameter outputs such as storage components, soil moisture content and snowmelt. HBV-Light simulated more snow in the catchment than TopNet, which was explained by the respective models complexities. TopNet uses a 30 m DEM which provides 3D gridded input data, allowing the catchment to be divided into high resolution 5 x 5 km sections. HBV-Light uses a 2D assumption, where one point in the catchment fits all, where the only change in snow accumulation is by specifying 3 to 5 different elevation zones, essentially providing lower resolution data points. Like the snowpack, HBV-Light simulated a soil moisture content for 2090, half that of TopNet, which was attributed to higher rates of snowmelt in TopNet, and a greater in-depth perception of precipitation infiltration to the soil moisture zone. Despite differences between key catchment parameters, HBV-Light performed well in representing future runoff responses to climate change in comparison to TopNet.

Chapter Seven
Conclusion

The research in question focused on the role hydrological model complexity plays in assessing the impacts that future climate change could have on New Zealand's freshwater resources. The first aim of this research was to determine whether a relatively simple hydrological model can realistically simulate an observed flow in an alpine catchment in New Zealand. Secondly, if a simple model could realistically simulate an alpine flow, the research would compare future climate change impacts on river flow between the simple hydrological model and that of a complex model. The two hydrological models chosen for comparison were the fully distributed TopNet (complex) and semi-distributed HBV-Light (less complex). TopNet has been well documented throughout New Zealand's freshwater catchments, and was developed by NIWA, whereas HBV-Light had only been used in two case studies within New Zealand, however, had been proved acceptable in over 30 different countries and 7 different continents. The HBV-Light model was run with a 26-year data set from within the Shotover Catchment, and runoff data for TopNet for the same observed period was kindly provided by NIWA. HBV-Light and TopNet were both run for two future periods, 2040 and 2090, under climate change conditions, as done previously in other New Zealand research.

The model performance results (Chapter Four) showed that the HBV-Light model performed well in the Shotover Catchment when replicating an observed data set of 13 years (1972−1984), returning a 'good' monthly NSE of 0.72 for the calibration period and an 'acceptable' 0.61 for the validation period (1985−1997). The hydrological model TopNet, although was not calibrated for the Shotover Catchment specifically, returned a 'good' monthly NSE value of 0.71 over a 20-year observed period (1980-1999). The use of HBV-Light in simulating future climate change, and the potential influence such changes could have on New Zealand's freshwater resources were also assessed (Chapter 5), and performed well. HBV-Light, using an IPCC SRES A1B climate scenario, and an ensemble of 12 GCM's suited to New Zealand's climate conditions, projected runoff increases to the Shotover River in the magnitude of 13.4 % for 2040 over a 20-year average (2030− 2049), and 17.4 % in 2090 (2080− 2099). In

comparison to TopNets assessment of climate change impacts for the same future time periods, using the same 12 GCM ensemble and IPCC SRES A1B climate scenario, HBV-Light over-stimulated TopNets projection for 2040 by 3.5 %, and under-simulated TopNets 2090 projection by 1.65 %, which could be considered relatively accurate. However, the monthly comparisons of runoff increase showed HBV-Light simulating a 90 % increase from the 1990 baseline to 2090 for the month of August, where TopNets highest increase was also in August but only by 56 %.

In the context of simulating model components responsible for estimating runoff, HBV-Lights performance was not as strong in comparison to overall runoff, with snowpack an exception. The snowpack volume as projected by HBV-Light for 2090 peaks in the same month (August) as when TopNet projects a peak in snowmelt, indicating the models have a similar response to changes in precipitation and temperature throughout the year. The soil moisture projected by HBV-Light also peaked the same month as TopNet (August), indicating the models responses to precipitation were the same, however, HBV-Lights yearly projection was 300 mm/yr^{-1} less, and was argued as a result of no infiltration excess component, where TopNet was retaining more soil moisture. Again, the differences in soil moisture values attributed to a function of TopNets complexity. AET peaked in September when projected by HBV-Light and October in TopNet, while also overestimating TopNet for the entirety of 2090-time period. The differences in AET between the two models was inferred as a combination of both model complexity and method used to calculate PET (Hargreaves verse Priestly-Taylor). TopNet includes a parameter that quantifies the AET occurring from precipitation stored on the canopy, allowing for more refined estimations of AET that could be occurring in the real-world environment.

Understanding the relationship between the input data available and the complexity of the hydrological model chosen to simulate future runoff is a critical point of the HBV-Light−TopNet comparison. Given a completely accurate and comprehensive input data set for all parameters, TopNet would be more realistic than HBV-Light due to its parameterisation of most catchment characteristics and inter-relationships, however, such a data set does not exist. The input data required run both models also plays a role in determining which one to use. HBV-Light uses point gauge data from within the catchment where as TopNet uses VCSN data, both of which have key differences. Although VCSN data is more likely to be realistic of a catchment compared to that from a single source point site low down in a catchment, crudely

lapsed by a few elevation zones, VCSN data is an interpolation only and not true physical data. On the other hand, climate variables within the intended field site may vary over the desired collection period and influence the physical data in the real world but not through the VCSN interpolation. The point gauge method of data collection as used to run HBV-Light gives true physical field data but the collection method and maintenance of such data can lead to uncertainties in the quality. Moreover, data collection from higher up in complex or mountainous catchments maybe impossible and therefore there is no information about what is going on in the upper catchment, usually where a lot of the precipitation occurs.

The results presented in this research are interpreted as such that the hydrological complexity outweigh those of the data limitations. As a perfect data set does not exist, there is a choice between a more realistic model that is run with limited, interpolated data (TopNet), and a more simplistic model that does not make as many demands in terms of input data (HBV-Light), which can be run with relatively accurate, albeit single point physical data. The more complex TopNet model simulated the largest monthly runoff increase within the Shotover Catchment for 2090 at 55 %, more in line with other research (50 % Lindis, 46 % Matukituki, 37 % Clutha) compared to HBV-Lights 90 %. Although HBV-Lights yearly interpretation of runoff increase (13 % in 2040, 17 % in 2090) was more realistic than the monthly runoff outputs, the simulations of runoff increase were more in line with results from the Lindis Catchment (10 % in 2040, 20 % in 2090) than catchments closer to the Shotover in nature like the Matukituki (7 % in 2040, 13 % in 2090). Therefore, in addressing the aims of this research, yes HBV-light can simulate an observed runoff data set to an acceptable standard as Chapter Four demonstrated. However, for the second aim, it is suggested that realistic simulations of climate change in complex catchments such as the Shotover in New Zealand requires more complex hydrological models like TopNet. In the absence of such high quality, comprehensive data such as VSCN, HBV-Light is an acceptable alternative to TopNet for assessing potential impacts of future climate change using point source data.

With the increasing threat of climate change and the potential influence that might have on the New Zealand's, and more importantly the world's freshwater resources, it is of great importance that time and energy continues to be centred towards hydrological modelling, to improve the methods and literature currently relied upon for such research. With the presentation of the results and discussion, this research concludes that hydrological complexity does not play a significant role in differences of projected changes to runoff under future

climate change conditions. HBV-Light provides a free easy to download modelling package that is easy to calibrate, which has now been proven sufficiently reliable in representing an observed runoff data set within the complex hydrological environment that New Zealand offers, with the ability to model influences to runoff under future climate change conditions. At a practical level, the findings of this research are beneficial for any person with the intent of assessing the impacts of climate change on freshwater resources in New Zealand, whom may not have the time or financial capability of using more complex hydrological models.

References

Abbott M.B., Bathrust J.C., Cunge J.A., O'Connell P.E., Rasmussen J., (1986). An introduction to European hydrological system - Systeme Hydrologique Europeen (SHE) Part 2. Structure of a physically based distributed modelling system. *J. Hydrol., 87, 61-77.*

Abbott M.B., Refsgaard J.C., (1996). *Distributed Hydrological Modelling.* Water Sciences and Technology, Kluwer Academic Publishers, Dordrecht, 22, 1-17, ISBN 978-94-009-0257-2.

Allen R.G., Pereira L.S., Raes D., Smith M., (1998). *Crop Evapotranspiration- Guidelines for Computing Crop Water Requirements*. FAO Irrigation and Drainage Paper 56. Food and Agriculture Organization, Rome.

Andersson L., Wilk J., Todd M.C., Hughes D.A., Earle A., Kniveton D., Layberry R., Savenije H.H.G., (2006). Impact of climate change and development scenarios on flow patterns in the Okavango River. *J. Hydrol., 331, 43-57.*

Anderton S., Latron J., Gallart F., (2002). Sensitivity analysis and multi-response, multi-criteria evaluation of a physical based distributed model. *Hydrol. Process, 16, 333– 353.*

Arnell N.W., (1999). A simple water balance model for the simulation of streamflow over a large geographic domain. *J. Hydrol., 217, 314–335.*

Arnold J.G., Srinivasan R., Muttiah R.S., Williams J.R., (1998). Large area hydrologic modelling and assessment part I: model development. *J. Amer. Wat. Res. Assoc. 34, 73–89.*

ASCE., (1993). Criteria for evaluation of watershed models. J. Irrigation Drainage Eng., 119(3): 429-442.

Bae D.H., Jung I.W., Lettenmaier D.P., (2011). Hydrologic uncertainties in climate change from IPCC AR4 GCM simulations of the Chungju Basin, Korea. *J. Hydrol., 401 (1-2), 90-105.*

Bandaragoda C., Tarborton D.G., Woods R., (2004). Application of TOPNET in the distributed model intercomparison project. *J. Hydrol., 298, 178-201.*

Barringer J.R.F., (1989). A variable lapse rate snowline model for the Remarkables, Central Otago, New Zealand. *J. Hydrol., 28 (1), 33-46.*

Bastola S., Murphy C., Sweeney J., (2011). The role of hydrological modelling uncertainties in climate change impact assessments on Irish river catchments. *Adv. Water Resour, 34, 562-575.*

Bates B.C., Kundzewicz Z.W., Wu S., Palutikof J.P., (2008). *Climate Change and Water.* Technical Paper of the Intergovernmental Panel on Climate Change, IPCC Secretariat, Geneva, 210 pp.

Berengena J., Gavilán P., (2005). Reference evapotranspiration estimation in a highly advective semiarid environment. *J. Irrig. Drain E.-ASCE, 131, 147–163.*

Bergstrom S., (1976). *Development and application of a conceptual runoff model for Scandinavian catchments*. SMHI, Report No. RHO 7, Norrkoeping, 134.

Bergstrom S., (1995). *The HBV model.* In: Singh, V.P. (Ed.) Computer Models of Watershed Hydrology. Water Resources Publications, Highlands Ranch, CO., pp. 443-476.

Bergstrom S., (2006). *Experience from applications of the HBV hydrological model from the perspective of prediction in ungauged basins.* In: Andréassian V., Hall A., Chahinian N., Schaake J., (Eds). Large Sample Basin Experiments for Hydrological Model Parameterization: Results of the Model Parameter Experiment - MOPEX. IAHS Publication 307, 97-109.

Beven K., (1979). A sensitivity analysis of the Penman–Monteith actual evapotranspiration estimates. *J. Hydrol. 44 (3–4), 169–190.*

Beven K., Lamb R., Quinn P., Romanowicz R., Freer J., (1995). Topmodel. In: Singh, V.P., (Ed.). *Computer Models of Watershed Hydrology.* Water Resources Publications, Highlands Ranch, CO, (Chapter 18), 627–668.

Beven K.J., (2001). How far can we go in distributed hydrological modelling? *Hydrol. Earth Syst. Sc., 5 (1), 1-12.*

Beven K.J., (2004). Infiltration excess overland flow at the Horton Hydrological Laboratory (or not?). *J. Hydrol., 293, 219-234.*

Beven K.J., (2010). *Environmental Modelling: An Uncertain Future?* Routledge, London, p. 310.

Beven K.J., Kirkby M.J., (1979). A physically-based variable contributing area model of basin hydrology. *Hydrol. Sci. Bull., 24 (1), 43–69.*

Beyene T., Lettenmaier D.P., Kabat P., (2010). Hydrologic Impacts of Climate Change on the Nile River Basin: Implications of the 2007 IPCC Scenarios. *Climatic change, 100:433-461.*

Biggs B.J.F., Duncan M.J., Jowett I.G., Quinn J.M., Hickey C.W., Davies-Colley R.J., Close M.E., (2010). Ecological characterisation, classification, and modelling of New Zealand rivers: An introduction and synthesis. *New Zeal. J. Mar. Fresh., 42 (3), 277-304.*

Bloom A.L., (1972). *Geomorphology: A systematic Analysis if Late Cenozoic Landforms.* Prentice Hall, New Jersey.

Bloschl G., Montanari A., (2010). Climate change impacts – throwing the dice? *Hydrol. Process, 24, 374–381.*

Bloschl G., Sivapalan M., (1995). Scale issues in hydrological modelling: a review. *Hydrol. Process, 9, 251-290.*

Brash, D.W., Beecroft, F.G., (1987). *Soil resources of Central Otago.* Proceedings of the New Zealand Grassland Association, 48, 23-30.

Breuer L., Huisman J.A., Willems P., Bormann H., Bronstert A., Croke B.F.W., Frede H.G., Graff T., Hubrechts L., Jakeman A.J., Kite G., Lanini J., Leavesley G., Lettenmaier D.P., Lindstrom G., Seibert J., Sivapalan M., Viney N.R., (2009). Assessing the impact of land use change on hydrology by ensemble modeling (LUCHEM). I: Model intercomparison with current land use. *Adva. Water Resour, 32, 129-146.*

Cao W., Bowden W.B., Davie T., Fenemor A., (2006). Multi-variable and multi-site calibration and validation of SWAT in a large mountainous catchment with high spatial variability. *Hydrol. Process, 20, 1057-1073.*

Chapon B., Delrieu G., Gosset M., Boudevillain B., (2008). Variability of rain drop size distribution and its effect on the Z-R relationship: A case study for intense Mediterranean rainfall. *Atmos. Res., 87, 52–65.*

Chattopadhyay N., Hume M., (1996). Evaporation and potential evapotranspiration in India under conditions of recent and future climate change. *Agri. Forest Manage, 87, 55-73.*

Christensen N.S., Lettenmaier D.P., (2007). A multimodel ensemble approach to assessment of climate change impacts on the hydrology and water resources of the Colorado River Basin. *Hydrol. Earth Syst. Sc., 11, 1417-1434.*

Chu T.W., and Shirmohammadi A., (2004). Evaluation of the SWAT model's hydrology component in the piedmont physiographic region of Maryland. *Trans. ASAE, 47(4): 1057-1073.*

Cichota R., Snow V.O., Tait A.B., (2008). A functional evaluation of virtual climate station rainfall data. *New Zeal. J. Agr. Res., 51, 317-329.*

Clark M.P., Ibbitt R.P., Woods R.A., (2007). Flood forecasts for New Zealand communities. *Water Atmosph, 15(3), 14–5.*

Clark M.P., Rupp D.E., Woods R.A., Aheng X., Ibbit R.P., Slater A.G., Schmidt J., Uddstrom M.J., (2008**A**). Hydrological data assimilation with the ensemble Kalman filter: Use of streamflow observations to update states in a distributed hydrological model. *Adva in Water Resour, 31, 1309-1324*.

Clark M.P., Schoenbohm, L.M., Royden, L.H., Whipple, K.X., Burchfiel, B.C., Zhang, X., Tang, W., Wang, E., Chen, L., (2004). Surface uplift, tectonics, and erosion of eastern Tibet from large-scale drainage patterns. *Tectonics, 23 (1), 1-20.*

Cole S.J., Moore R.J., (2008). Hydrological modelling using rain-gauge and radar-based estimators of areal rainfall. *J. Hydrol., 358, 159–181.*

Collins M., Knutti R., Arblaster J., Dufresne J.-L., Fichefet T., Friedlingstein P., Gao X., Gutowski W.J., Johns T., Krinner G., Shongwe M., Tebaldi C., Weaver A.J., Wehner M., (2013). *Long-term Climate Change: Projections, Commitments and Irreversibility*. In: Climate Change 2013: The Physical Science Basis. Contribution of Working Group I to the Fifth Assessment Report of the Intergovernmental Panel on Climate Change [Stocker, T.F., D. Qin, G.-K. Plattner, M. Tignor, S.K. Allen, J. Boschung, A. Nauels, Y. Xia, V. Bex and P.M. Midgley (eds.)]. Cambridge University Press, Cambridge, United Kingdom and New York, NY, USA.

Collischonn W., Allasia D.G., Silva B.C., Tucci E.M., (2007). The MGB/IPH model for large-scale rainfall-runoff. *Hydrolog. Sci. J., 52, 878–895.*

Cummins B., (2007). *Biological Science with Mastering Biology*. (3rd ed), Freeman, Scott (ed), p 215. ISBN-13: 9780321543271

Cuo L., Lettenmaier D.P., Mattheussen B.V., Storck P., Wiley M., (2008). Hydrologic prediction for urban watersheds with the Distributed Hydrology-Soil-Vegetation Model. *Hydrol. Proc., 22, 4205–4213.*

Daley R., (1991). *Atmospheric data analysis*. Cambridge Atmospheric and Space Science Series, Cambridge University Press, Cambridge. ISBN 0521 382157.

Daniels A.E., Morrison J.F., Joyce L.A., Crookston N.L., Chen S.C., McNully S.G., (2012). Climate projections FAQ. General Technical Report. Fort Collins, CO, U.S. Department of Agriculture, Forest Service, Rocky Mountain Research Station: 1-32.

Devi G.K., Ganasri B.P., Dwarakish G.S., (2015). A review of hydrological models. *Aquatic Procedia, 4, 1001-1007.*

Devkota R.P., Bhattarai U., (2015). Assessment of climate change impacts on floods from a techno-social perspective. *J. Flood Risk Manage.*, doi:10.1111/jfr3. 12192.

Dibike Y.B., Coulibaly P., (2005). Hydrologic impact of climate change in the Saguenay watershed: comparison of downscaling methods and hydrologic models. *J. Hydrol., 307, 145-163.*

Doll P., Kaspar F., Lehner B., (2003). A global hydrological model for deriving water availability indicators: model tuning and validation. *J. Hydrol., 270, 105–134.*

Donigian A.S., Imhoff J.C., Bicknell B.R., (1983). *Predicting Water Quality Resulting From Agricultural Nonpoint Source Pollution Via Simulation –HSPF*. In: Agricultural Management and Water Quality, F.W. Schaller and G.W. Bailey (Editors). Iowa State University Press, Ames, Iowa, pp. 200-249.

Driessen T.L.A., Hurkmans R.T.W.L., Terink W., Hazenberg P., Uijlenhoet R., (2010). The hydrological response of the Ourthe catchment to climate change as modelled by the HBV model. *Hydrol. Earth Sci., 14, 651-665.*

Elsner M.M., Cuo L., Voisin N., Deems J.S., Hamlet A.F., Vano J.A., Mickelson K.E.B., Lee S., Lettenmaier D.P., (2010). Implications of 21st Century Climate Change for the Hydrology of Washington State. *Climatic Change 102, 225-260.*

Fenicia F., Savenije H.H.G., Matgn P., Pfister L., (2006). Is the groundwater reservoir linear? Learning from data in hydrological modelling. *Hydrology and Earth System sciences Discussions, Copernicus Publications, 10 (1), 139-150.*

Fitzharris, B., (2004). *Report prepared for NIWA, Ministry for the Environment, and Statistics New Zealand.* Climate Management Centre, Department of Geography, University of Otago. PP 8.

Fooladmand H.R., Hosein Z.H., Ravanan M.H., (2008). Comparison of different types of Hargreaves equation for estimating monthly evapotranspiration in the south of Iran. *Archives of Agronomy and Soil Science, 54 (3), 321–330.*

Frederick K.D. Gleick P.H., (1999). *Water and Global Climate Change: Potential Impacts on U.S. Water Resources*. Prepared for the Pew Center on Global Climate Change, Arlington, Virginia.

Gangopadhyay M., Uryvaev V.A., Oman M.H., Nordenson T.J., Harbeck GE., (1966). *Measurement and estimation of evaporation and evapotranspiration*. WMO Technical No. 83, Geneva, Switzerland.

Gash J.H.C., Wright I.R., Lloyd C.R., (1980). Comparative estimates of interception loss from three coniferous forests in Great Britain. *J. Hydrol., 48, 89-105.*

Gawith D., Kingston D.G., McMillan H., (2012). The effects of climate change on runoff in the Lindis and Matukituki catchments, Otago, New Zealand. *J. Hydrol., 51 (2), 121-135.*

Giorgi F., Mearns L.O., (1991). Approaches to regional climate change simulation: A review. *Rev. Geophys., 29, 191-216.*

Goring D.G., (1994). *Kinematic shocks and monoclinal waves in the Waimakariri, a steep, braided, gravel-bed river, Proceedings of the International Symposium on Waves.* Physical and Numerical Modelling, University of British Columbia, Vancouver, Canada, 21–24 August, 336–345.

Gosain A.K., Mani A., Dwivedi C., (2009). *Hydrological modelling literature review: Report No.1.* Indo-Norwegian Institutional Cooperation Program 2009–2011.

Gosling S.N., Arnell N.W., (2010). Simulating current global river runoff with a global hydrological model: model revisions, validation and sensitivity analysis. *Hydrol. Proc., 27 (7), 1129-1145.*

Gosling S.N., Taylor R.G., Arnell N.W., Todd M.C., (2011). A comparative analysis of projected impacts of climate change on river run-off from global and catchment-scale hydrological models. *Hydrol. Earth Syst. Sci., 15, 279-294.*

Graham L.P., Jacob D., (2000). Using large-scale hydrologic modelling to review runoff generation processes in GCM climate models. *Meteorol. Z. 9, 49-57.*

Griffiths G.A., (1981). Some suspended sediment yields from South Island catchments, New Zealand. *Water Resour. Bull., 17 (4), 662-671*.

Gupta H.V., Sorooshian S., Yapo P.O., (1999). Status of automatic calibration for hydrologic models: Comparison with multilevel expert calibration. *J. Hydrologic Eng., 4(2): 135-143*.

Guyennon N., Romano E., Portoghese I., Salerno F., Calmanti S., Perangeli A.B., Tartari G., Copetti D., (2013). Benefits from using combined dynamical-statistical downscaling approaches – lessons from a case study in the Mediterranean region. *Hydrol. Earth Syst. Sci., 17 (2), 705-720*.

Haddeland I., Clark C., Franssen W., Ludwig F., Voß F., Arnell N.W., Bertrand N., Best S., Folwell S., Gerten D., Gomes S., Gosling S.N., Hagemann S., Hanasaki N., Harding R., Heinke J., Kabat P., Koirala S., Polcher J., Stacke T., Viterbo P., Weedon G., Yeh P., (2011). Multi-model estimate of the global terrestrial water balance: Setup and first results. *J. Hydrometeorol., 12, 869-884.*

Hagemann S., Chen C., Clark D.B., Folwell S., Gosling S.N., Haddeland I., Hanasaki N., Heinke J., Ludwig F., Voß F., Wiltshire A.J., (2012). Climate change impact on available water resources obtained using multiple global climate and hydrology models. *Earth Syst. Dyn. Discuss. 3, 1321-1345.*

Hamlet A.F., Salathe E.P., Carrasco P., (2010). *Statistical Downscaling Techniques for Global Climate Model Simulations of Temperature and Precipitation with Application to Water Resource Planning Studies*. The Columbia Basin Climate Change Scenarios Project (CBCCSP) report, Chapter 4, in review.

Hargreaves G.H. and Z.A. Samani, (1985). Reference Crop Evapotranspiration From Temperature. *Applied Engrg. in Agric. 1 (2), 96-99.*

Hattermann F., Krysanova V., Wechsung F., Wattenbach M., (2004). Integrating groundwater dynamics in regional hydrological modelling. *Environ. Modell. Softw., 19 (11), 1039-1051.*

Haughton N., Abramowitz G., Pitman A., (2014). On the generation of climate model ensembles. *Clim. Dynam., 43, 2297-2308.*

Henderson R.D., Singh S., Woods R.A., Zammit C., (2011). *Surface water components of New Zealand's National Water Accounts, 1995–2010.* NIWA Client Report No. CHC2011-051.

Hendrikx, J., Clark M., Hreinsson E.O., Tait A., Woods R., Slater A., Mullan B., (2009). *Simulations of Seasonal Snow in New Zealand: Past and Future.* In: Ninth International Conference on Southern Hemisphere Meteorology and Oceanography. American Meteorological Society-Australian Meteorological and Oceanographic Society, Melbourne, Australia. http://www.canterburywater.org.nz/downloads/Stage-3-report.pdf, accessed on November 5, 2016.

Henriksen H.J. Troldborg L., Hojberg A.L., Refsgaard J.C., (2008). Assessment of exploitable groundwater resources of Denmark by use of ensemble resource indicators and a numerical groundwater-surface water model. *J. Hydrol., 348, 224-240.*

Herbst M., Rosier P.T.W., McNeil D.D., Harding R.J., Gowing D.J., (2008). Seasonal variability of interception evaporation from the canopy of a mixed deciduous forest. *Agri Forest Meteorol, 148 (11), 1655-1667.*

Hicks M.D., Shankar U., McKerchar A.I., Basher L., Lynn I., Page M., Jessen M., (2011). Suspended sediment yields from New Zealand rivers. *J. Hydrol. (NZ), 50 (1), 81-142.*

Houghton, J. T., L. G. Meira Filho, B. A. Callander, N. Harris, A. Kattenberg, and K. Maskell (Eds), 1996. *Climate Change 1995: The Science of Climate Change.* Contribution of Working Group I to the Second Assessment Report of the Intergovern.

Huntington T.G., (2006). Evidence for intensification of the global water cycle: review and synthesis. *J. Hydrol., 319 (1–4), 83-95.*

Hurd B., Leary N., Jones R., Smith J., (1999). Relative regional vulnerability of water resources to climate change. *J. Am. Water Resour. As., 35 (6), 1399-1409.*

Ibbitt R., Thompson C., Turner R., (2005). Skill assessment of a linked precipitation-runoff flood forecasting system. *J. Hydrol. (NZ), 44 (2), 91-104.*

IPCC (1996). Climate Change 1995. The Science of Climate Change. Cambridge University Press, Cambridge.

IPCC (2000). *Special report on emissions scenarios (SRES): a special report of working group III of the intergovernmental panel on climate change.* Cambridge University Press, Cambridge, pp 599.

IPCC (2007). *Summary for policymakers.* In: Climate change 2007: The physical science basis. Contribution of working group I to the Fourth Assessment Report of the Intergovernmental Panel on Climate Change. Solomon S., Qin D., Manning M., Chen Z., Marquis M., Averyt K.B., Tignor M., Millar H.L. (Eds.).

IPCC, (2007). *Climate Change 2007: Synthesis Report*. Contribution of Working Groups I, II and III to the Fourth Assessment Report of the Intergovernmental Panel on Climate Change [Core Writing Team, Pachauri, R.K and Reisinger, A. (eds.)]. IPCC, Geneva, Switzerland, 104 pp.

Islam Z., (2011). A review on physically based hydrological modelling. Technical Report, Unpublished. DOI: 10.13140/2.1.4544.5924.

Jiang T., Chen Y.D., Xu C., Chen X., Chen X., Singh V.P., (2007). Comparison of hydrological impacts of climate change simulated by six hydrological models in the Dongjiang Basin, South China. *J. Hydrol., 336, 316-333.*

Johansson B., Seuna P., (1994). Modelling the effects of wetland drainage on high flows. *Aqua Fennica, 24(1), 59–68.*

Johnson R.C., (1990). The interception, throughfall and stemflow in a forest in Highland Scotland and comparison with other upland forests in the UK. *J. Hydrol, 188, 281–287.*

Kenny G.J., Warrick R.A., Campbell B.D., Sims G.C., Camilleri M., Jamieson P.D., Mitchell N.D., McPherson H.G., Salinger M.J., (2000). Investigating climate change impacts and thresholds: An application of the climpacts integrated assessment model for New Zealand Agriculture. *Climate Change, 46, 91-113.*

Kim J., Miller N.L., Farrara J.D., Hong S., (2000). A seasonal precipitation and stream flow hindcast and prediction study in the Western United States during the 1997/98 winter season using a dynamic downscaling system. *Am. Meteorol. Soc., 1, 311-329.*

Kingston D.G., Todd M.C., Taylor R.G., Thompson J.R., Arnell N.W., (2009). Uncertainty in the estimation of potential evapotranspiration under climate change. *Geophys. Res. Lett., 36,* L20403, doi:10.1029/2009GL040267.

Klemes, V., (1986). Operational testing of hydrological simulation models. *Hydro. Sci. J., 31 (1), 13-24.*

Koedyk L.P., Kingston D.G., (2016). Potential evapotranspiration method influence on climate change impacts on river flow: a mid-latitude case study. *Hydrology Research, 47.5, 951-963.*

Legates D.R., McCabe G.J., (1999). Evaluating the use of "goodness-of-fit" measures in hydrologic and hydroclimatic model validation. *Water Resour. Res., 35(1): 233-241.*

Lettenmaier D.P., Wood A.W., Palmer R.N., Wood E.F., Stakhiv E.Z., (1999). Water resources implications of global warming: a U.S. regional perspective. *Climatic Change, 43 (3), 537-79.*

Lill B., (2003). Climate Change and Alpine Catchment Discharge. Unpublished MSc thesis, University of Otago.

Lindström G., Johansson B., Persson M., Gardelin M., Bergström S., (1997). Development and test of the distributed HBV-96 model. *J. Hydrol., 201, 272–288.*

Lindstrom, G. and Bergstrom, S., (1992). Improving the HBV and PULSE-models by use of temperature anomalies, *Vannet i Norden, 16– 23.*

Lu J., Sun G., McNulty S., Amatya D., (2005). A comparison of six potential evapotranspiration methods for regional use in the southeastern United States. *J. Am. Water Resour. As., 41, 621–633.*

Madden R.A., Kidson J.W., (1997). The Potential Long-Range Predictability of Temperature Over New Zealand. *Int. J. Climatol., 17, 483-49.*

Madden R.A., Shea D.J., Katz R.W., Kidson J.W., (1999). The Potential Long-Range Predictability of Precipitation Over New Zealand. *Int. J. Climatol., 19, 405-421.*

Manabe S., (1969). Climate and ocean circulation, I, The atmospheric circulation and the hydrology of the earth's surface. *Mon. Weather Rev., 97, 739-774.*

McCraw, J.D. (1956). Soil survey of Upper Catchment. In Shotover River Survey (Upper Catchment). Otago Catchment Board Bull., 1, 16-23.

McCraw, J.D. (1966). Soils of Lower Shotover Catchment, Western Otago. In Shotover River Survey (Lower Catchment). Otago Catchment Board Bull. 2

McGlone M.S., Moar N.T., Meurk C.D., (1997). Growth and Vegetation History of Alpine Mires on the Old Man Range, Central Otago, New Zealand). *Arctic and Alpine Research, 29 (1), 32-44.*

McGlynn B.L., McDonnell J.J., Seibert J., Kendall C., (2004). Scale effects on headwater catchment runoff timing, flow sources and groundwater-streamflow relations. *Water resour. Res., 40,* W07504, doi:10.1029/2003WR002494.

McKenney M.S., Rosenberg N.J., (1991). Simulating the impacts of climate change on potential evapotranspimtion: a comparison of the climate sensitivity to selected methods. *Mitigation and Adaption Strategies for Global Change, 15 (5), 413-431*.

McMahon T.A., Peel M.C., Lowe L., Srikanthan R., McVicar T.R., (2013). Estimating actual, potential, reference crop and pan evaporation using standard meteorological data: a pragmatic synthesis. *Hydrol. Earth Syst. Sci., 17, 1331–1363.*

McMillan H., Jackson B., Clark M., Kavetski D., Woods R., (2011). Rainfall uncertainty in hydrological modelling: An evaluation of multiplicative error models. *J. of Hydrol., 400 (1-2), 83-94.*

McMillan H.K., Booker D.J., Cattoen C., (2016). Validation of a national hydrological model. *J. Hydrol., 800-815.*

McMillan, H.K., Hreinsson, E.Ö., Clark, M.P., Singh, S.K., Zammit, C., Uddstrom, M.J., (2013). Operational hydrological data assimilation with the recursive ensemble Kalman filter. *Hydrol. Earth Syst. Sci., 17 (1), 21–38.*

Mearns L.O., Bogardi I., Giorgi F., Matyasovszky I., Palecki M., (1999). Comparison of climate change scenarios generated from regional climate model experiments and statistical downscaling. *J. Geophys. Res., 104 (D6), 6603-6621*.

Meehl G.A., Covey C., Delworth T., Latif M., McAvney B., Mitchell J.F.B., Stouffer R.J., Taylor K.E., (2007). The WCRP CMIP3 multimodel dataset: A new era in climate change research. B. *Am. Meteorol. Soc., 88, 1383–1394.*

Ministry for the Environment (2008). *Climate Change Effects and Impacts Assessment*. A Guidance Manual for Local Government in New Zealand. 2nd Edition. http://www.mfe.govt.nz/publications/climate/climate-change-effect-impacts-assessments-may08/index.html. Accessed on September 15, Otago, New Zealand.

Moeletsi M.K., Walker S., Hamandawana H., (2013). Comparison of the Hargraves and Samani equation and the Thornthwaite equation for estimating decadal evapotranspiration in the Free State Province, South Africa. *Phys. Chem. Earth, Pt. A/B/C, 66, 4-15.*

Montzka C., Canty M., Kunkel R., Menz G., Vereecken H., Wendland F., (2008). Modelling the water balance of a mesoscale catchment basin using remotely sensed land cover data. *J. Hydrol., 353, 322-334.*

Moore R.D., Owens I.F., (1984). A conceptual runoff model for a mountainous rain-on-snow environment, Craigieburn Range, New Zealand. *J. Hydrol. (NZ), 23, 84-99.*

Moradkhani H., Sorooshian S., (2008). *General review of rainfall-runoff modelling: model calibration, data assimilation, and uncertainty analysis*. Hydrological modelling and the water cycle. Springer. 291 p. ISBN 978-3-540-77842-4.

Moriasi D.N., Arnold J.G., Van Liew M.W., Bingner R.L., Harmel R.D., Veith T.L., (2007). Model evaluation guidelines for systematic quantification of accuracy in watershed simulations. *ASABE-American Society of Agricultural and Biological Engineers, 50(3): 885−900.*

Moulin L., Gaume E., Obled C., (2009). Uncertainties on mean areal precipitation: assessment and impact on streamflow simulations. *Hydrol. Earth Syst. Sci., 13, 99-114.*

Mullan A.B., Wratt D.S., Renwick J.A., (2001). Transient model scenarios of climate changes for New Zealand. *Weather and Climate, 21, 3-33*.

Nash J.E., Sutcliffe J.V., (1970). River Flow Forecasting Through Conceptual Models. Part 1: A Discussion of Principles. *J. Hydrol., 10(3):282-290.*

National Water and Soil Conservation Organisation (1977). *Shotover River Catchment, Report on Sediment Sources Survey and Feasibility of Control, 1975.* Ministry of Works and Development Water and Soil Division Technical Publication No. 4, 38 pp.

Osborn T.J., Conway D., Hulme M., Gregory J.M. Jones P.D. (1999). Air flow influences on local climate: observed and simulated mean relationships for the UK. *Clim. Res., 13, 173-191.*

Otago Regional Council, (2003). Wakatipu Basin Groundwater Investigation. Unpublished technical report for ORC, prepared in February 2003, Dunedin. (ORC 2003).

Pacific Climate Impacts Consortium (PCIC), University of Victoria, (2014). Statistically Downscaled Climate Scenarios. Downloaded from http://www.cccsn.ec.gc.ca/?page=downscaling on 23/03/17.

Penman H.L., (1948). Natural evaporation from open water, bare soil and grass. *Proc. R. Sot. Ser. A 193, 120-145.*

Pereira A.R., Pruitt W.O., (2004). Adaption of the Thornthwaite scheme for estimating daily reference evapotranspiration. *Agric. Water Manage., 66, 251-257.*

Poyck S., Hendrix J., McMillan H., Hreinsson E.O., Woods R., (2011). Combined snow and streamflow modelling estimate of climate change on water resources in the Clutha River, New Zealand. *J. Hydrol. (NZ), 50 (2), 293-313.*

Priestley C.H.B., Taylor R.J., (1972). On the assessment of surface evaporation using largescale parameters. *Mon. Weather. Rev., 100, 81-92.*

Prudhomme C., Davies H., (2009). Assessing uncertainties in climate change impacts analyses on the river flow regimes in the UK. Part 1: baseline climate. *Clim. Change.* doi:10.1007/s10584-008-9464-3

Prudhomme C., Davis H., (2009). Assessing uncertainties in climate change impact analysis on the river flow regimes in the UK. Part 2: future climate. *Climatic Change, 93, 197-222.*

Reeves E., (2014). *Modelling the hydrological impacts of land use change and integrating cultural perspectives in the Waikouaiti Catchment, Otago, New Zealand*. Unpublished MSc thesis, University of Otago.

Rowe L.K., (1983). Rainfall interception by an evergreen beech forest, Nelson, New Zealand. *J. Hydrol., 66, 143-158.*

Rutter A.J., Morton A.J., Robins P.C., (1975). A predictive model of rainfall interception in forests, II. Generalization of the model and comparison with observations in some coneferous and hardwood stands. *J. Appl. Ecol., 12, 367-380.*

Saelthun N.R., Aittoniemi P., Bergström S., Einarsson K., Jóhannesson T., Lindström G., Ohlsson P.E., Thomsen T., Vehviläinen B., Aamodt K.O., (1998). *Climate change impacts on runoff and hydropower in the Nordic countries.* Final report from the project "Climate Change and Energy Production". Tema Nord 1998, 552, Oslo, Norway.

Saelthun N.R., Bergstrom S., Einarsson K., Johannesson T., Lindstrom G., Thomsen T., Vehvilainen B., (1999). *Potential impacts of climate change on floods in Nordic hydrological regimes.* In: Balabanis P., Bronstert A., Casale R., Samuels P., (Eds), Proceedings from the Ribamod - River Basin Modelling, Management and Flood Mitigation Concerted Action -Final Workshop. Wallingford, UK, 26-27 February 1998, 103-115.

Schneider S.H., (1983). *CO2, climate and society: a brief overview*. In: Chen R.S., Boulding E., Schneider S.H., (Eds). Social science research and climate change: an interdisciplinary appraisal. Reidel, Dordrecht, p viii, 255p

Seaby L.P., Refsgaard J.C., Sonnenborg T.O., Stisen S., Christensen J.H., Jensen K.H., (2013). Assessment of robustness and significance of climate change signals for an ensemble of distribution-based scaled climate projections. *J. Hydrol., 486, 479-493.*

Segond M.L., Wheater H.S., Onof C., (2007). The significance of spatial rainfall representation for flood runoff estimation: A numerical evaluation based on the Lee catchment, UK. *J. Hydrol., 347, 116-131.*

Seibert J., (1997). Estimation of parameter uncertainty in the HBV model. *Nord Hydrol, 28 (4/5), 247-262.*

Seibert J., (2005), HBV light version 2, User's manual, Dept. of Physical Geography and Quaternary Geology, Stockholm University.

Seibert J., Vis M.J.P., (2012). Teaching hydrological modelling with user-friendly catchment-runoff-model software package. *Hydrol. Earth Syst. Sci., 16, 3315-3325.*

Singh J., Knapp H.V., Arnold J.G., Demissie M., (2005). Hydrologic modelling of the Iroquois River watershed using HSPF and SWAT. *J. Am. Water Resour. As., 41(2), 361-375.*

Snelder T.H., Biggs B.J.F., (2002). Multi-scale river environment classification for water resources management. *J. Am. Water Resour. As., 38, 1225-1239.*

Srinivasan M.S., Schmidt J., Poyck S., Hreinsson E., (2011). Irrigation reliability under climate change scenarios: A modelling investigation in a river-graysonased irrigation scheme in New Zealand. *J. Am. Water Resour. As., 47 (6), 1261-1274.*

Stainforth A., Aina T., Christensen C., Collins M., Faull N., Frame D.J., Kettleborough J.A., Knight S., Martin A., Murphy J.M., Piani C., Sexton D., Smith L.A., Spicer R.A., Thorpe A.J., Allen M.R., (2005). Uncertainty in predictions of the climate response to rising levels of greenhouse gases. *Nature, 433, 403-406.*

Tait A., Henderson R., Turner R., Zheng X., (2006). Thin plate smoothing spline interpolation of daily rainfall for New Zealand using a climatological rainfall surface. *Int. J. Climatol., 26, 2097-2115.*

Thompson J.R., Green A.J., Kingston D.G., Gosling S.N., (2013). Assessment of uncertainty in river flow projections for the Mekong River using multiple GCMs and hydrological models. *J. Hydrol., 486, 1-30.*

Tilahun K., (2006). Analysis of rainfall climate and evapo-transpiration in arid and semi-arid regions of Ethiopia using data over the last half a century. *J. Arid Environ., 64, 474-487.*

Todd M.C., Taylor R.G., Osborn T.J., Kingston D.G., Arnell N.W., Gosling S.N., (2011). Uncertainty in climate change impacts on basin-scale freshwater resources: Preface to the special issue: The QUEST-GSI methodology and synthesis of results. *Hydrol. Earth Syst. Sci., 15 (3), 1035-1046.*

Vehvilainen B., Huttunen M. (1997). Climate change and water resources in Finland. *Boreal Envi. Res. 2, 3-18.*

Vehvilainen B., Lohvansuu J., (1991). The effects of climate change on discharges and snow cover in Finland. *Hydro. Sci. J., 36, 109-121.*

Vogel R.M., Fennessey N.M., (1995). Flow duration curves II: A review of applications in water resources planning. *J. Am. Water Resour. As., 31 (6), 1029-1039.*

Wagener T., McIntyre N., (2007). Tools for teaching hydrological and environmental modelling. *Computers in Education Journal, 17, 16-26.*

Wigley T.M.L., (1999). *The Science of Climate Change: Global and U.S. Perspectives*. Pew Center on Global Climate Change, Arlington, Virginia.

Willmott C.J., Rowe C.M., (1985). Climatology of the terrestrial seasonal water cycle. *J. Clim., 5, 589-606.*

Woods R., Tait A., Mullan B., Hendrikx J., Diettrich J., (2008). *Projected Climate and River Flow for the Rangitata Catchment for 2040.* National Institute of Water & Atmospheric Research Report CHC2008-097, Christchurch, New Zealand.

Zorita E., von Storch H., (1999). The analog method as a simple statistical downscaling technique: comparison with more complicated methods. *J. Clim., 12 (8), 2474-2489*